To the Graduate Council:

I am submitting herewith a thesis written by Sudhakar Jagannathan entitled “Process - structure – property relationships of electrospun nano fibers”. I have examined the final electronic copy of this thesis for form and content and recommend that it be accepted in partial fulfillment of the requirements for the degree of Master of Science, with a major in Polymer Engineering.

Kevin M. Kit

_____

Major Professor

We have read this thesis and recommend its acceptance:

Joseph E. Spruiell

_____

Committee Advisor

Roberto S. Benson

_____

Committee Advisor

Accepted for the Council:

Anne Mayhew

_____

Vice Provost
and Dean of Graduate Studies

(Original signatures are on file with official student records.)

Process - structure – property relationships of electrospun nano fibers

A Thesis Presented for the Master of Science Degree

The University of Tennessee, Knoxville

Sudhakar Jagannathan

December 2003

Dedicated to

My parents

J. Kasthuri and J. Jagannathan,

My sisters

Thara & Guna,

My Gurus

M. Abdul Kader, Jai Singh, Joseph E. Spruiell, Kevin M. Kit, Marion G. Hansen, Mohammed Ansari, Mohammed Nabi, Roberto S. Benson, K. Ramamurthy, Syed Amanullah

My cousins

Balu, Bharath, Bhaskar, Chitra, Dhana, Dinesh S, Dinesh G, Divakar, Gautham, Gyanam, Indhu, Kavitha, Kumar, Latha, Logi, Malini, Meena, Mohana, Mythili, Nalini, Nithya, Nivetha, Raju, Ramesh, Ramya, Rani, Selvi, Shankar, Sunitha, Suresh G, Suresh J, Thyagu, Uma, Vandhana, Viji.

&

My friends

Abhijeeth, Akbar, Akila, Anita, Ashwin, Atul, Bill, Balaji, Balaji R, Bruce, Chris, Demit, Dhanapathi, George, Girish, Guruprasad, Hari, Haroon, Indraneel, Imran, Javeed, Joseph, Kannan, Kamal, Karthik, Kaushik, Lakshmi, Leina, Madan, Madhavan, Madhan, Madhusudan, Magesh, Mahalingam, Mary, Mayilvelan, Muruganandham, Narayan, Narayan R, Naseema, Neelima, Nirisha, Padmaja, Pandurangan, Parag, Prakash, Prashanth, Praveen, Puja, Rahul S, Rahul P, Rajesh, Ramanathan, Ramesh, Ravi, Rodger, Saif, Sampath, Sarojini, Sathya B, Sathya M, Sathya R, Sekar, Senthil, Sethuraman, Shelley, Sherry, Shreeram, Sowjanya, Sridhar, Srikanth, Srilalitha, Srinivas, Srinivasan, Sriram MP, Sriram S, Srividhya, Subi, Sundar, Thenbavanam, Thirupathi, Umayal, Venkat, Vijay A, Vijay M, Vijay P, Vijay R, Vivek, Vivekanandan.

Acknowledgements

The author wishes to express a sincere gratitude to his advisor, Dr. Kevin M. Kit for his continuous encouragement, support and guidance throughout the course of this project. The gratitude is also extended to his committee advisors Dr. Roberto S. Benson for his advise on measurement of mechanical properties and orientation of fibers using DMA and FTIR and Dr. Joseph E. Spruiell for his advise on crystallinity measurement using WAXD.

The author also thanks Dr. Jochen Weiss and Dr. Ghajanan Bhat for their help in handling of DSC. The author also thanks each one in Material Science and Engineering department for their support at different stages of this project. A special thank is extended to Greg Jones and Dr. Dunlop for their help in handling of SEM, Doug Fielden & his team for fabrication of different equipments used in this project and Frank Holiway & Randy Stooksbury for their help in obtaining the supplies. This project submitted as thesis work for Master of Science diploma was funded in part by Dupont Textiles and Tnteriors. The author also thanks Dr. Hao Chang of Dupont Textiles and Interiors for his suggestions.

The author is also grateful to his colleagues Abhijeeth Godbole, Anita Dimeska, Asif Rasheed, Atul Dahiya, Chris Stephens, Evyn Childress, George Jacob, Hoaming Rong, Indraneel Sen, Leina Toccheto, Rahul Seshadri, Rodgerio Toccheto, Sathyaprasad Malapudi, Shreeram Wadekar, William Barlow, Xiaoyu Luo, Xiaoyun Ling, Xiaoping Guan for their help and support. Finally and most importantly, the author wishes to thank his Indian friends in Knoxville, who kept his spirit alive away from home, for their love and affection.

Abstract

Electrospinning is a process by which fibers with diameters as small as 15 nanometers are produced when a polymer solution is accelerated from a capillary towards a grounded target by an electric field. An investigation on the electrospinning process and the effect of its process variables on orientation, crystallinity, microstructure and mechanical properties of the fibers produced are made.

Nylon 6, nylon 66 fibers and their blends from a solution of formic acid were produced on a stationary copper target as well as on a metal disc rotating at discrete variable speeds. The solution concentration of the polymers, distance of the target from the syringe, the voltage applied and concentration of moisture were varied and their effect on the structure, morphology and properties were studied using scanning electron microscopy, dynamic mechanical analysis, fourier transform infrared spectroscopy, wide angle x-ray diffraction and density gradient column.

This electrospinning process was used to produce PA66 fibers as small as 15 nm. The fibers were produced by electrospinning process only if the applied voltage is above a given limiting value. The diameter of the fiber obtained varied with the solution concentration, which in turn depends on solution charge density, type of polymer, and the solvent used. The diameter of nylon 66 fibers under conditions studied here does not depend on the target distance from the tip of syringe and the voltage applied. The amount of fibers spun by electrospinning process increases with the applied voltage.

The orientation of fibers can be increased by collecting the fiber in a rotating wheel or annealing the fibers at high temperature and load. The fiber and molecular orientations and tensile modulus of electrospun nylon 6,6 fibers increase with orienatation of fibers.

Poly(ethylene terepthalate) from a solution in trifluoroacetic acid and polystyrene/poly(methyl methacrylate) from tetrahydrofuran were also spun at a stationary target. A membrane like structure observed on spinning nylon 6 urged us to

study the effect of moisture content on morphology and mechanical properties of fibers. The preliminary results show better processability of polymers spun from acidic solutions than from organic solvents. Therefore an attempt has also been made to increase the conductivity of the organic solvents like THF by addition of soluble salts and hence improve the electrospinning capabilities of polystyrene and PMMA in THF.

The information available in the literature was considered together with the experimental results to determine the effect of process variables on the nano sized polymer fibers spun.

Table of Contents

List of Figures

Chapter 1

Introduction

1. 1 History

The demand for synthetic fibers has increased drastically over the last 50 years. The first synthetic fiber, nylon 66, was developed by Wallace H. Carothers in the laboratories of DuPont in the year 1937. Paul Shlack of IG Farbenindustrie then invented nylon 6 fiber processing technique in 1938. DuPont and Calico printers association, UK, developed first acrylic and polyester fibers respectively. In 1954, Natta and Ziegler patented a process for industrial production of polypropylene fibers. The poly(vinylalcohol) fiber was developed in Germany during the second world war[1].

These polymer fibers are traditionally produced spinning from solution, melt, liquid crystalline state, or gel state are now also used in wide range of applications from textiles to composite reinforcement [2]. Low tenacity, high surface area to volume ratio, superior mechanical, chemical and biological properties were the ideal requirements of fibers produced. The diameter of fibers produced by these conventional processes typically varied from 10 to 500 μm [3]. A constant attempt has been made to produce fibers with diameter of sub-micron size for various kinds of applications. The increase in surface area of the polymer fibers with the reduction of fiber size is demonstrated in Figure. 1.1.

Unlike conventional fiber spinning techniques, electrostatic spinning or electrospinning is a process that is capable of producing polymer fibers in the nanometer diameter range. This electrospinning process uses a high voltage electric field to produce fibers of nano scale diameter from a polymer melt or solution. The significance of these nanofibers is their small diameters, their large surface area per unit mass, and small pore size between fibers. The ease with which the deposition of polymer fibers on a target substrate can be controlled enables formation of complex three-dimensional shapes. The electrospinning of two different polymers together is also possible to achieve intermediate properties of

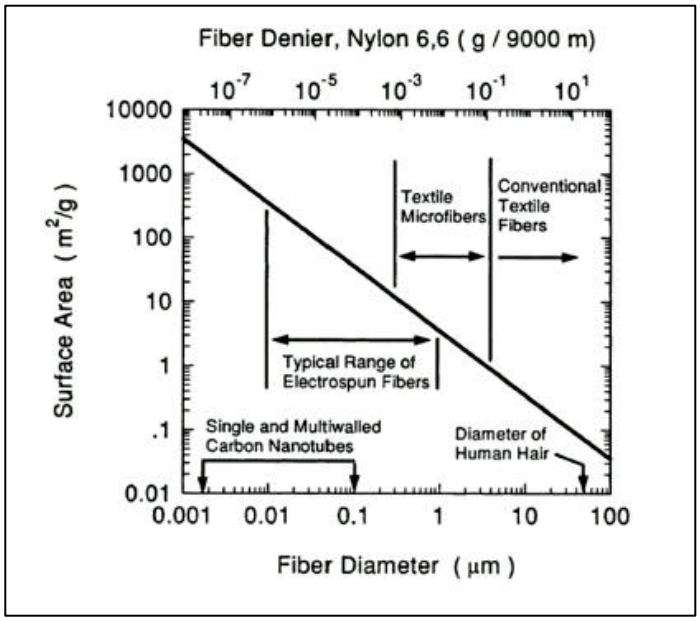

Figure 1.1 Increase in surface area of fibers with decrease in diameter [4].

the two polymers. A wide range of properties can be achieved by varying the type of polymer spun. Small insoluble particles, soluble drugs, and anti-bacterial agents can also be incorporated into the fiber to achieve the desired end properties [5].

Though the technology of producing polymer fibers from an electro statically driven jet of polymer solution or melt has been known for more than 100 years, it was first patented in the year 1934 (US patent, 1-975-504) [5]. Since then many detailed studies have been carried out to study the electrospinning process from both solution and melt. To date, more than 30 natural and synthetic fibers have been electrospun for different applications [6].

In 1981, Larrondo and Manley [7] were able to produce nano sized fibers by electrospinning rapidly crystallizing polyethylene and polypropylene from the melt. Reneker and Chun [8] revived the interest in electrospinning process in the early 1990's by producing more than 20 polymers in their laboratory; demonstrating the ability to produce nano sized fibers from many polymers. Most of the fibers spun by Reneker were spun from solution though a few polymers were spun from melt using vacuum and air. Subsequently, wide ranges of polymers used in conventional fiber spinning process were spun using the electrospinning process. These include nylons(66, 6, 64), poly(ethylene terepthalate), poly(ethylene oxide), polystyrene, polycarbonate, Kevlar®, polyacrylonitrile, poly(vinyl alcohol), poly(benzimidazole), polyaniline and biopolymers like proteins, DNA, polypeptides produced from solution. The poly(ethylene terepthalate), polyethylene and polypropylene have also spun from melt. The electrospinning process is also used to spin some of the electrically conducting and photonic polymers [5,7,8].

The important properties of these nano size fibers, which make them commercially important, are small diameter, large surface area, and small pore size; the ideal requirements for filtration, catalysis and adsorption applications. Large length to diameter ratio and small mass to volume ratio of these nano-sized fibers widens the areas of their

application further. These properties of nano fibers are exploited by current researchers to determine appropriate conditions for electrospinning various polymers and biopolymers for eventual applications including multifunctional membranes, biomedical structural elements (scaffolding used in tissue engineering, wound dressing, drug delivery, artificial organs, vascular grafts), protective shields in speciality fabrics, filter media for sub-micron particles in separation industry, composite reinforcement and structures for nano-electronic machines among others[5].

Another interesting application of the electrospinning process is the possibility of spinning two mutually insoluble polymers by spinning them from a common solvent. When polymer blends are spun from a common solvent using this method, there is possibility of phase separation like any other method used to produce polymer fibers. However the rapid evaporation of the solvent may prevent phase separation; making this method suitable to produce a homogenous phase for almost any polymer pair that is melt immiscible but soluble in a common solvent. The homogenous blend can be annealed to allow phase separation to occur which can result in very fine nano-scale morphology, depending on annealing conditions. The final morphology of these immiscible blends, often difficult to control, is determined by the processing conditions and the properties of its components.

1. 2 Objective

The main objective of this project is to investigate processing – structure – property relationships in polymer fibers with nano size diameters produced by the electrospinning process. The effect of processing parameters and blending of commercially important nylon and PET fibers on orientation, crystallinity, fiber diameter, microstructure, and mechanical properties will be determined. The literature review of previous works on electrospinning reveal that very little information has been reported on aligning the electrospun fibers and measurement of its orientation. Hence a study has been made to understand the effect of orientation and blending on structure and properties of electrospun fibers and non-woven mats collected on a rotating disc, which allows aligned

fibers to be collected and orientation to be measured. The effect of orientation on crystallinity, structure and properties has also been studied.

The nylon 6 and nylon 66 were spun from a solution of formic acid at different concentrations. The membrane like structure observed on spinning nylon 6 urged us to study the effect of moisture content on morphology and mechanical properties of fibers. An attempt has also been made to increase the conductivity of the organic solvents like tetrahydrofuran by addition of soluble salts and improve the electrospinning capabilities of polystyrene and poly(methylmethacrylate) in tetrahydrofuran.

Chapter 2

Background and Literature Review

2.1 Introduction

The electrospinning process produces thin polymer fiber from a polymer melt or solution at high voltage and electrostatic field. Studies have been made to understand the relationship between the electrospinning process, structure of fibers formed, and their properties. This process has been used to produce fibers as small as 15 nm by varying the processing conditions. When a high potential difference is maintained between the capillary and metal target, the droplet at the tip of capillary forms a cone, which on exceeding a critical voltage forms a jet of fluid ejected from the cone tip. When the viscosity of the solution spun is low, a jet of droplets results whereas high viscosity polymer solutions result in a thin fiber with evaporation of solvent before reaching the target [9]. A schematic representation of the electrospinning process is given in Figure 2.1.

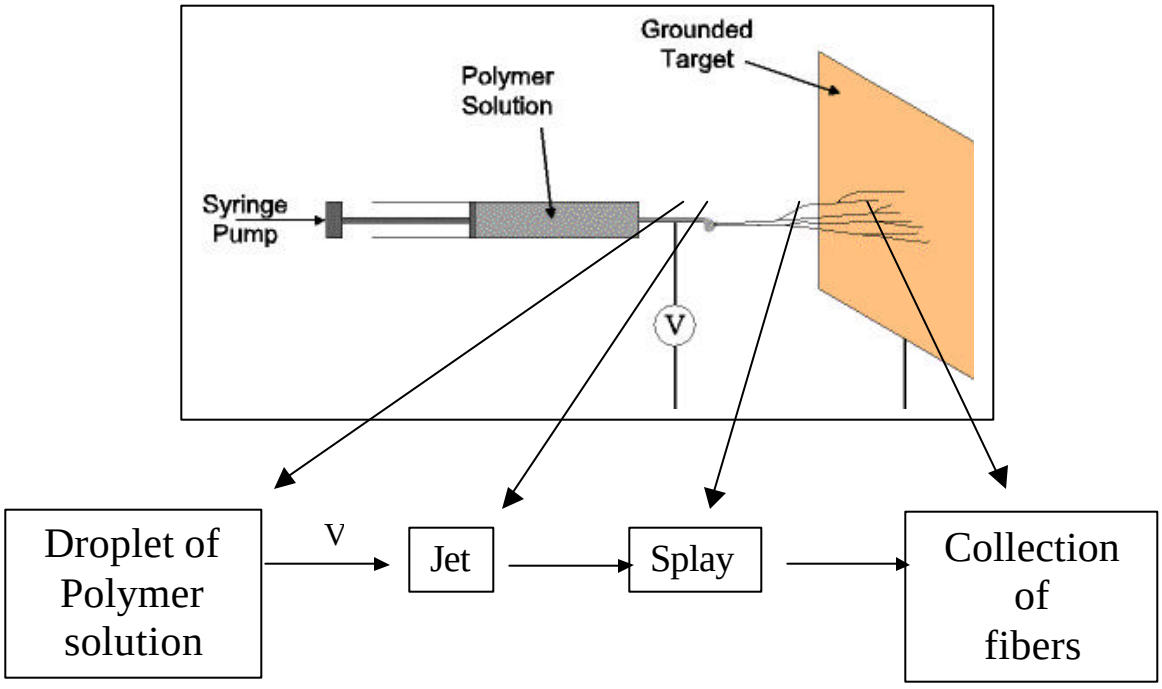

Figure 2.1 Electrospinning process representation

Various researchers have used different types of methods for producing nano sized fibers by electrospinning process. Reneker and Koombhongse[10] mounted the capillary in the vertical direction using gravity to produce a droplet on the tip of capillary for displacement. In other cases the capillary is mounted at an angle to control the flow of the droplet. Many used a setup with a horizontal capillary with a displacement pump to generate a droplet at its tip. A high voltage is applied at the capillary by connecting an electrode at the tip of the capillary. A metal sheet is generally used as a target for collection of fibers spun. However, researchers have also used a grounded water bath [11] and a rotating aluminum cylinder [12] to collect the fibers as non-woven fabric. Zussman [13] used the electrospinning process to align the individual nano fibers on a tapered and grounded wheel like bobbin. The bobbin was able to wind continuously at its tip like edge.

The electrospinning process is driven by the electrical forces on the surface or inside a polymeric liquid. When an electric field is applied between the capillary and the target, the pendant drop at the tip of capillary is deformed into a conical shape known as Taylor's cone shown in Figure 2.2. At a critical voltage, the electrostatic forces overcome the surface tension of the drop and a jet is ejected from the cone. When the voltage is lowered after formation of the jet, thinner fibers are produced without any instability in the jet. A splaying of the jet is observed in some polymer systems by narrowing the jet by reducing the voltage, stretching the jet in electrostatic field, or by evaporation of solvent. The increase in the charge density on the jet due to reduction of its diameter leads to destabilization resulting in splaying which move towards capillary on further reduction in voltage. The fibers are collected on the target as a non-woven fabric if the solvent evaporates during the travel from the capillary [9]. Reneker and Chun[8] divided a stable electrospinning jet into four regions. The jet emerges from the charged surface at the base region, travels through the jet region, divides into many fibers in the splaying region, and stops in the collection region.

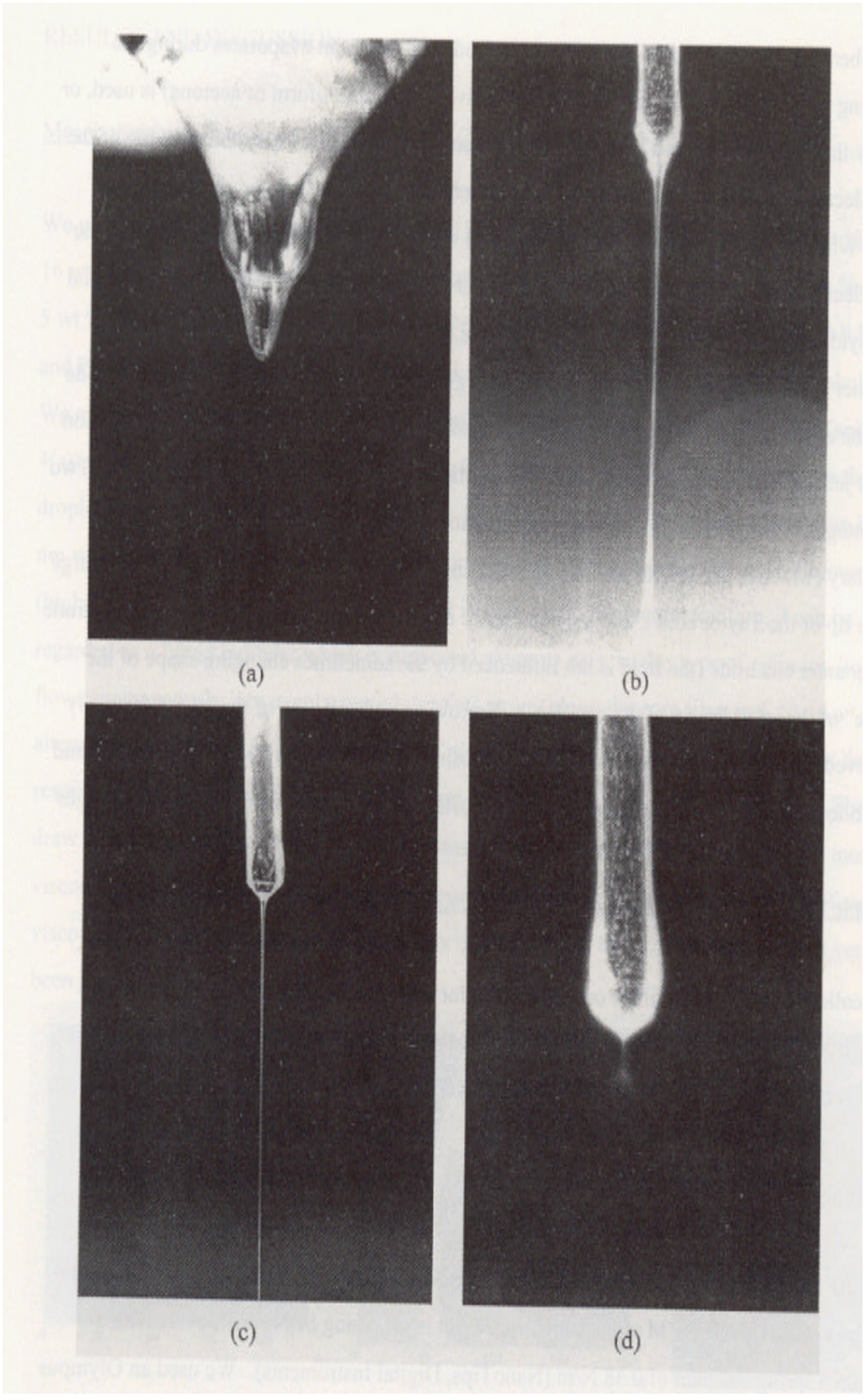

Figure 2.2 Taylor cone (a), Initiation (b), Stretching (c), and splaying (d) of jet [9]

2.2 Structure-property-process relationship

Most of the research work done on electrospinning has explored the types of polymer solvent systems used for nano fiber spinning. Only a few researchers have shown interest in studying processing – property relationships. The processing parameters considered include solution concentration, tip to target distance, spinning voltage, feed rate of fluid to the tip, polarity of the solvent and the viscosity of the solution [2]. The amount of fibers produced depends on the amount of polymer present in the solution, the voltage applied and the distance of the target from the syringe.

2.2.1. Concentration dependence

The viscosity and the surface tension of the solution have an important role in fiber formation in the electrospinning process. The type of polymer used in the preparation of the solution affects the viscosity of solution and in turn the fiber structure formed. The solution viscosity has been found to influence fiber diameter, the droplet shape and the jet trajectory [2]. Solutions with lower viscosity may result in formation of droplets instead of fibers.

Deitzel [2] studied the influence of concentration of poly (ethylene oxide) in HPLC grade water on processability and structure of fibers formed. A concentration of 4-10 wt% of PEO (mw : 400,000) produced fibers. At concentrations below 4%, a mixture of fibers and droplets were observed while for concentration above 10%, high viscosity made solutions extremely difficult to be forced through the syringe. Even within the processing window, the fibers produced from a lower concentration solution were more irregular with undulating morphology and large variations in diameter along a single fiber while fibers produced from a higher concentration solution produced more uniform fibers. Solutions with higher polymer concentration have enough entanglements to prevent breakdown into droplets. Hence the higher concentration solution has more non-woven fabric like structure than the lower concentration solution. electrospun fiber also

increased with solution concentration through a power law relationship [2]. The average diameter of electrospun fiber also increased with solution concentration through a power law relationship [2].

Both Buchko [14] and Zong [15] observed a similar effect in silk like polymer with fibronectin functionality (SLPF) in formic acid and poly (D,L–lactic acid) in dimethylformamide respectively. The concentration effect of PDLLA in DMF given in Figure 2.3 shows a decrease in irregularity of fiber morphology with increase in solution concentration.

2.2.2. Voltage dependence

The electrospinning process produces fibers only if the applied voltage is above the given limiting value required to overcome the surface tension of the solution. In electrospinning experiments, the electric current associated with the process can typically be measured with a microamp-meter. The droplets or fibers transport charge across the gap between the charged needle and the electrically grounded target, closing the circuit. The voltage applied between the capillary and the metal target can be used to control the amount of polymer reaching the target. The number of droplets or fibers reaching the target is a function of the current flowing across the circuit. Hence the amount of fiber spun can be easily controlled by varying the voltage. At low voltage, a droplet of solution remains suspended at the end of the syringe needle, and the fiber jet originates from the cone at the bottom of the droplet. The size of the droplet formed at the end of capillary is large as the voltage is not high enough to transfer all of the solution to the target. The nanofibers produced under this condition will typically have cylindrical morphology with few bead defects. The bead like structures are undesirable “by products” of the electrospinning process caused due to instability of the jet of polymer solution [16]. When voltage is increased, the cone will have receded and the jet originates from the liquid surface within the syringe tip. The fiber morphology still remains cylindrical but with more bead defects [2]. The voltage effect on fiber morphologies of PEO and polyamides are shown in

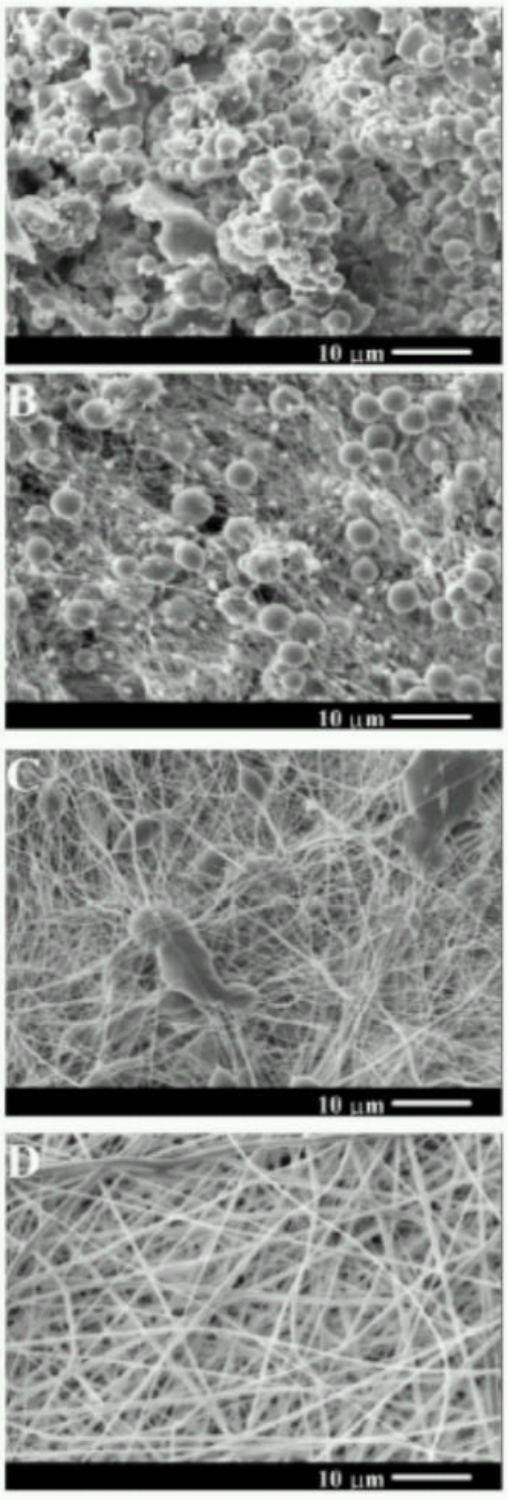

Figure 2.3 Concentration effects on morphology of electrospun PDLLA nanofibers (A) 20wt%, (B) 25wt%, (C) 30wt% and (D) 35wt% [15]

Figure 2.4 and 2.5. Figure 2.4 show that the amount of bead defects increases with the increase in the voltage. Figure 2.5 show the decrease in fiber diameter with increase in voltage applied between the syringe and target.

2.2.3. Dependence on target distance

The polymer fibers collected at longer target distance have a possibility of formation of more uniform structure due to complete evaporation of the solvents. The fibers collected at shorter distance are expected to have more membrane like structure due to incomplete evaporation of solvents. The sizes of the fiber produced at different target distance may also vary. Figure 2.6 illustrates the difference between deposition distance of 0.5 cm and 2 cm in the Silk like Polymer with Fibronectin functionality (SLPF) fibers spun from tetrahydrofuran by Buchko[14]. Figure 2.6a show fine fiber morphology of SLPF spun from a distance of 2 cm. The morphology of SLPF spun from a distance of 0.5 cm show more of membrane like morphology as given in Figure 2.6b.

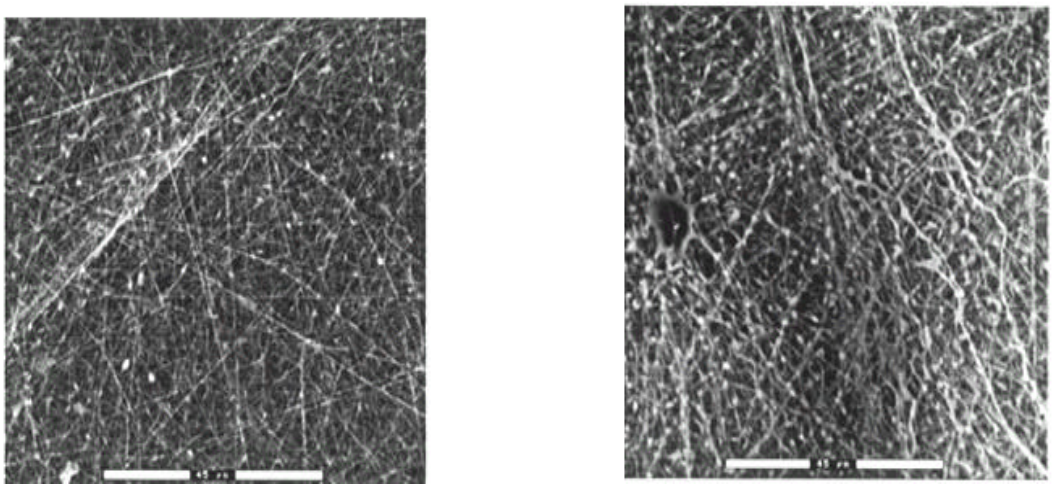

Figure 2.4 The voltage effect on fiber morphology of PEO/water solution (A) 7kV (B) 9kV [2]

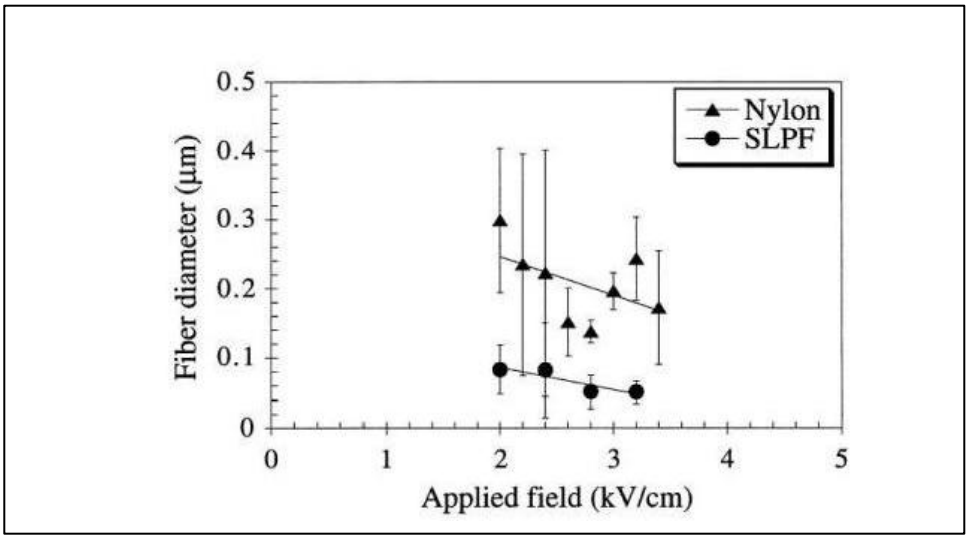

Figure 2.5 Fiber diameters decreases with increasing voltage for Nylon 6,6 and SLPF in formic acid [2]

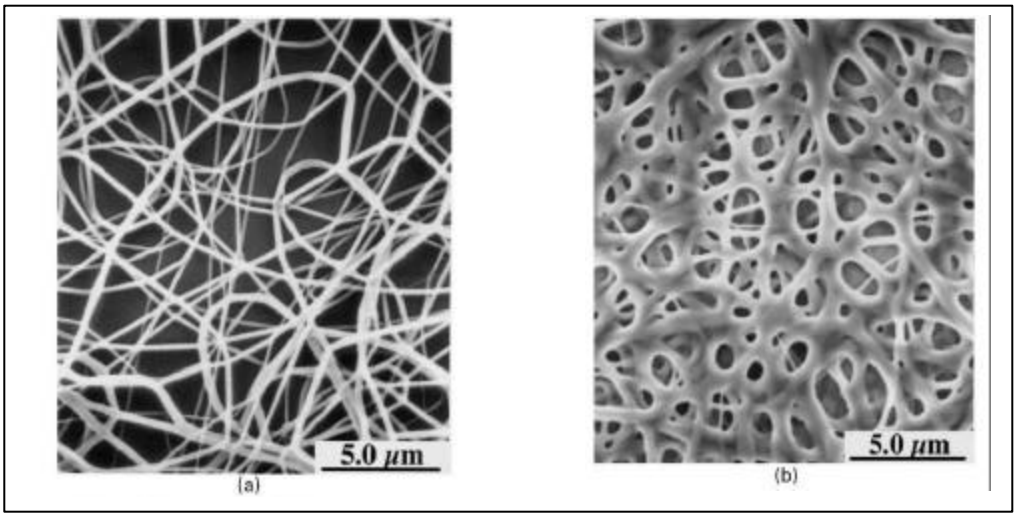

Figure 2.6 The effect of variation in target distance on fiber morphology of SLPF in formic acid [2] (a) 2 cm and (b) 0.5 cm

2.2.4 Surface tension effect on fiber morphology

The electrospun fibers spun do not always have regular morphology and is often characterized by bead defects in regular array. Fong [16] observed the influence of viscosity of the solution, charge density of the jet and the surface tension of the solution to be key factors for the bead defects. The surface tension drives a reduction in the surface area of the fibers by changing jets into spheres. He observed formation of more uniform spherical fibers with the decrease in surface tension of poly(ethylene oxide) in a mixture of ethanol and distilled water. This effect of surface tension on the PEO fibers is explained in the Figure 2.7. With the increase in the concentration of ethanol the surface tension decreases. Hence as shown in the Figure 2.7, surface tension is decreased with the addition of ethanol/water ratio from 0.0 to 0.702 to causes spinning of more uniform fiber with less bead defect.

2.2.5 Effect of charge density

Previous studies show that the polymers spin well from acidic solutions having higher polarity [16,17,18]. However experiments to spin polymers like polystyrene and poly(methyl methacrylate) from organic solvents have shown poor processability due to low charge carrier density in organic solvents. Wang [17] were able to increase the processability of polystyrene/methyletherketone system by addition of 0.5% by weight of LiCl salt. Jagodzinski [18] used $LiClO_4$ to increase the conductivity of THF. Therefore an attempt has also been made to increase the conductivity of the organic solvents like THF by addition of conductive salts and improve the electrospinning capabilities of polystyrene and PMMA in THF reported in section 4.4. Fong [16] studied the change in net charge density with the addition of NaCl to the solution of poly(ethylene oxide) in a mixture of ethanol and distilled water. Figure 2.8 shows the morphology of poly(ethylene oxide) spun with different concentration of NaCl; charge density varied from 1.23 to 28.8 coulomb/liter. The increase in the salt concentration causes production for more uniform and fine fibers.

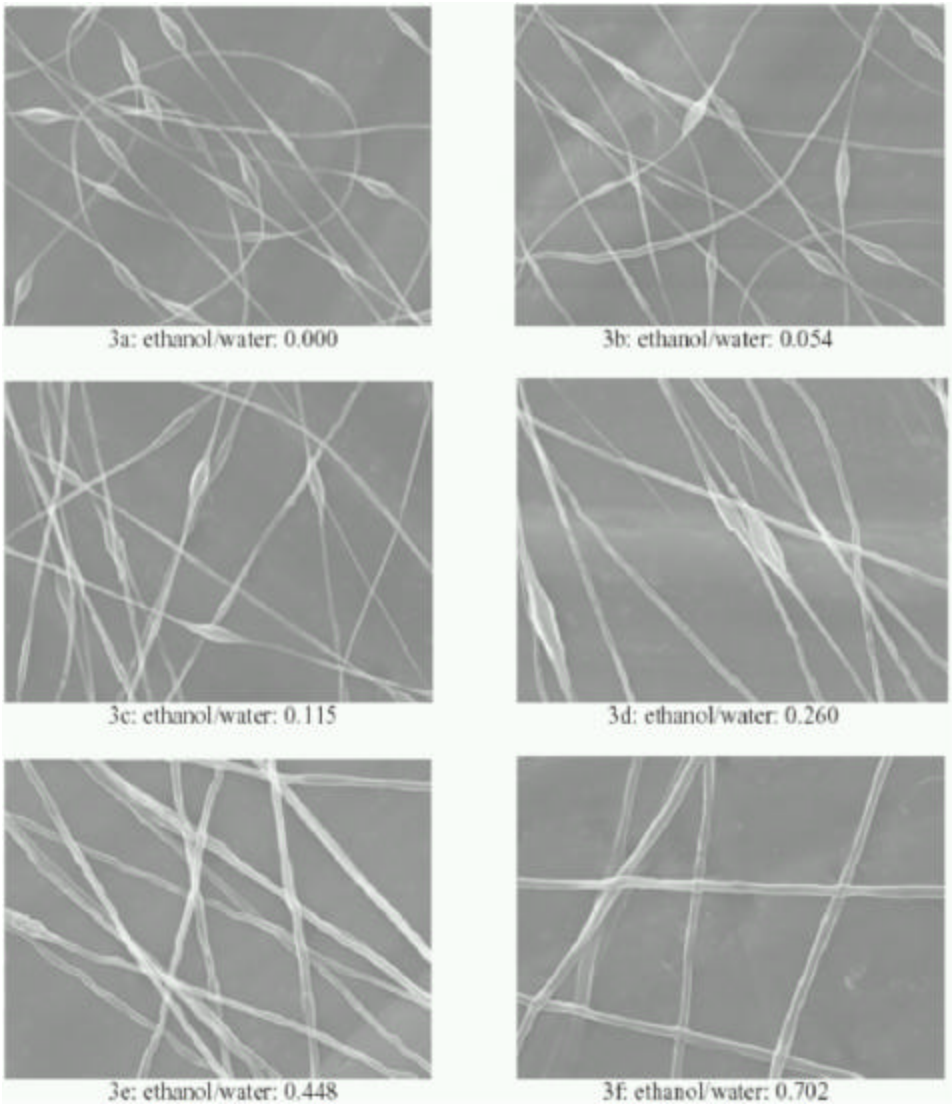

Figure 2.7. The effect of surface tension on PEO fibers spun from ethanol/water [16]

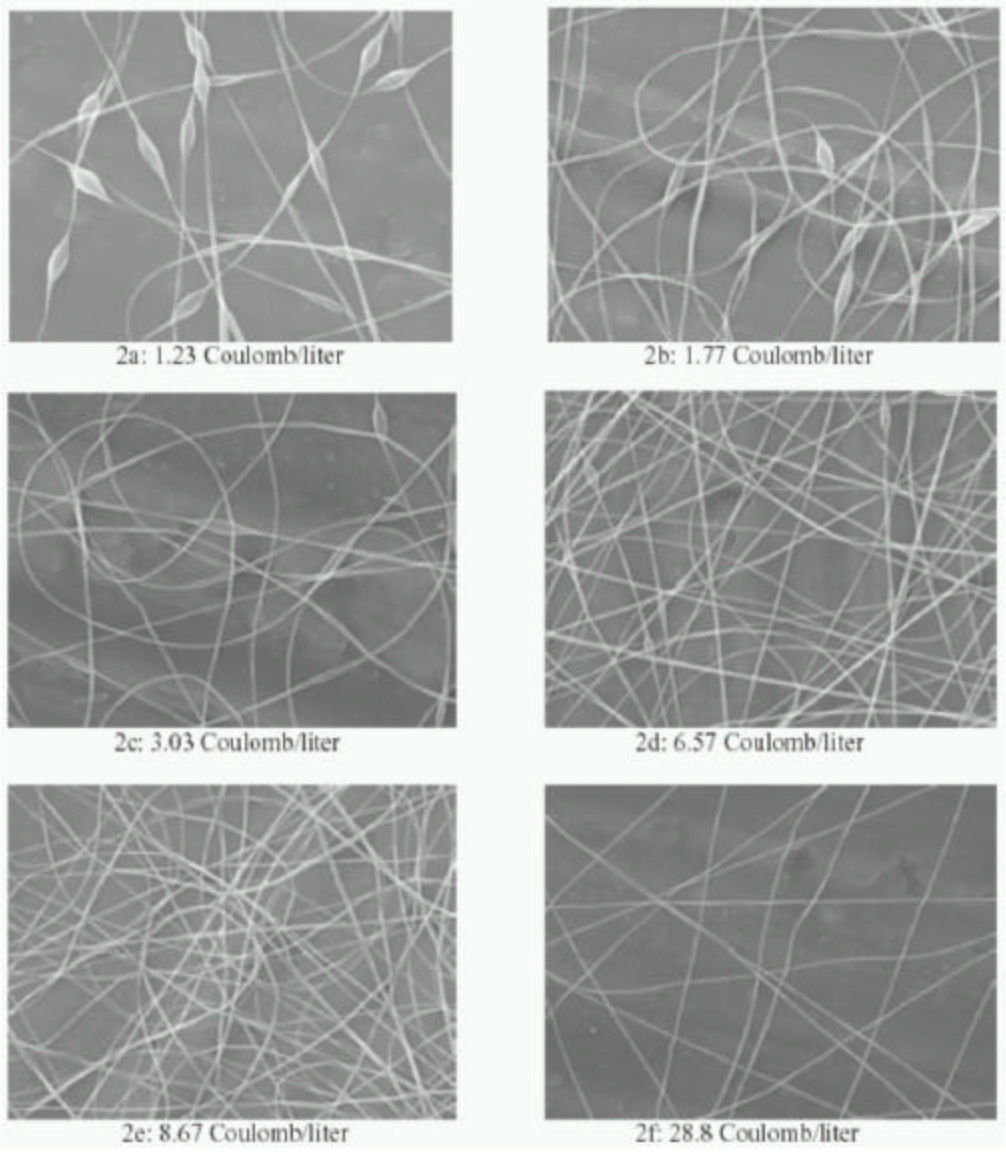

Figure 2.8 The effect of solution conductivity on PEO fibers spun from ethanol/water [16]

2.3 Orientation of fibers

Zussman [13] have described a possibility of increasing the crystallinity and mechanical properties of the electrospun fibers by an electrostatic field-assisted assembly technique combined with an electrospinning process to align the individual nano fibers on a tapered and grounded wheel like bobbin. This paper explains in detail the jet paths in which a polymer fiber travels from a syringe tip to the rotating wheel. In this method, the pendant droplet forms a taylor cone similar to common electrospinning process. At a certain potential difference, a jet emerges and moves towards the rotating wheel. After the jet traveled away from the droplet in a nearly straight line, it bent into a complex path whose envelope can be described by a cone. At certain point of travel, the envelope cone starts to shrink resulting in an inverted envelope cone with its apex resting on the wheel's edge. The setup used by Zussman[13] and the explanation of jet path is given in Figure 2.9. This technique also demonstrates the possibility of continuous winding of the fibers when electrospun from multiple capillaries for a commercial scale production of nano fibers. By designing the winding wheel as a disk (5 mm thick, 20 cm diameter) with a tapered edge (53.1°) instead of a drum, they were able to force the jet into a path within a conical cone whose apex coincided with the tapered edge of the disk. They also performed electrostatic field simulations that showed that this geometry focuses the electric field lines onto the tapered edge of the disk. With this experimental arrangement, they were able to collect highly aligned yarns of electrospun poly(ethylene oxide) given in Figure 2.10.

2.3.1. Birefringence and dichroism of oriented fibers

Vasanthan [18] studied the birefringence of melt spun nylon 66 fibers as a function of draw ratio. The samples were drawn to different draw ratio in a tensile testing machine at room temperature. He observed that the crystallinity measured as 35% did not increase significantly with the increase in the draw ratio.

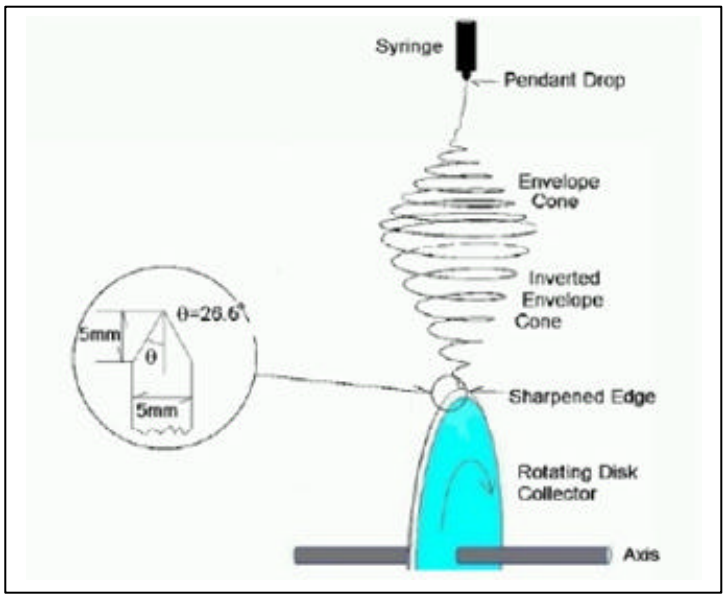

Figure 2.9 Representation of setup used by Zussman[13] and the explanation of jet path.

.

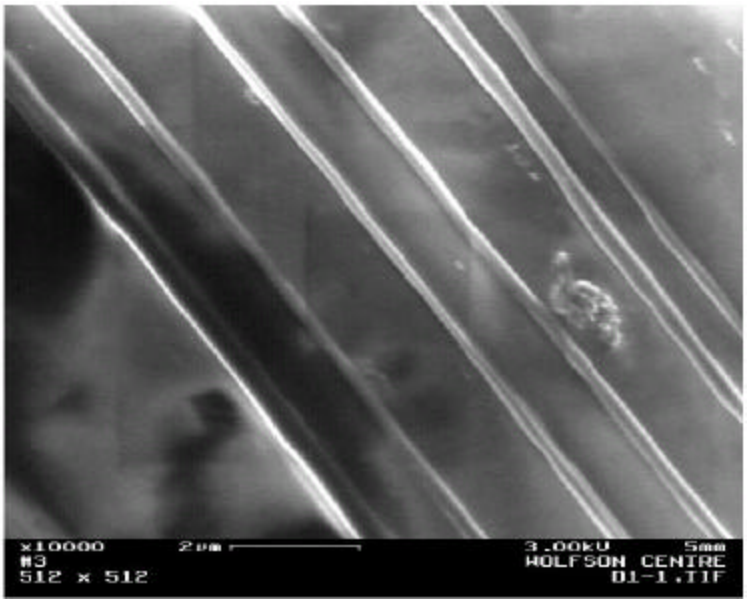

Figure 2.10 SEM images of highly aligned yarns of electrospun poly(ethylene oxide) collected by Zussman [13].

However, Figure 2.11 shows a significant increase in the birefringence value with the draw ratio for 2 different sets of nylon 66 denoting that crystalline or amorphous orientation increases with the increase in draw ratio without increase in crystallinity. It was also observed that the amorphous orientation developed more slowly than the crystalline orientation, a typical behavior of flexible chain polymers. He also measured the dichroic ratio of the nylon 66 fibers as a function of draw ratio with the help of Fourier transform infrared spectroscopy. The dichroic ratio of the crystalline bands at 936 and 906 cm^{-1} corresponding to parallel and perpendicular dichroism and amorphous band of 924 cm^{-1} were considered. Figure 2.12 show the dichroic ratios of 936 and 906 cm^{-1} as a function of draw ratios. The increase in the dichroic ratio for the band corresponding to 936 cm^{-1} and decrease in value corresponding to 906 cm^{-1} shows that the molecules are oriented in the direction of collection of fibers. The crystalline and amorphous orientation functions, given in Figure 2.13 shows an increase in orientation of fibers with respect to the draw ratio. Lee [19] measured the dichroic ratio of the peak 842 cm^{-1} corresponding to $-CH_2$ rocking motion for the electrospun poly(ethylene oxide) fibers collected at two different voltages. He found that the dichroic ratio decreased with the increase in the target distance from the electrode.

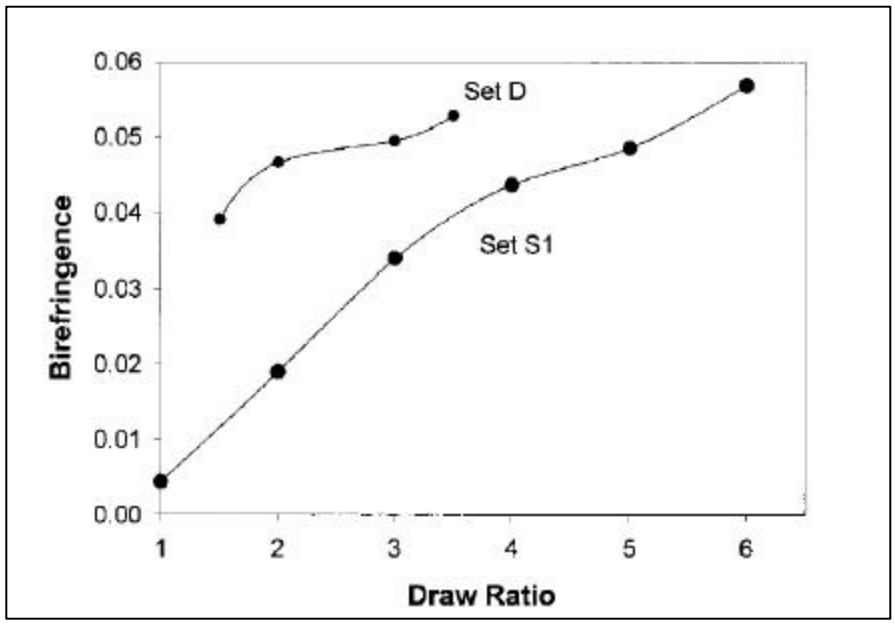

Figure 2.11 Birefringence of 2 different sets of nylon 66 measured as a function of draw ratios [18].

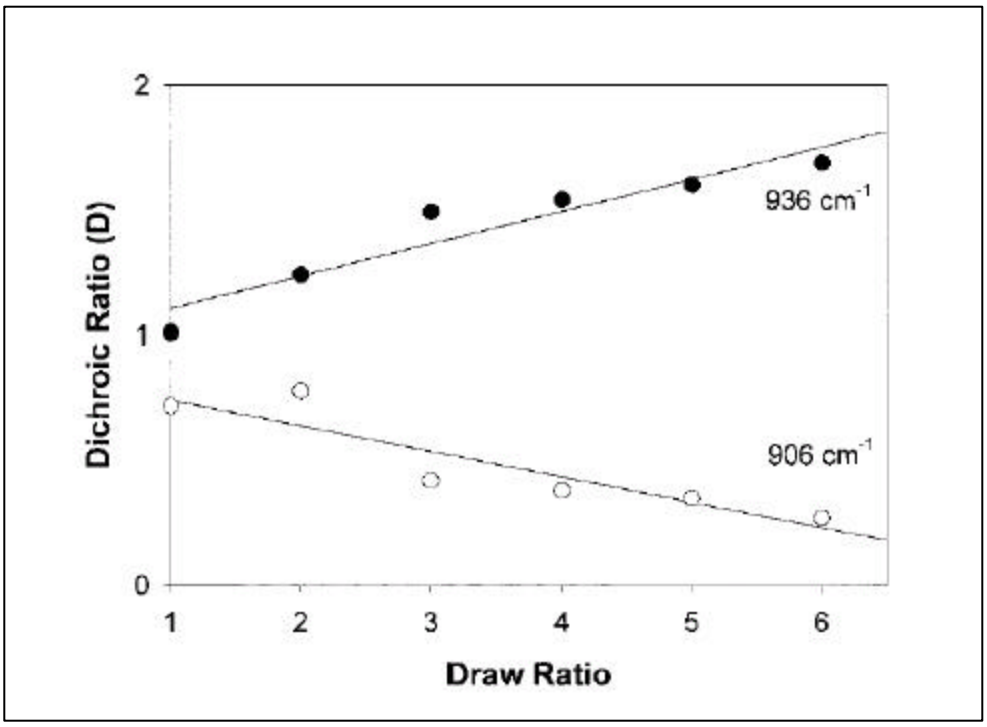

Figure 2.12 Dichroism of 936 and 906 cm^{-1} as a function of draw ratios [18].

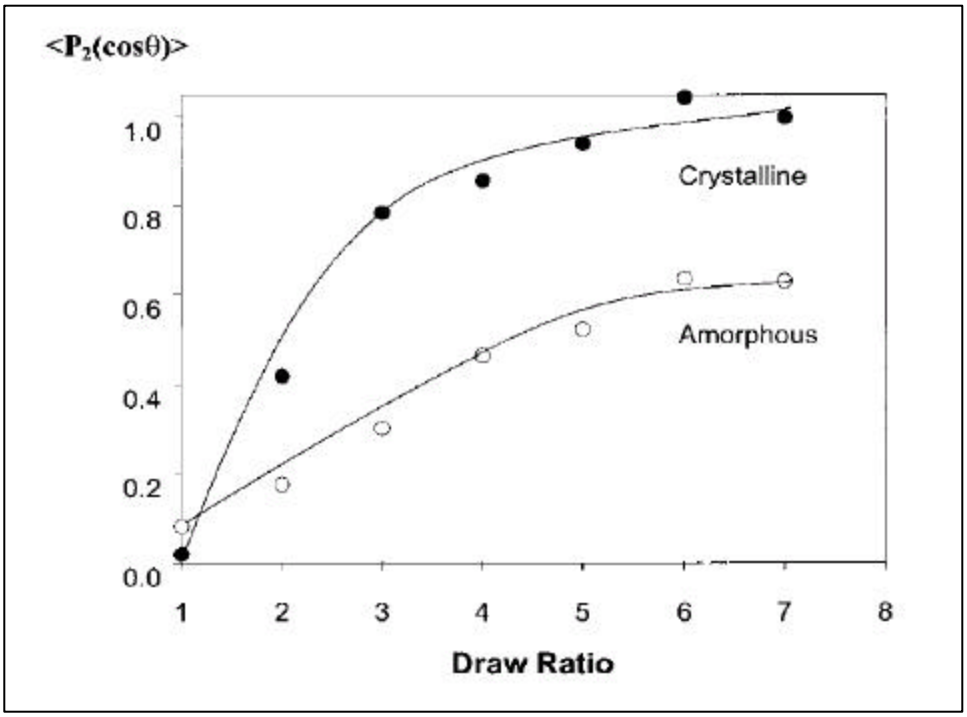

Figure 2.13 Crystalline and amorphous orientation functions versus draw ratios [18].

2.3.2. Crystallinity of oriented fibers

Many research scientists have studied the structure of nylon fibers that are produced from melt spinning and spinning from a solution [4, 20, 21]. Most of them predicted that the Nylon 6 and 66 fibers do not crystallize as soon as they are spun from the capillary. The fibers spun are unoriented and uncrystallized when they are produced from the capillary. The crystallization of the fibers takes place during drawing. The force applied on the fiber by the bobbin induces a stress in the sample, which causes it to crystallize. The molecules also orient in the direction of rotation of the bobbin. Several studies made reveal that the Nylon 6 and Nylon 66 form alpha monoclinic structure on winding in the bobbin and when quenched at a rapid rate forms pseudo hexagonal structure. Further crystallization takes place when the sample is annealed at higher temperature under higher stress which causes stress induced crystallization. The rate of crystallization is found to depend upon the take up velocity of the fibers in the bobbin, the crystallization temperature, rate of cooling of the sample, and annealing conditions. The degree of crystallinity is found to increase with increase in take up velocity, and decrease in cooling rate. The proximity of transition temperatures of the nylon to the annealing temperature also affects the crystal dimensions. The crystallization kinetics and the degree of crystallinity are found by measuring the specific volume or the amount of crystals formed or by directly observing the rate of formation and growth of sperulites.. The meridian 2 theta scans of the as spun fibers and fibers drawn at a spin draw ratio of 15 is given in the Figure 2.14 [20]. Clearly the crystallinity of the samples drawn at higher speed is more than the as spun fibers. Salem [22] measured the volume fraction crystallinity as function of take-up speed for nylon 6 fibers as shown in Figure 2.15. He observed that the alpha phase contribution remained constant while the gamma phase increased with the increase in winding speed. Schultz [21] found an increase in total and alpha phase crystallinity index with winding speed while the contribution due to the gamma phase remained constant.

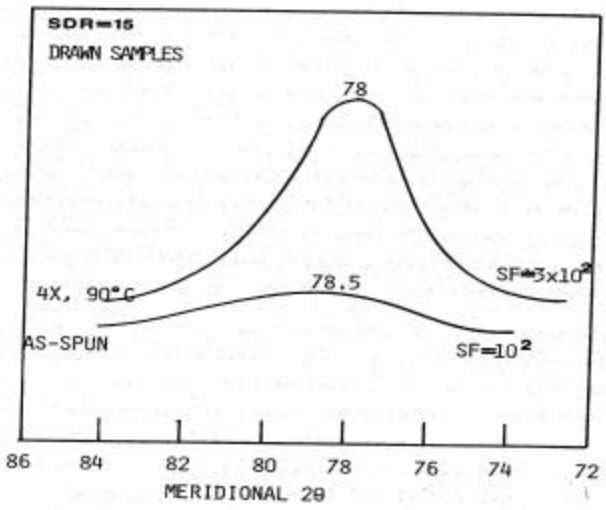

Figure 2.14 Crytallinity of as spun and drawn nylon 6 fibers [20].

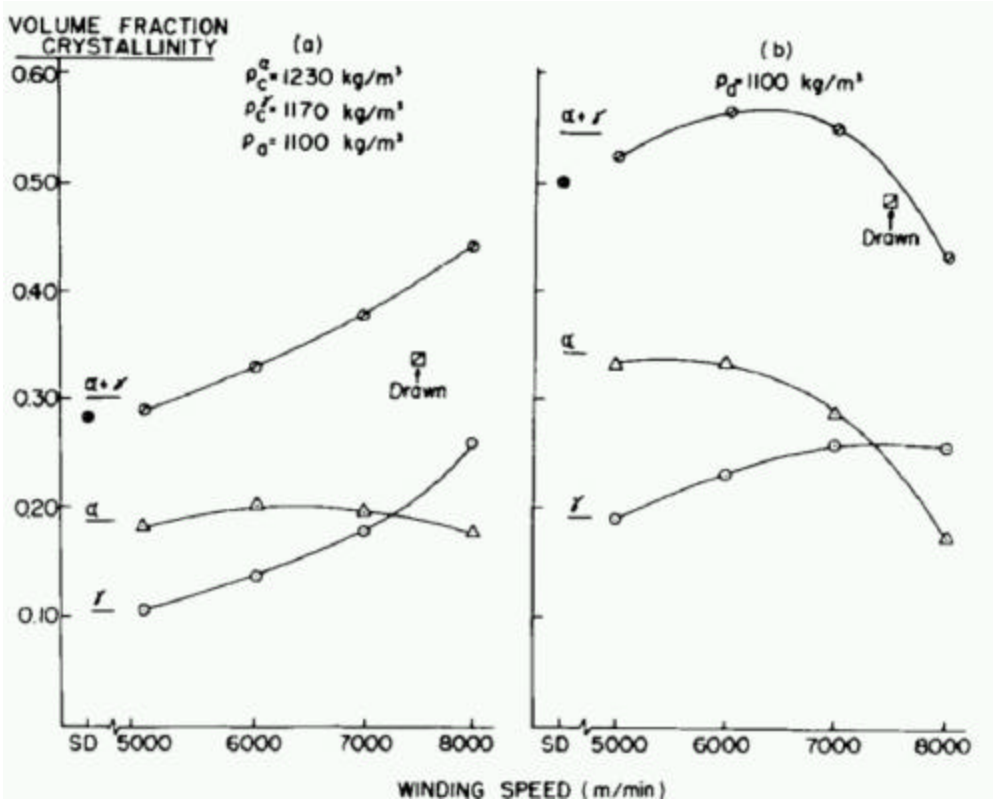

Figure 2.15 Volume fraction crystallinity versus the winding speed of nylon 6 fibers [22].

2.3.3 Mechanical properties of oriented fibers

The mechanical properties of polymer fibers depend on molecular orientation, degree of crystallinity, polarity of the polymer, and presence of plasticizer. The orientation of fibers by aligning them in a rotating wheel typically increases the mechanical property of the fibers due to increase in the orientation and degree of crystallinity of fibers. The change in the modulus can be due to changes in orientation of fibers or molecular orientation within the fiber. Murase [23] measured the Young's modulus of melt spun nylon 6 as a function of winding speed as shown in Figure 2.16. He observed an increase in modulus with the increase in the winding speed and attributed it to both increase in crystallinity and orientation of fibers.

The non-woven fabric resulting from the electrospinning process has high porosity, an important requirement for the filtration application. The fibers produced are laid down in layers that have high porosity but very small pore size. Gibson [4] studied the filtration efficiency of nylon 66 fibrous membranes with void fraction between 0.3 – 0.6. The fibers spun from the polymer solutions create a strong cohesive porous structure because of presence of residual solvent in the electrospun fibers facilitating bonding of intersecting fibers. Hence the non-woven membranes produced would have superior mechanical properties, which could be increased further if the fibers were aligned in a single direction.

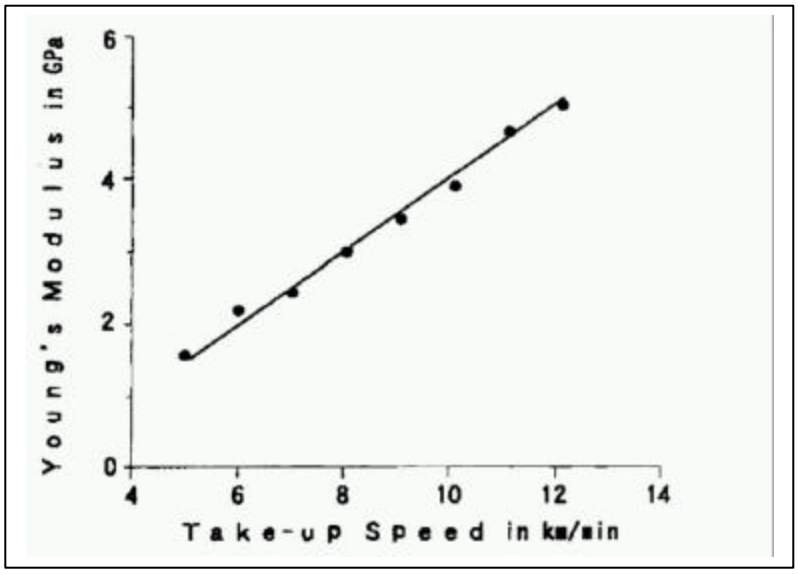

Figure 2.16 Young's modulus versus the winding speed of nylon 6 fibers [23].

2.4 Characterization techniques

2.4.1 Scanning electron microscopy

The scanning electron microscope is an instrument used to examine and analyze microstructures of solid objects. The optical microscopes are used to obtain images with resolution as small as 300 nm. However, the resolution and depth of focus obtained by this technique are poor. The main advantage of SEM is the high resolution, typically 2-5 nm, which can be obtained when bulk objects are examined. Another important feature of SEM is the three-dimensional appearance of the sample examined due to a large depth of field, which provides much more information about the specimen. A typical SEM has a lens system, electron gun, electron collector, visual and recording cathode ray tubes and the electronics associated with it. Figure 2.17 shows the operation of a typical SEM [2,3,4].

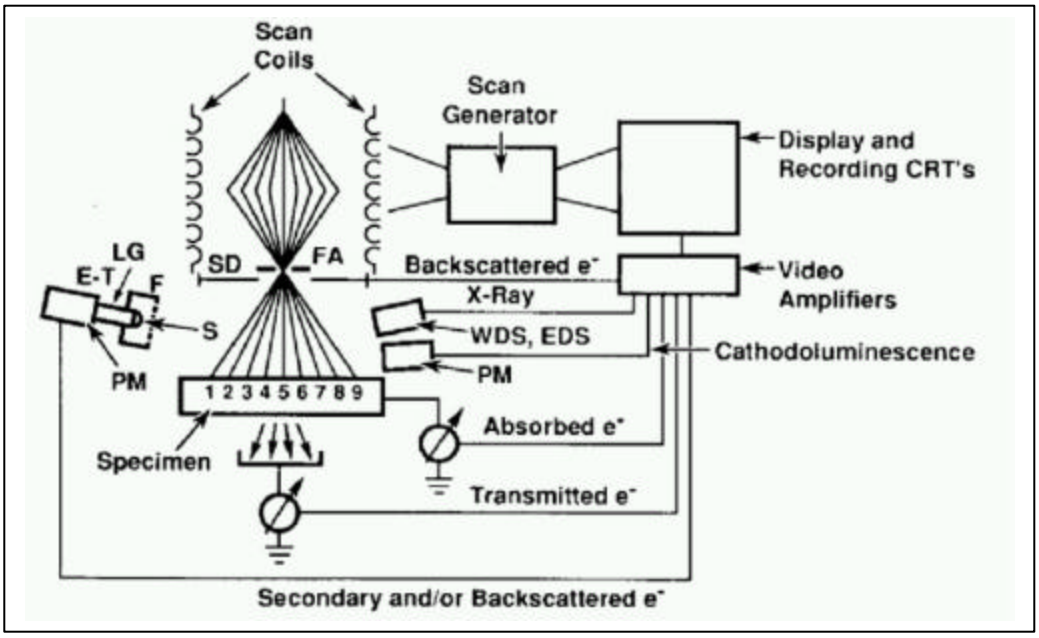

Figure 2.17 Operation of typical Scanning electron microscope [24].

The electron beam from the electron column given in Figure 2.17 enters the specimen chamber striking the specimen at a single location, interacting elasticlly and inelastically and forming a limited interaction volume in the specimen from which the various types of radiation emerge including back scattered, secondary and absorbed electrons, characteristic x-rays and cathodoluminescence radiation. The surface and bulk properties of the sample is determined by measuring the magnitude of signals from a single location or a scan of signals from different locations. To form a SEM image with which we are most familiar, the beam is scanned on the specimen in a X-Y pattern while the CRT is scanned in the same X-Y pattern given in Figure 2.18. A one to one correspondence is established between the set of beam locations on the specimen to points on the CRT with a linear magnification [24].

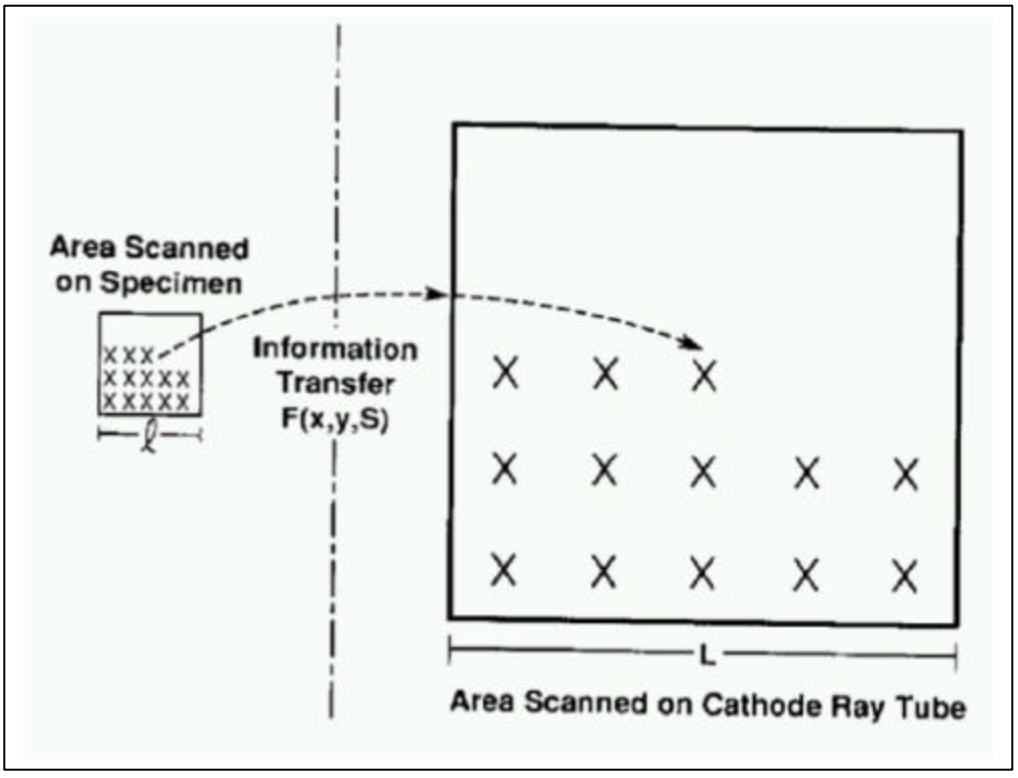

Figure 2.18 The principle of image display by area scanning [24]

2.4.2 Dynamic mechanical analysis

The dynamic mechanical analyzer is an instrument used to determine the mechanical properties of the polymeric material under dynamic conditions. This instrument is useful to explain the various structural parameters like crystallinity, molecular weight, orientation, cross-linking, co-polymerization, and their effect on the properties of the material. The effect of variation of the temperature, time, frequency, and type of deformation can also be studied[25].

The elastic materials have the capacity to store mechanical energy without any dissipation whereas the viscous liquids in a non hydrostatic stress state has a capacity for dissipating energy without any storage. The polymeric material having the characteristic of both elastic solid materials and viscous fluids, when deformed, stores part of work done as potential energy and remaining is dissipated as heat energy. The part of energy that is dissipated as heat is due to the internal friction between the polymeric chains. This character of dissipation of heat is made use of in damping applications to reduce the noise level of the instruments. The dynamic mechanical analyzer measures two responses as two different moduli: *Storage modulus*, the elastic component of the modulus in-phase with the applied load and the *Loss modulus*, the viscous and damping component of the modulus out of phase with the input signal. The ratio of the two moduli is the constant tan δ, which represents relative damping ability of the material.

When a polymer undergoes a relaxation or transition when there is a marked change in the properties at that particular temperature. The tan δ, called loss tangent shows a peak at this region of transition. The polymeric material at lower temperature is rigid with its chains having little internal energy to move. When the thermal energy is supplied to the material, the internal energy of the material increases. The rigid polymer chains expands on application of thermal energy and begin to exhibit cooperative motion when the temperature reaches a critical value called the glass transition temperature often called the α relaxation. The α relaxation is the most prominent transition, which occurs when the

micro Brownian movement of the polymer chains is initiated. A number of factors including the flexibility of the polymer chain, bulkiness of the side groups, polarity of the molecules, percent crystallinity of the sample, and presence of diluents affect the glass transition. Relaxation which occur faster than the glass transition - β, γ, etc. correspond to end group rotation, side-group motion, backbone chain rotation of small segments, etc [25].

The properties of polymeric material are different at different temperatures. The plastic material is rigid at lower temperatures, which softens on increasing the thermal energy to form a rubbery substance. On further increase in temperature, the sample melts at its characteristic melt temperature for crystalline polymers and the sample softens over a range of temperature for amorphous polymers. The rubbers, which are flexible at room temperature, when cooled below room temperature, form a rigid substance [26].

The temperature and frequency dependence of modulus of a polymeric material is demonstrated in Figure 2.19. The modulus of the polymer given in Figure 2.19(a) decreases with the increase in temperature. This decrease is more marked at the transition temperatures reflected by the peaks in tan δ curves. A sharp decrease in modulus of this polymer at glass transition temperature of 90° C shows that the polymer is highly crystalline. The duration of application of force on the polymer has an effect on the mechanical properties of the polymer. The effect of frequency on modulus of polymeric material is given in Figure 2.19(b). The modulus of the material, when measured over shorter time/high frequency, shows a higher value when compared to the longer times/shorter frequency. When time duration for the force is longer, the polymer chains have enough time to change configuration hence the measured values are lower. Whereas, when the time is shorter, the polymer chain does not have enough time to respond to the applied load. Hence it is more rigid at shorter times and higher frequency [26].

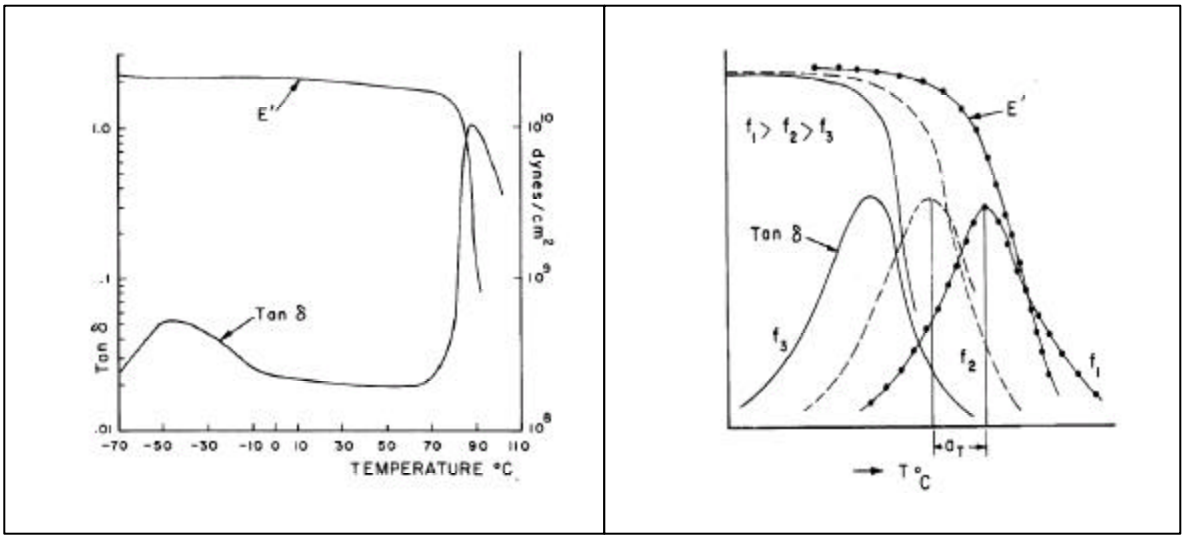

(a) (b)

Figure 2.19 Temperature (a) and frequency (b) dependence of a polymeric material [25].

2.4.3 Differential scanning calorimetry

The differential scanning calorimetry uses the difference in heat flow to a sample, when it is heated at a constant rate through a range of temperatures, to measure crystallinity. A small amount of sample is heated at a constant rate along with a standard. At the beginning a constant heat flows to both the pans that can be used as a reference line to monitor transitions. During transitions, the amount of heat flowing to the sample will increase or decrease depending on whether the transition is endothermic or exothermic. This difference in heat flow is monitored against temperature continuously [27].

From the plot of differential power of heat flow versus the temperature, the area under the curve representing the transitions is calculated. This area is directly proportional to the heat of fusion of the sample. Then the crystallinity can be calculated from the equation

Degree of crystallinity $\mathbf{Xc = \Delta Hf / \Delta Ho}$

Where ΔHf is the heat of fusion for the sample and ΔHo is the theoretical heat of fusion of the fully crystalline polymer.

2.4.4 Wide angle x-ray diffraction

The Wide angle X-ray diffraction works on the principle that the integrated area under the curves corresponding to the crystalline and amorphous regions in x-ray diffraction pattern of the polymer sample is directly proportional to the mass of the corresponding phase. The crystalline phase of the polymer has the basic ability to diffract x-rays under the conditions specified by Braag's law

$$\mathbf{n\lambda = 2 d_{hkl} \sin\theta}$$

where n is order of diffraction, λ is the wave length of incident x-rays, d_{hkl} is the interplanar spacing in the crystal and θ is the angle of diffraction[28].

A sample produces characteristic peaks at positions corresponding to the structures present in it, when scanned through the given range. These characteristic peaks and intensities are compared with the already established polymers to identify the reflections observed. A typical WAXD curve resolved for amorphous and crystalline peaks of nylon is given in Figure 2.20 [28]

The degree of crystallinity is calculated using the following formula

Degree of crystallinity $\mathbf{Xc = 1/(1+KR)}$

where K=1 and R is the ratio of amorphous and crystalline area counts.

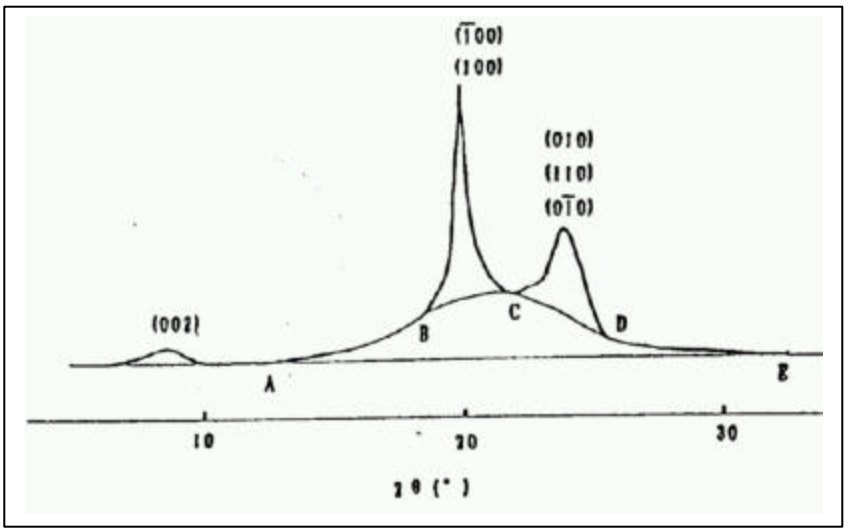

Figure 2.20 WAXD curve resolved for amorphous and crystalline peaks of Nylon [28]

unit cell axis with respect to a specific direction in the specimen. For polymeric fiber, it is usually the spinning direction of the fiber. This degree of preferred orientation will be higher if the fiber has more crystals aligned in the direction of the c-axis.

The second moment is a cosine-squared average of ϕ for the distribution of hkl poles about the fiber axis and is given by

$$< \cos^2 f_{hkl}, z > = \frac{\int_0^{2p} I(f) \sin f \cos^2 f \, df}{\int_0^{2p} I(f) \sin f \, df}$$

The orientation functions, the values generally used to represent the preferred orientation of fibers are functions of the second moments $<\cos^2\phi_{a,z}>$, $<\cos^2\phi_{b,z}>$ and $<\cos^2\phi_{c,z}>$.

$$f_{a,z} = \frac{3 < \cos^2 f_{a,z} > -1}{2}$$

$$f_{b,z} = \frac{3 < \cos^2 f_{b,z} > -1}{2}$$

$$f_{c,z} = \frac{3 < \cos^2 f_{c,z} > -1}{2}$$

2.4.5 Fourier transform infrared spectrophotometer

The Infra red spectroscopy is one of the techniques used to measure orientation of fibers. The FTIR works on the principle that "When the frequency of incident infrared radiation is the same as the frequency of vibration of grouping of atoms in a molecule and there is a change in dipole moment during that vibration, all or part of the incident infrared radiation will be absorbed by resonance"[29].

The interferometer controls the intensity of the infrared rays to the sample. It basically has two mirrors, one fixed and one movable, with a beam splitter. The IR rays when passed through beam splitter is reflected and transmitted to fixed and movable mirror. The two beams reflected from these mirrors recombine to form the required beam based on the position of the movable mirror.

Then the beam is passed through the sample where the rays corresponding to the characteristic vibrations of the sample are absorbed. A detector senses the missing frequencies in the beam and signals are sent to computer for Fourier transform calculations. The resulting spectrum is displayed in screen for interpretation [29].

Chapter 3

Experimental

3.1 Materials

Dupont Textiles & Interiors and Scientific Polymer Products Inc. supplied the polymers used in this project. The solvents used were obtained from Acros Organic and Fisher Scientific. The salts used to increase the conductivity of tetrahydrofuran were obtained from Acros Organic, Mallinckrodt Analytical Reagent and Fisher Scientific. The following polymers and solvents were used in this project.

a. Nylon 6/6 (Mn: 12,600 g/mol, Mw: 36,150 g/mol) from Dupont in solution of formic acid 99% from Acros Organic.
b. Nylon 6 from Dupont in solution of formic acid 99% from Acros Organic.
c. Nylon 6(3)T – Poly(trimethyl hexamethylene terephthalamide) from Scientific Polymer Products Inc in solution of formic acid 99% from Acros Organic.
d. Poly(ethylene terepthalate) (Crystar) from Dupont in solution of triflouroaceticacid 99% from Acros Organic.
e. Polycarbonate – Poly(bisphenol-A carbonate) from Scientific Polymer Products Inc. (Mw: 60,000 g/mol) in solutions of toluene and chloroform from Fisher Scientific.
f. Polystyrene from Scientific Polymer Products Inc. (Mw: 280,000 g/mol) in solutions of toluene, chloroform and tetrahydrofuran from Fisher Scientific.
g. Poly(methyl methacrylate) from Scientific Polymer Products Inc. (Mw: 75,000 g/mol) in solution of tetrahydrofuran from Fisher Scientific.
h. Poly(vinyl chloride) from Scientific Polymer Products Inc. (Mw: 215,000 g/mol) in solution of tetrahydrofuran from Fisher Scientific.
i. Polycaprolactone from Scientific Polymer Products Inc. (Mw: 120,000 g/mol) in solution of formic acid 99% from Acros Organic.
j. Lithium perchlorate from Acros Organic (Mw: 106.39).
k. Sodium chloride from Fischer Scientific (Mw: 58.44)

l. Potassium chloride from Mallinckrodt Analytical Reagent (Mw 74.55)

m. Potassium iodide from Fischer Scientific (Mw: 166.01)

3.2 Electrospinning process

The electrospinning process is used to produce the nano-sized fibers. A 10 cm^3 reusable syringe from Fisher Scientific is used for spinning the fiber through a capillary with 0.42 mm diameter. A 30 kV, 20 W DC power supply from Gamma High Voltage Research, Inc. is used to maintain high voltage difference between the capillary and a stationary copper target or a 25 cm diameter, 6.35 mm thick stainless steel rotating disc. A Harvard apparatus syringe pump from Fisher Scientific is used to feed the solution to capillary tip continuously. The polymers used for electrospinning are nylon 6, nylon 66, poly(ethylene terepthalate), polystyrene, polycarbonate, poly(methyl methacrylate), poly(vinyl chloride), poly(caprolactone) and poly(trimethyl hexamethylene terepthalamide) in different solvents. The solutions are prepared by stirring the required weight percent of each polymer in given solvent for 3 to 4 hours till it is completely dissolved. The polymers nylon 6, nylon 66, poly(ethylene terepthalate) produced very fine fibers without any difficulty. Hence these polymers were used to study the process – structure – property relationship. The solutions of 5 to 20% concentration by weight were prepared from nylon 6, nylon 66 and their blends from Dupont Textiles & Interiors in formic acid from Fisher Scientific and poly(ethylene terepthalate) in triflouro acetic acid by stirring the required weight percent of polymers in solvents till it is completely dissolved.

The copper metal sheet or a rotating disc 25 cm in diameter and 6.35 mm thick with a tapered edge machined to an angle of 64° are used as a stationary and rotating target respectively grounded to a water tap. The rotating disc is connected to a variable frequency motor with operating range of 5 Hz to 60 Hz which corresponds to a speed range of 233 to 2833 m/min at the edge of the disc. The ease with which nylon 66 spins urged us to use this polymer for all the process – structure – property relationship studies by varying process conditions. A constant velocity is applied to the syringe to produce a flow rate of 10 μliters/min, which forms a droplet at the tip of the capillary. The voltage

is varied between 5 to 25 kV to initiate the formation of jet. The fibers formed are collected at the copper target/rotating disc for 8 - 24 hours. The experiment is repeated with solution concentration as 5, 10 and 20 wt%, the distance of copper target as 5, 10 and 20 cm from the capillary and voltage of 5 to 25 kV. The same procedure is repeated for different composition of the nylon 6/66 and for PET using trifluoro acetic acid solution. Figures 3.1 (a) & 3.1 (b) show the experimental setup of the electrospinning process.

The nonwoven fibers produced by electrospinning process is aligned in a single direction to improve the orientation, crystallinity and mechanical properties. The fibers were oriented by either collecting them in a rotating wheel or by annealing under constant stress. The speed of rotating wheel was varied from 233 m/min to 2833 m/min to achieve different levels of orientation and crystallnity. The nonwoven fibers spun were also annealed at 95º C under different constant stress levels for 1 hour. The tensile clamp of the dynamic mechanical analyzer DMTA V was used to grip the bundle of nano sized fibers. Different constant loads were attached to these grips to induce stresses on the samples ranging from 0.5 to 7 MPa. These annealed and wound samples were tested for orientation, crystallinity and mechanical properties using the characterization techniques discussed in this chapter.

3.3 Characterization techniques

3.3.1 Scanning electron microscopy

The fibers spun from various polymer systems at different process conditions were analyzed with the Leo 1525 scanning electron microscope shown in Figure 3.2 to determine the morphology and dimensions of the fibers formed. A minimum emission voltage is varied between 1 - 5 KV depending on amount of charge accumulation in the sample. Any metallic coating of the fibers was avoided so that the actual dimensions of the fibers are not affected. The sample was placed on a carbon tape and transferred to a sample stool.

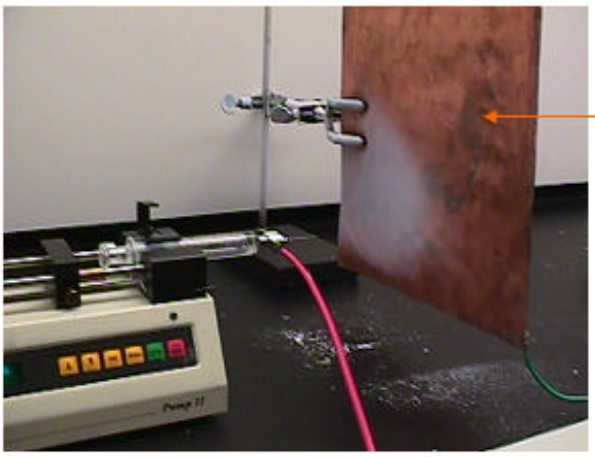

(a)

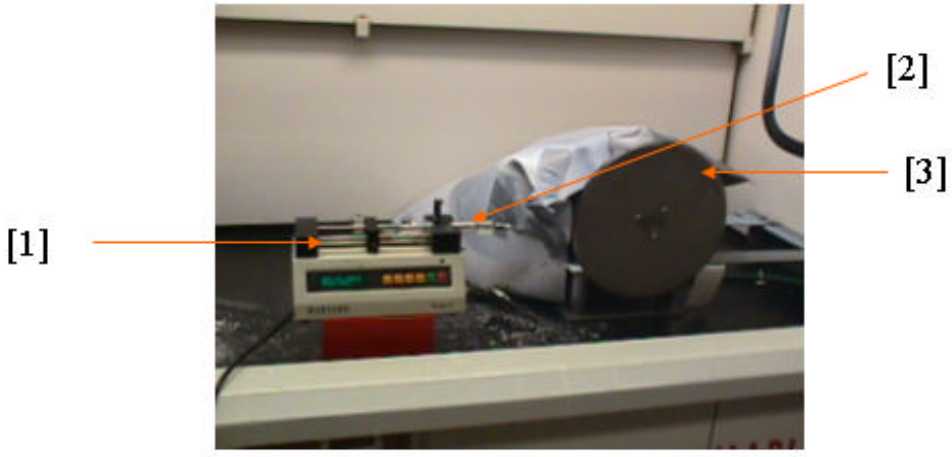

(b)

Figure 3.1 Electrospinning process setup with copper target (a) and rotating disc(b) [1] Displacement pump, [2] Syringe, [3] Rotating Wheel, [4] Copper target.

Figure 3.2 Scanning Electron Microscope Leo 1525

A number of these sample stools are placed on a sample holder before loading on a vacuum chamber. The vacuum is then lowered to 1.5 x 10^{-5} Torr before the voltage is turned on. The sample image is then captured by aligning and focusing the image to required magnification. This image obtained is then saved as a TIFF file.

3.3.2 Dynamic mechanical analysis

The rheometrics DMTAV dynamic mechanical analyzer given in Figure 3.3 was used for the test. Bundles of different polymer fiber samples are tested from a temperature of –150 to +200° C at frequencies 0.1, 1, 10 Hz at the rate of 2 degrees per minute using the tensile clamp. The liquid nitrogen gas is used to cool the sample below the room temperature. The static force applied to the sample, is always maintained at 10 % more than the dynamic force so that the sample is always in tension. The cross sectional areas of the polymer fiber bundles are calculated using the density of the polymer, mass of the sample and the length.

Cross sectional area A = m/(r xl)

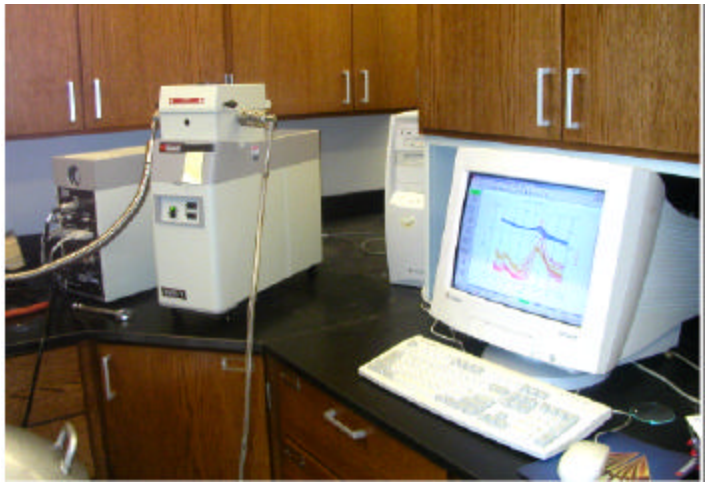

Figure 3.3 Dynamic Mechanical Analyzer Rheometrics DMTA V

Where m is the mass of the sample in grams, ρ is density in grams/ cubic millimeter and l is length in millimeter.

The tensile strength and modulus of bundle of nano fibers are determined by testing the samples in dynamic mechanical analyzer parallel to winding direction in strain rate test mode at a constant strain rate of 1.5 %/second until the sample failed.

3.3.3 Differential scanning calorimetry

TA instruments DSC 2590 differential scanning calorimeter given in Figure 3.4 is used to measure crystallinity of annealed as well as wound nylon 66 samples. The sample is placed in standard aluminum pan, weighed accurately and placed in the DSC chamber. The calibration is done using indium standard with melting temperature of 156.61° C. The base line correction is made by scanning the sample through required temperature range without polymer sample. The flow rate of nitrogen is maintained at 20 cc/min and a scan range of -50 to +300° C was chosen at the rate of 5° C/min. The degree of

Figure 3.4 Differential Scanning Calorimeter TA instruments 2590

crystallinity is automatically calculated, by selecting the required curve peak, using the thermal analyzer software by entering the ΔHo value of 200 J/g for the fully crystalline nylon 66 polymer using the above-mentioned formula[30].

From the plot of differential power of heat flow versus the temperature, the area under the curve representing the transitions is calculated. This area is directly proportional to the heat of fusion of the sample. Then the crystallinity can be calculated from the equation

$$\text{Degree of crystallinity } \mathbf{Xc} = \Delta\mathbf{Hf}/\Delta\mathbf{Ho}$$

Where ΔHf is the heat of fusion for the sample and ΔHo is the theoretical heat of fusion of the fully crystalline polymer.

3.3.4 Wide angle x-ray diffractometer

The polymer fiber samples are tested for crystallinity in Philips' x'pert x-ray diffractometer shown in Figure 3.5 with a proportional counter and CuKα radiation for 2θ range of 10 to 40 degrees at 45 kV and 40 mA with step size of 0.03 degree and dwell time of 0.5 seconds. The percent crystallinity developed in fibers at different loads, are calculated by measuring the area under the crystalline and amorphous peaks of WAXD.

The degree of preferred orientation is expressed as a second order moment of a specific unit cell axis with respect to a specific direction in the specimen. For polymeric fiber, it is usually the spinning direction of the fiber. This degree of preferred orientation will be higher if the fiber has more crystals aligned in the direction of the fiber axis.

The second moment is a cosine-squared average of ϕ for the distribution of hkl poles about the fiber axis and is given by

$$< \cos^2 f_{hkl}, z > = \frac{\int_0^{2p} I(f) \sin f \cos^2 f \, df}{\int_0^{2p} I(f) \sin f \, df}$$

The orientation functions, the values generally used to represent the preferred orientation of fibers are functions of the second moments $<\cos^2\phi_{a,z}>$, $<\cos^2\phi_{b,z}>$ and $<\cos^2\phi_{c,z}>$.

$$f_{a,z} = \frac{3 < \cos^2 f_{a,z} > -1}{2}$$

$$f_{b,z} = \frac{3 < \cos^2 f_{b,z} > -1}{2}$$

$$f_{c,z} = \frac{3 < \cos^2 f_{c,z} > -1}{2}$$

Figure 3.5 Philips x'pert X-ray diffractometer

3.3.5 Fourier Transform Infrared Spectroscopy (FTIR)

A Biorad FTS6000 shown in Figure 3.6 was used for the experiment. The mid IR range has been used as source with mid IR deuterated tri-glycine sulfate(DTGS) as detector and potassium bromide as beam splitting crystal. The initial settings of the spectrometer were as follows:

a. Speed – 5 KHz
b. Filter – 1.2
c. Resolution – 4
d. Sensitivity – 1
e. Scans to co-add – 256
f. IR range – 400-4000 cm-1

As the sensitivity was lower, it has been increased in steps to 4. The scanning was carried out without the sample for the background information. The scanning was

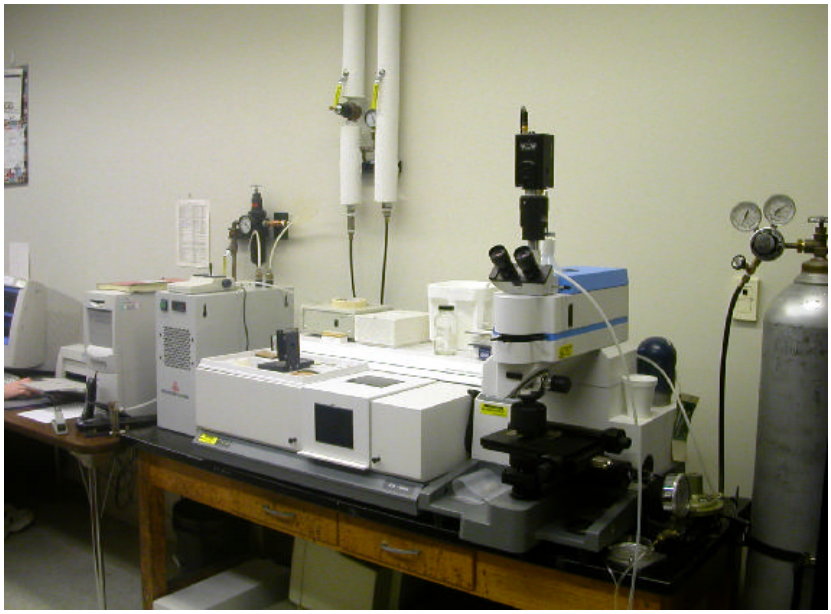

Figure 3.6 Fourier transform infrared spectrometer Bio Rad FTS 6000

repeated with the nylon 66 and PET fiber samples to get the characteristic peaks. The absorbance of the infrared rays in the characteristic bands of NH stretching at 3300 and CH in benzene ring stretching at 730 are noted for nylon66 and PET respectively.

Dichroism was determined with the use of polarizing filter. If $\mathbf{A}_{||}$ is the measured absorbance when the polarization direction is parallel to alignment of fibers and $\mathbf{A}_{\perp}$ in normal direction to alignment of fibers then the dichroism D, is defined by the following formula.

$$\mathbf{D = A_{||} / A_{\perp}}$$

The orientation function f, for each sample produced by annealing with different loads are calculated from the dichroism given by

$$f = \frac{C\,(D-1)}{(D+2)}$$

Where

$$C = \frac{(2\cot^2 b + 2)}{(2\cot^2 b - 1)}$$

Where **ß** is the angle the group, whose characteristic band is considered, makes with the polymer backbone [31]. The bond angle for both CH and NH groups considered is 90º. Hence the equation for the orientation function reduces to

$$f = \frac{-2\,(D-1)}{(D+2)}$$

3.3.6 Conductivity measurement

A study has been made on methods of improving the conductivity of polymer solutions by additions of salts like lithium perchlorate, sodium chloride, potassium chloride and potassium iodide. The conductivity of the solutions was measured using a conductivity-resistivity meter.

The conductivity or specific conductance (K) is related to the resistance (R in ohms) of a liquid sample and the cell constant (C in cm^{-1}) of the conductivity meter.

$$\mathbf{K = C/R}$$

The cell constant is equal to the distance between the parallel electrodes (L) in cm divided by the cross-sectional area of the electrodes (A), in cm^2 all multiplied by the efficiency, C.

$$\mathbf{C = L/A}$$

A YSI model 34 with a standard dip type cell with constant of 10 S/cm is used to measure the conductivity of the solutions of THF with different concentration of salts - lithium per chlorate, sodium chloride, potassium chloride and potassium iodide.

3.3.7 Image analysis

The orientation of fibers relative to a given reference axis can be determined by the analyzing the Fourier transformed image of fiber pictures obtained by the SEM. The orientation function in the direction of preferred orientation is determined with the help of the SEM images of fibers collected in rotating disc at different speeds. The SEM picture obtained as a ".tif" image of size 512 x 512 pixels is converted to a Fourier transformed image using the Scion Image software. This Fourier transformed image gives output as a 512x512 matrix with each value representing intensity at each pixel of the image. The average intensity at each orientation angle and the second moment is calculated using the formula given below with the help of a Fortran 77 program.

$$< \cos^2 f > = \frac{\int_0^{2p} I(f) \cos^2 f \, df}{\int_0^{2p} I(f) \, df}$$

where I(F) is the integrated intensity of the pixels along the radial direction for each F given by the following equation

$$I(f) = \int_0^R I(f, r) \, dr$$

A radius of R = 64 pixels was chosen and r = 0 corresponds to the center of image.

Then the orientation function for preferred orientation along the c-axis is calculated using the formula

$$f = 2 < \cos^2 f > -1$$

3.3.8 Manual measurement of orientation of fibers

The directions of orientation of fibers collected at different speeds in rotating disc are measured manually using a protractor. These distribution functions plotted versus the direction of fiber angle are used to find the orientation factor. The direction of spinning

is taken as $\phi = 0$. The orientation factor measured for each speed of collection of fibers, is calculated using the formula

$$f = 2 < \cos^2 f > -1$$

where $\cos^2\phi$ is calculated from the formula

$$< \cos^2 f > = \frac{\int_0^{2p} N(f) \cos^2 f \, df}{\int_0^{2p} N(f) \, df}$$

and $N(\phi)$ is the number of fibers oriented in the direction ϕ.

Chapter 4

Results and Discussion

4.1. Polymer systems

The polymer systems listed in the Table 4.1. were used to study the structure – property – process relationship of the fibers produced by the electrospinning process. A nominal test condition of 10 wt% solution concentration, 10 cm target distance and 10 kV potential difference is used for studying the process. The size of fibers produced varied from tens of nanometers to as large as few microns depending on the viscosity, solution concentration and polarity of polymer/solvent. A few of the polymer systems did not produce fibers when electrospun due to difference in molecular weight, viscosity, surface tension and polarity of polymer/solvent. The clarity of the solution was checked inside the syringe and at the tip of the capillary to assure the miscibility of the system. The solutions that were cloudy either in the bulk solution or at the tip of capillary are phase separated, and hence were not spun.

Table 4.1. The polymer systems used to study the structure – property – process relationship of the fibers produced by the electrospinning.

Polymer (10 wt%) + Solvent	Bulk Solution	Solution at Capillary Tip	Comments
nylon 6 in formic acid	clear	clear	~50 nm size fibers formed
nylon 66 in formic acid	clear	clear	~50 nm size fibers formed
PET in triflouroacetic acid	clear	clear	~150 nm size fibers formed
PS in toluene/chloroform	clear	clear	~2 μm size fibers formed
PMMA in THF	clear	clear	powder only

4.2. Effect of process variables

Earlier studies on electrospinning process show that the amount of fibers produced depends on the amount of polymer present in the solution, the voltage applied and the distance of the target from the syringe [2,14]. The fibers are produced by electrospinning process only if the applied voltage is above the given limiting value. This voltage is required to overcome the surface tension of the solution.

4.2.1. Effect of solution concentration

The size and structure of the fibers produced was studied by varying the concentration of the solution. The solution concentration determines the viscosity and surface tension of the droplet formed at the tip of the capillary. The solutions with lower concentrations have lower polymer content. Therefore the surface tension of the droplet should dominate over the formation of fibers. The size of the cone formed at the tip of the capillary will be smaller, which results in smaller diameter fiber. Processing of the polymeric material becomes more difficult when the viscosity of the polymer solution increases. Also, if the surface tension of the polymer-solvent system is lower, more non-woven fabric like structure will be produced. The surface tension of the system depends on the exact solvent and polymer used. The variation in the concentration of the solution gives a range of diameters for each concentration as shown in Figure 4.1. The plot of logarithmic diameter against concentration of fibers produced given in Figure 4.1 shows increase in size of the fiber with the increase in the concentration of the solution. The solution concentration of 5, 10 and 20% of nylon 66 in formic acid produced fibers with diameters in the range 15 – 30 nm, 40 – 60nm and 180 – 680 nm respectively. Our results also follow the power law relationship observed by Deitzel[2] with the exponential value of 2.11 and R^2 value of 0.93. If d is the average diameter of fibers in nm and c is the solution concentration in weight %, then

$$\mathbf{d = c^{2.11}}$$

The fibers formed at higher concentration also have uniform cross section due to larger size of the tip of the cone formed resulting from lower surface tension. The picture of nylon 66 produced by varying the solution concentration is given in Figures 4.2.

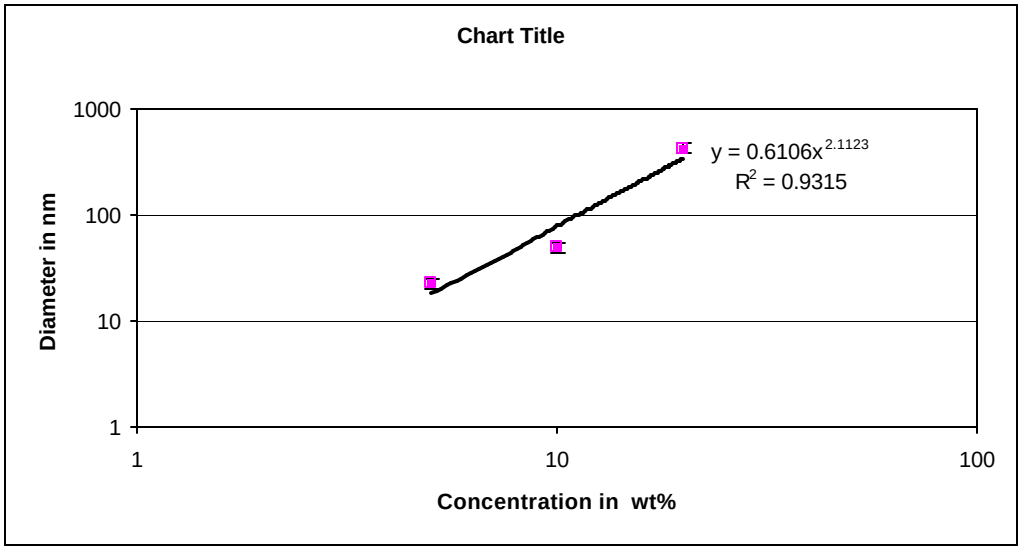

Figure 4.1 Effect of solution concentration on nylon 66 average fiber diameter at 10 cm target distance and 10 kV voltage. The error bars, insignificant in the plot due to small range, denote the maximum and minimum values.

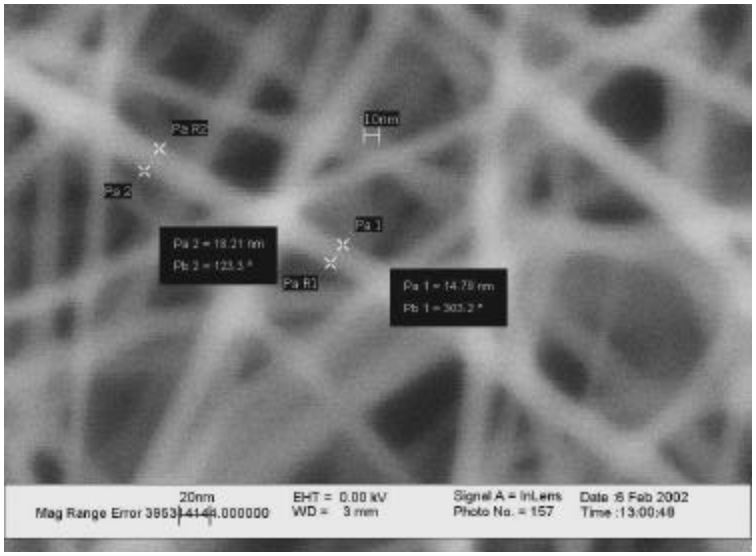

(a)

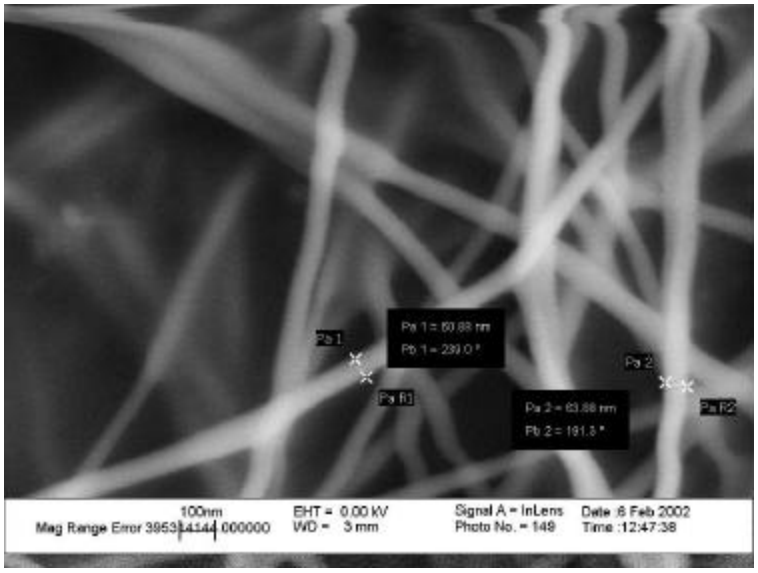

(b)

Figure 4.2 Nylon 66 spun at 10 cm target distance and 10 kV voltage at solution concentration (a) 5% (b) 10% and (c) 20%

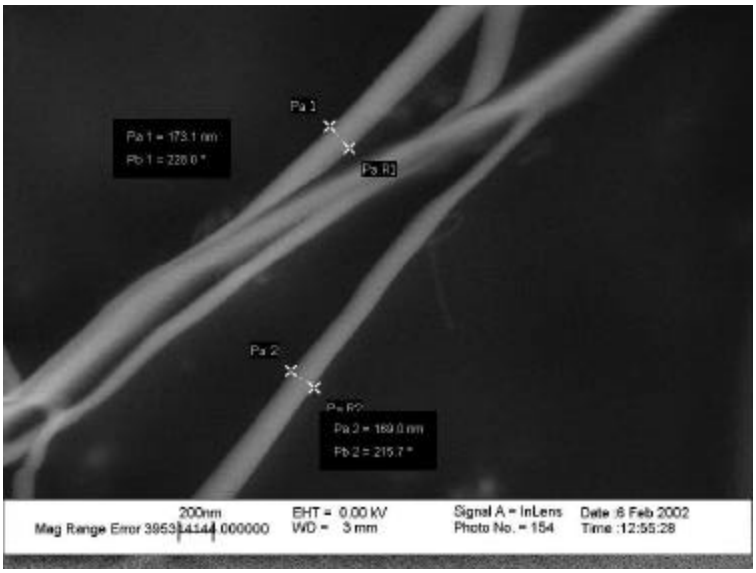

(c)

Figure 4.2 continued

4.2.2. Effect of applied voltage

The voltage applied between the capillary and the metal target can be used to control the amount of polymer reaching the target. The number of droplets or fibers reaching the target is a function of the current flowing across the circuit. The current flowing and hence the amount of fiber spun can be easily controlled by varying the voltage. At low voltage, the size of the droplet formed at the end of capillary is large as the voltage is not high enough to transfer all of the solution to the target. The diameter of fiber spun from this droplet will be larger. When the voltage is increased, the diameter of the droplet will be less and hence the diameter of the tip of cone formed is also smaller resulting in smaller fibers [2]. When voltage is increased, the amount of fiber formed increases. A study on fiber size of nylon 66 fibers formed by varying the voltage shows a decrease in diameter for voltage above 10 kV as shown in Figure 4.3.

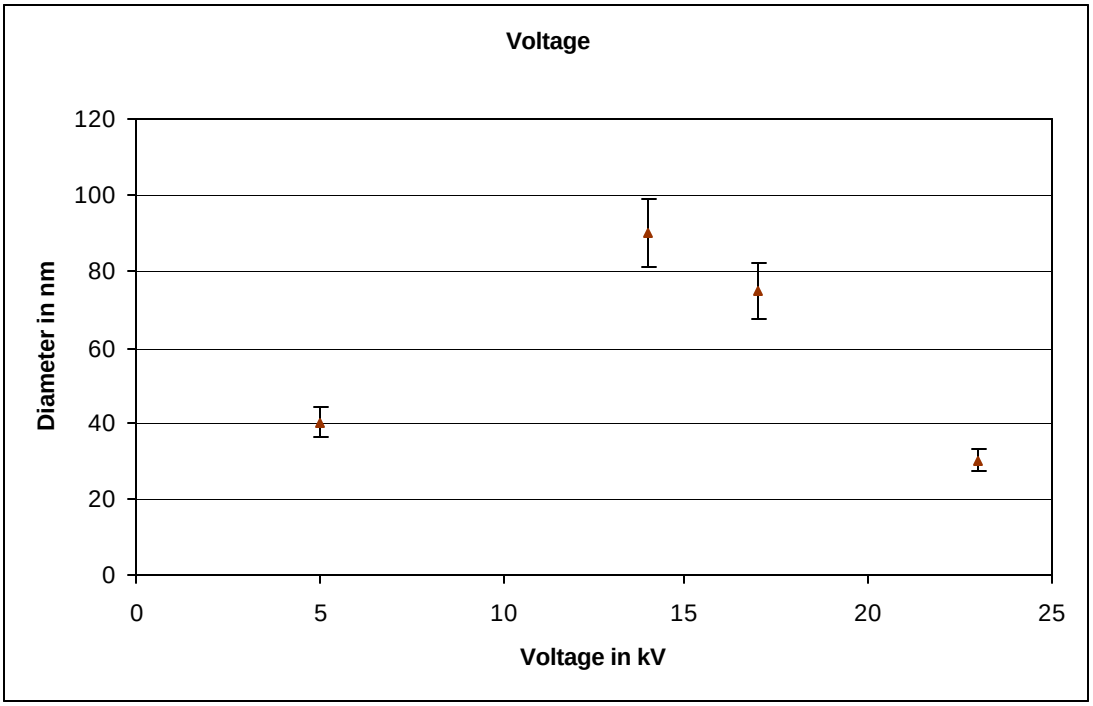

Figure 4.3 Effect of variation in voltage applied on nylon 66 average fiber diameter at 10 cm target distance and 10 wt% concentration. The error bars denote the maximum and minimum values.

The amount of nylon 66 fibers produced at nominal test conditions of 10 wt% solution concentration, 10 cm target distance is measured by varying the voltage applied. The mass throughput is plotted against the applied voltage shows an increasing trend in figure 4.4. The throughput of fibers increases with the increase in the voltage. A drastic increase in output of fibers is noticed around 15 kV voltage. This could be critical voltage that produces enough current to overcome the surface tension of the droplets formed at the tip of the cone. There is also a possibility of increasing the output of fibers by increasing the concentration of solution.

4.2.3. Effect of target distance

The polymer fibers collected at longer target distance have a possibility of formation of more uniform structure due to complete evaporation of the solvents. The fibers collected at shorter distance are expected to have non uniform structure due to presence of more solvent in them. The sizes of the fiber produced at different target distance were measured. The increase in the target distance does not seem affect the diameter of the nylon 66 fibers. Figure 4.5 shows the diameter of nylon 66 fibers spun measured as a function of target distance. The picture of nylon 66 fibers produced by varying the target distance is given in Figure 4.6. The diameter of fibers collected at each target distance varied typically between 50 – 80 nm though few fibers were noticed with diameters outside this range as shown in Figure 4.6c.

4.3. Winding of fibers

Previous researchers have tried to increase the crystallinity and hence the mechanical properties of the electrospun nano-fibers by aligning them in a rotating wheel in place of stationary target [18]. A similar attempt has been made here by aligning nylon 66 fibers electrospun at nominal test conditions of 10 wt% concentration, 10 cm target distance, and 15 kV voltage on a 25 cm rotating metal disc at a fixed constant speeds ranging from 233 m/min to 2833 m/min. The scanning electron microscopic pictures of these fibers are shown in Figure 4.7.

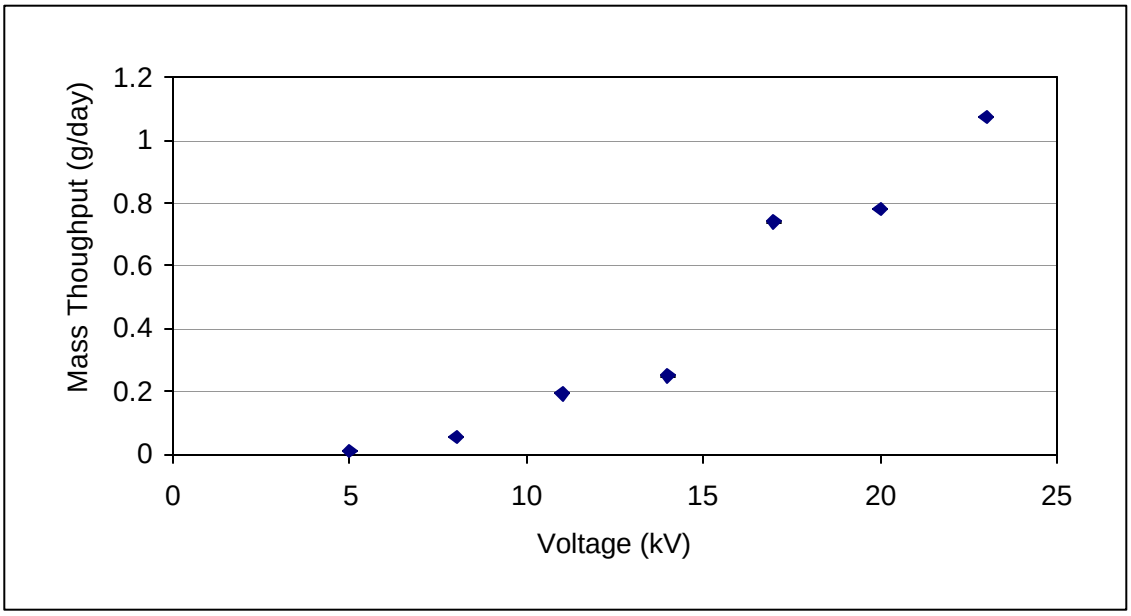

Figure 4.4 Effect of voltage on amount of nylon 66 fibers produced with 10 cm target distance and 10 wt% concentration. The measurement had an insignificant error value of 0.001g/day and hence not visible in the plot.

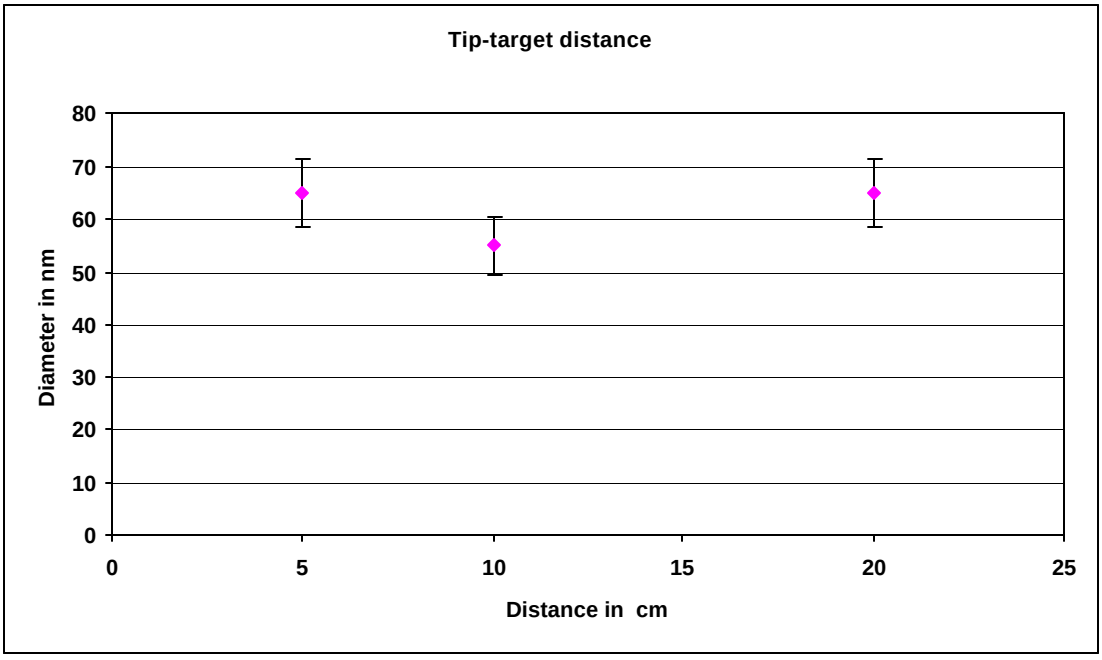

Figure 4.5 Effect of variation in target distance on nylon 66 fiber diameter at 10 kV voltage and 10 wt% concentration.

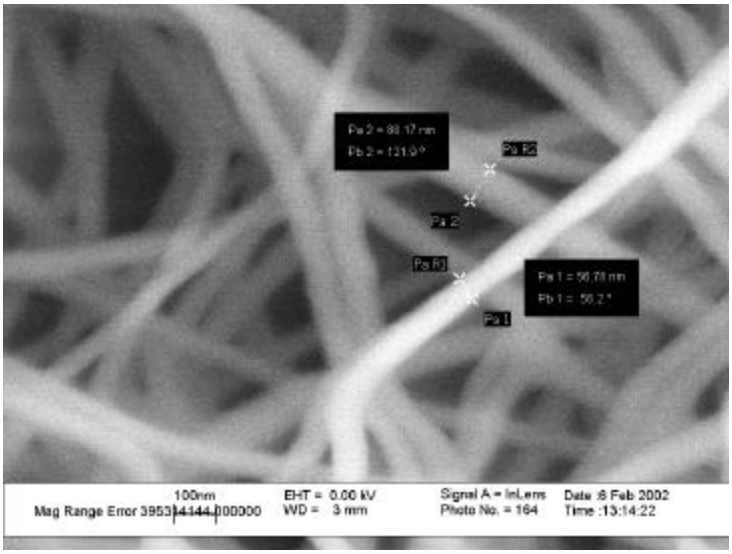

(a)

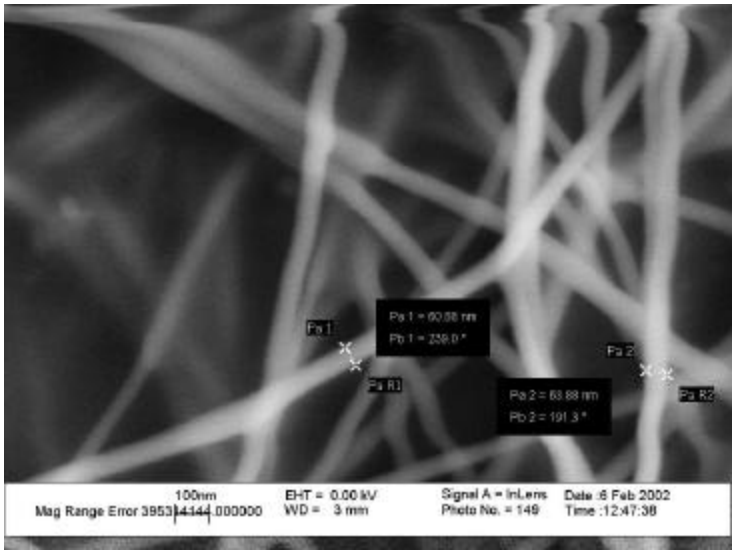

(b)

Figure 4.6 Nylon 66 spun at 10% solution concentration and 10 kV voltage with target distance (a) 5 cm, (b) 10cm and (c) 20cm

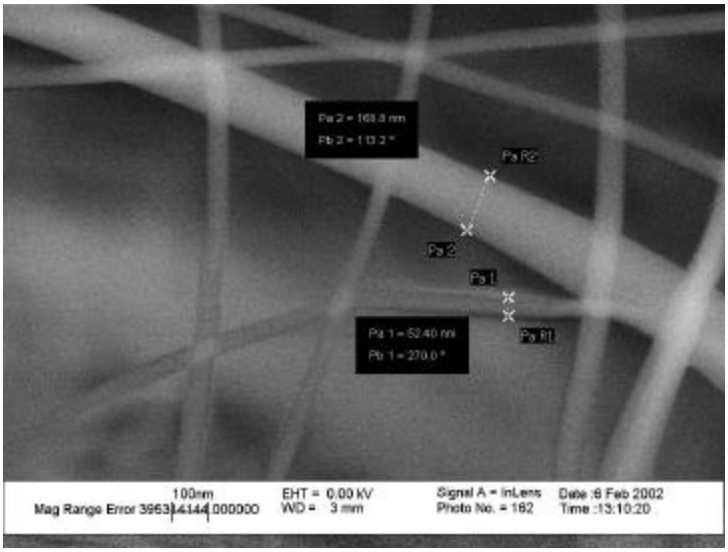

Figure 4.6 continued

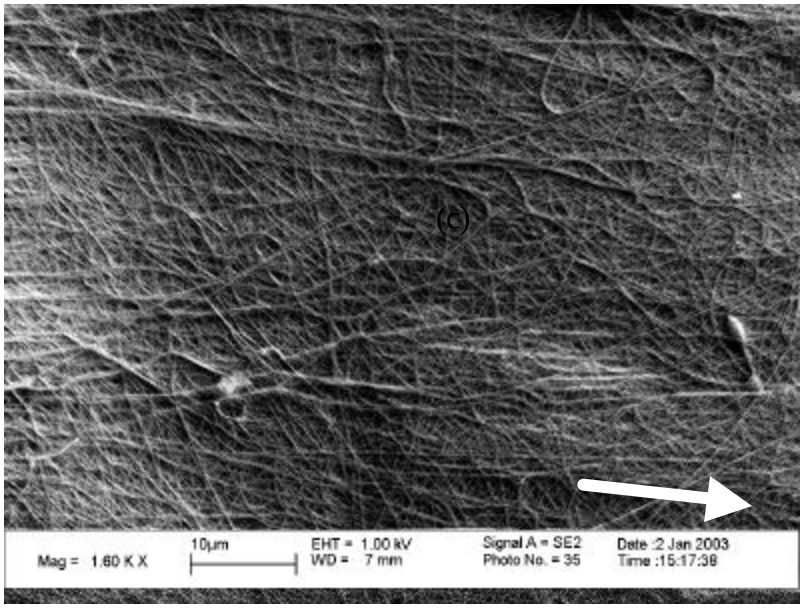

(a)

Figure 4.7 Nylon 66 fibers wound collected at 10 wt% concentration, 10 cm target distance, and 15 kV voltage at a speed of (a) 233 m/min, (b) 465 m/min, (c) 926 m/min, (d) 1868 m/min and (e) 2833m/min

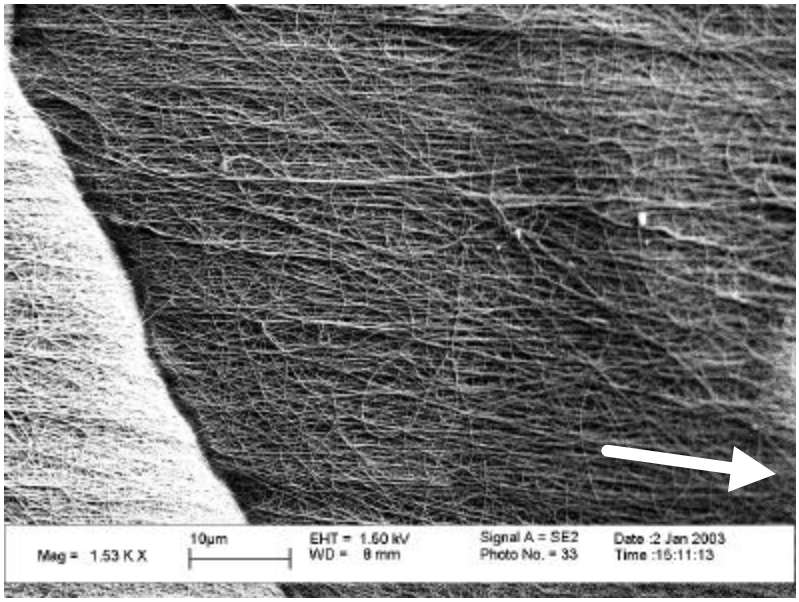

(b)

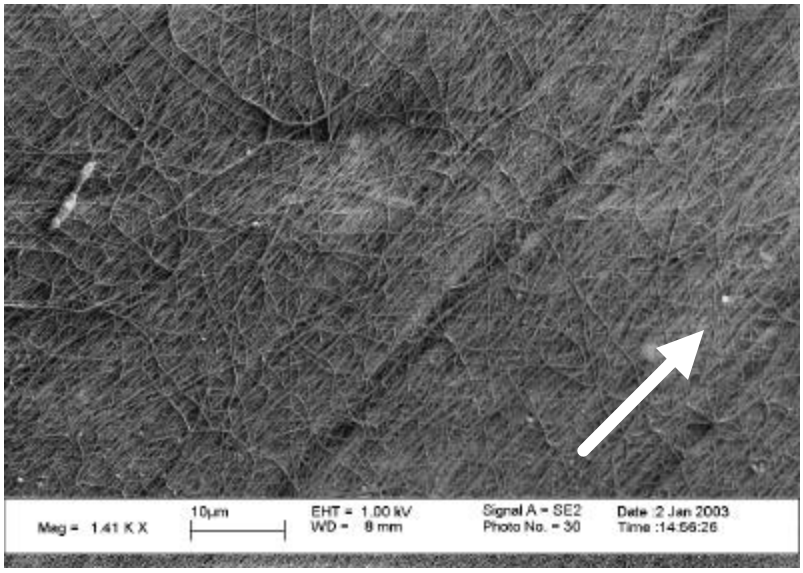

(c)

Figure 4.7 continued

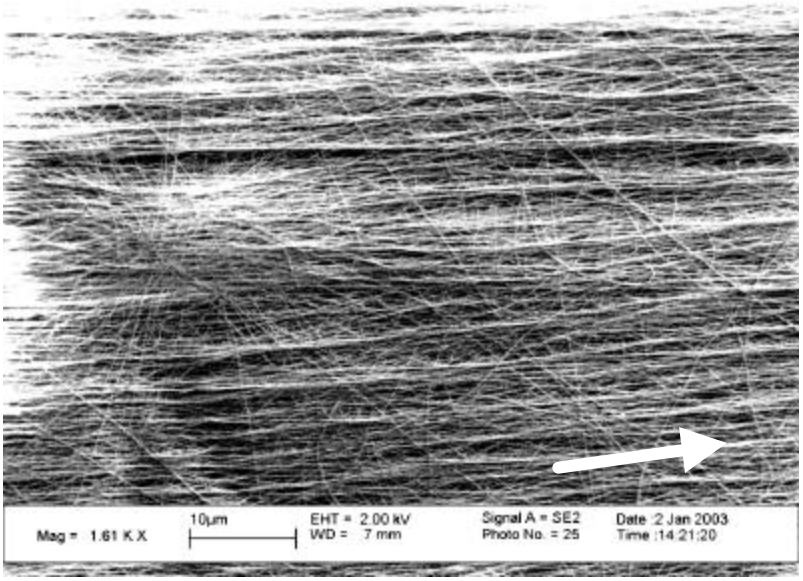

(d)

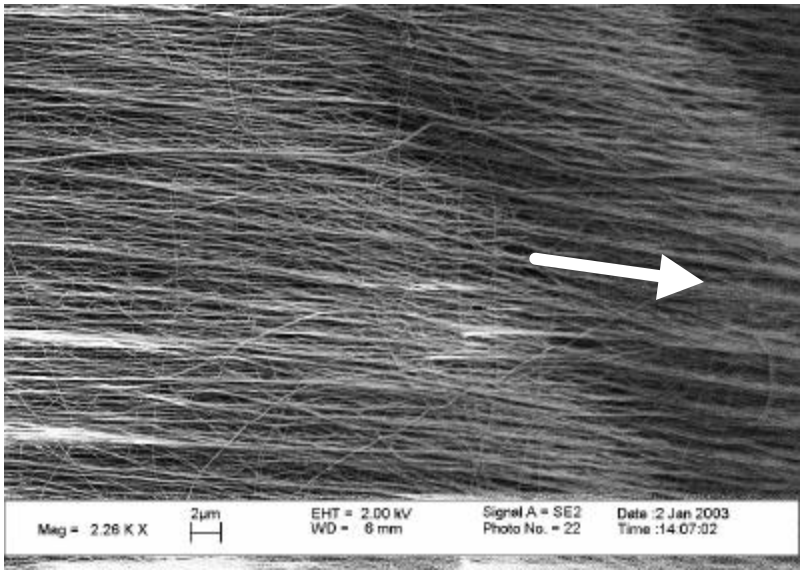

(e)

Figure 4.7 continued

4.3.1. Orientation of wound fibers

The SEM pictures given in Figure 4.7 clearly show an increase in orientation of fibers in the direction of rotation of wheel. The orientations of fibers are quantified by a factor called orientation factor, the value of which gives the degree of fiber orientation. The orientation factor for the fibers is calculated by the following 2 methods.

a. ***Manual measurement*** of orientation of fibers.

b. Measurement of orientation using fourier transform obtained by an ***Image analysis*** software and measurement of orientation using a computer program.

The molecular orientation of the fibers is measured by the Fourier transform infra red spectroscopy and the crystalline orientation was determined by the psi scan in x-ray diffractometer.

The orientation factor calculated for the samples collected at 15 kV, with tip to target distance of 10 cm and solution concentration 10 wt % from all four methods is shown in Figure 4.8a. This shows a definite increase in orientation of fibers with increase in speed of the rotating wheel. The fiber orientation increases from a random orientation to orientation along the fiber axes.

4.3.1.1.Manual measurement of orientation of fibers

The directions of orientation of fibers in Figure 4.7 are measured manually using a protractor. The distribution of fibers spun at different speeds is given in Figure 4.9. These distribution functions are used to find the orientation factor shown in Figure 4.8a as manual technique. The Figure 4.10 shows the angular distributions with $\phi = 0$ corresponding to the winding direction. The orientation factor given in legend of Figure 4.10 is found to increase with the increase in speed of collection of fibers.

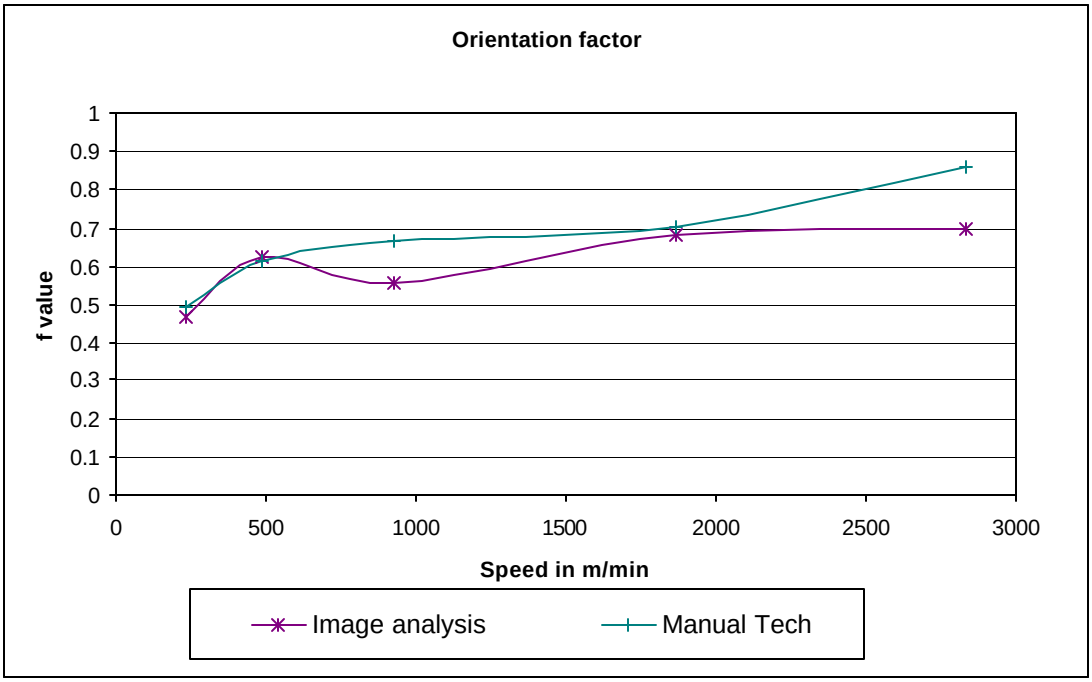

(a)

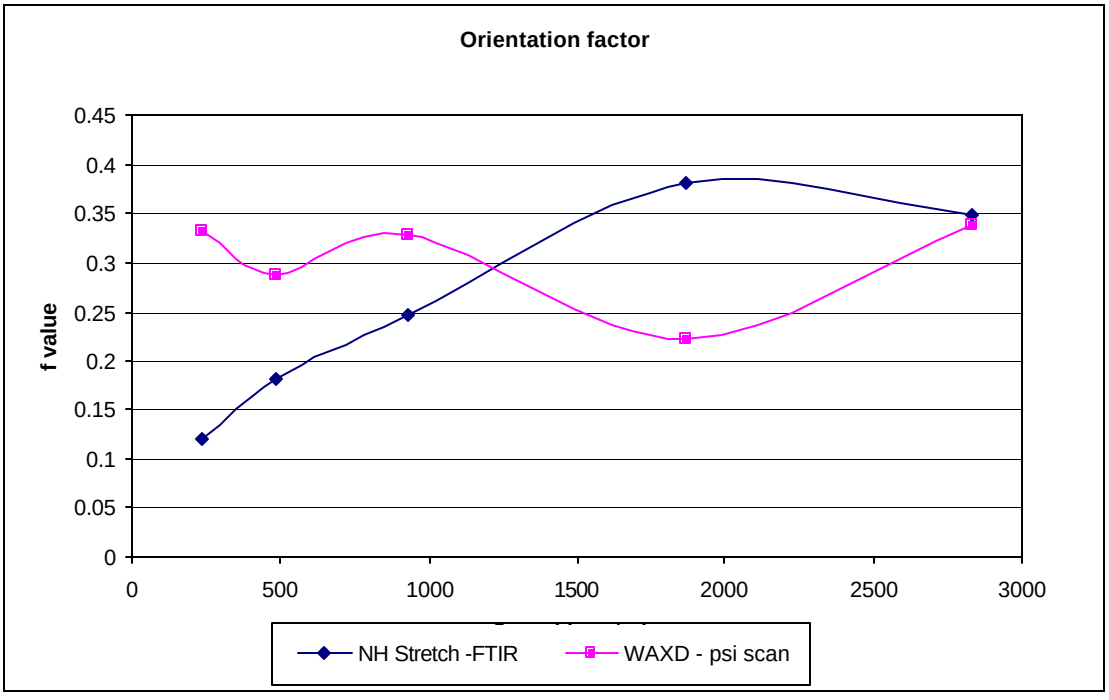

(b)

Figure 4.8 Orientation factors for nylon 66 fibers measured by various methods corresponding to (a) orientation of fibers (b) molecular orientation

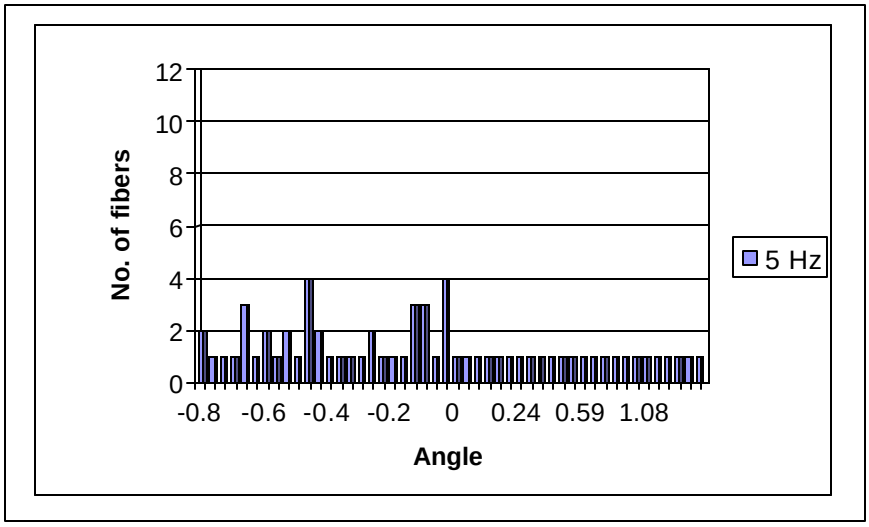

(a)

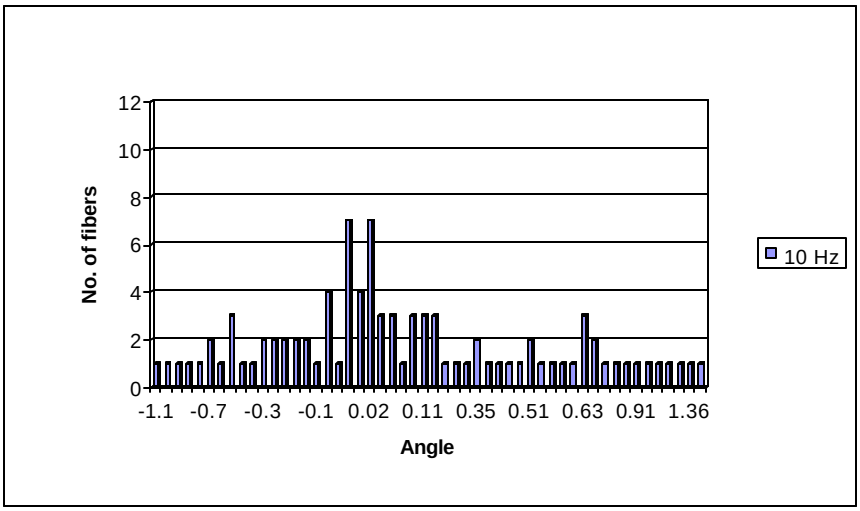

(b)

Figure 4.9 Orientation of fibers spun at 10 wt% concentration, 10 cm target distance, and 15 kV voltage at speeds (a) 233 m/min (b) 465 m/min, (c) 926 m/min, (d) 1868 m/min and (e) 2833m/min

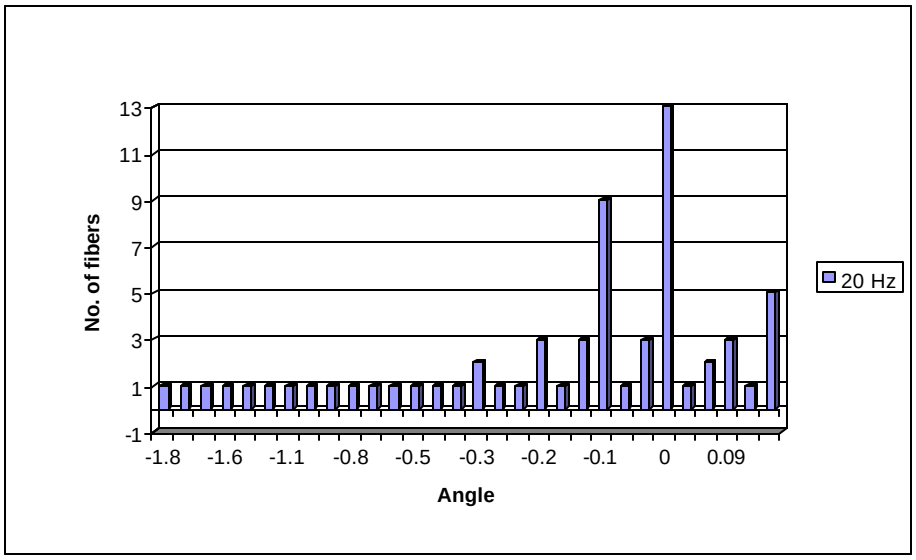

(c)

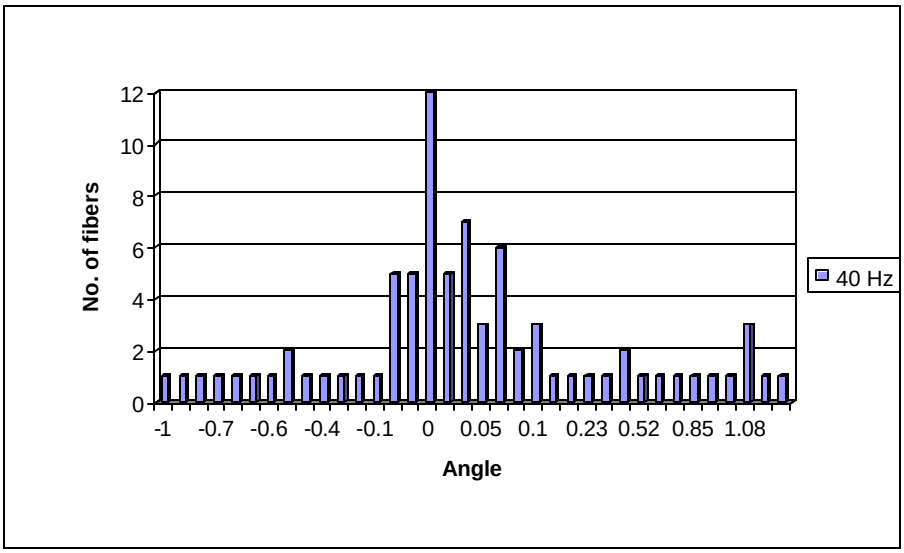

(d)

Figure 4.9 continued

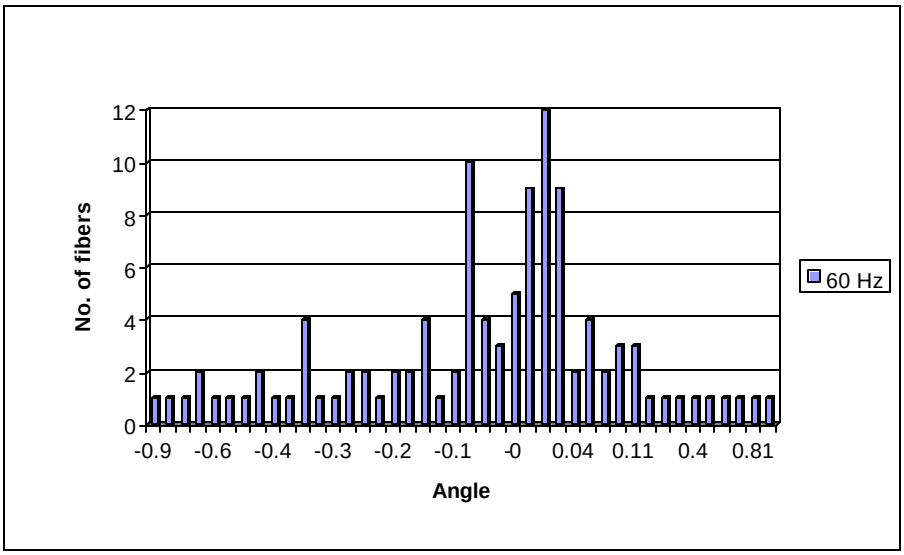

(e)

Figure 4.9 continued

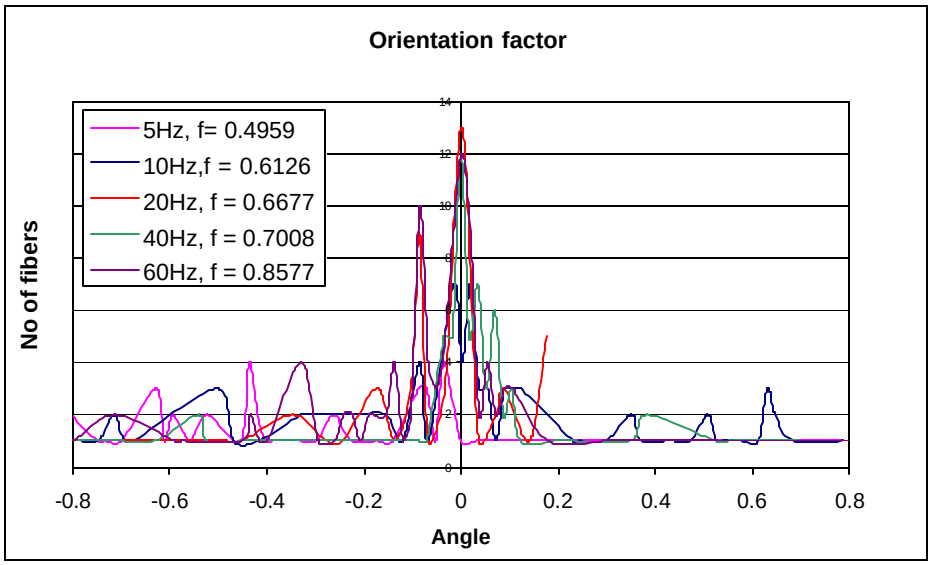

Figure 4.10 Orientation of fibers by making direction of maximum orientation as zero measured manually.

4.3.1.2.Measurement of orientation using image analysis

The orientation of fibers given in Figure 4.7 are measured from Fourier transformed image obtained using Scion image software. The data file with the intensity of each pixel of the fourier transformed image given in Figure 4.11 are used as an input for the Fortran program given in appendix I to calculate the orientation factor. The FFT image corresponding to the fibers spun at 233 m/min show a weak angular dependence whereas the FFT images corresponding to higher speeds show a stronger angular dependence with intensity increasing in the direction perpendicular to the direction of fibers. The measure of intensity, I, at angles ϕ is given in the Figure 4.12. The orientation factors given in legend of Figure 4.12 are calculated using this method shows an increasing trend with increase in speed of rotation of wheel and is given in Figure 4.8a.

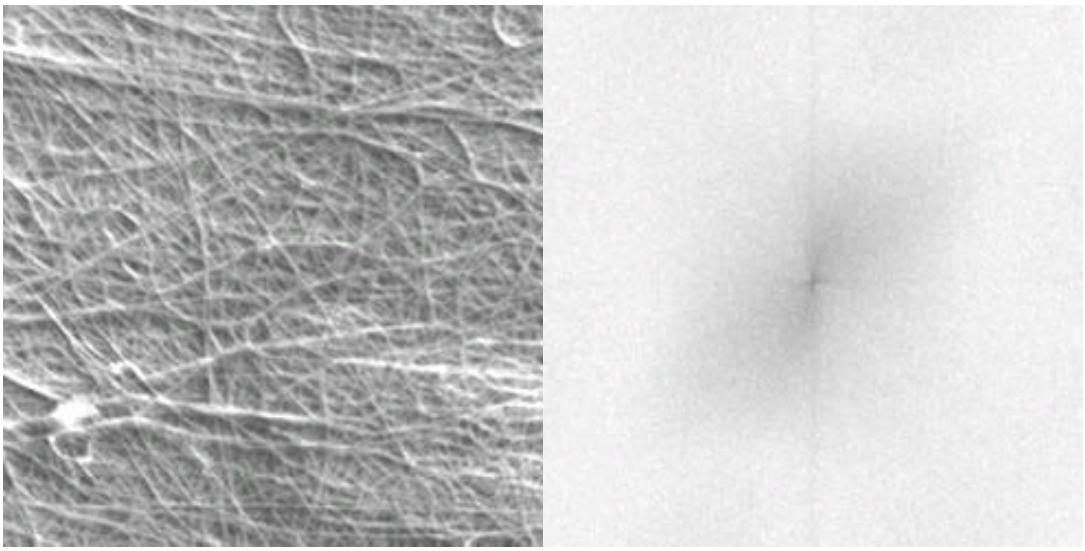

(a)

Figure 4.11 Original and Fourier transformed image of nylon 66 fibers collected at 10 wt% concentration, 10 cm target distance, and 15 kV voltage spun at speeds (a) 233 m/min (b) 465 m/min, (c) 926 m/min, (d) 1868 m/min and (e) 2833m/min

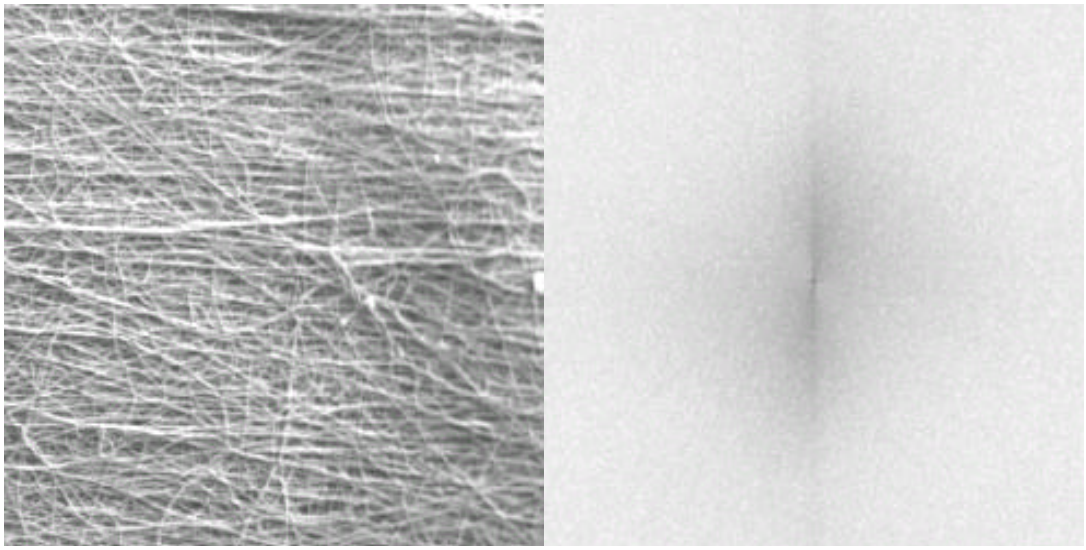

(b)

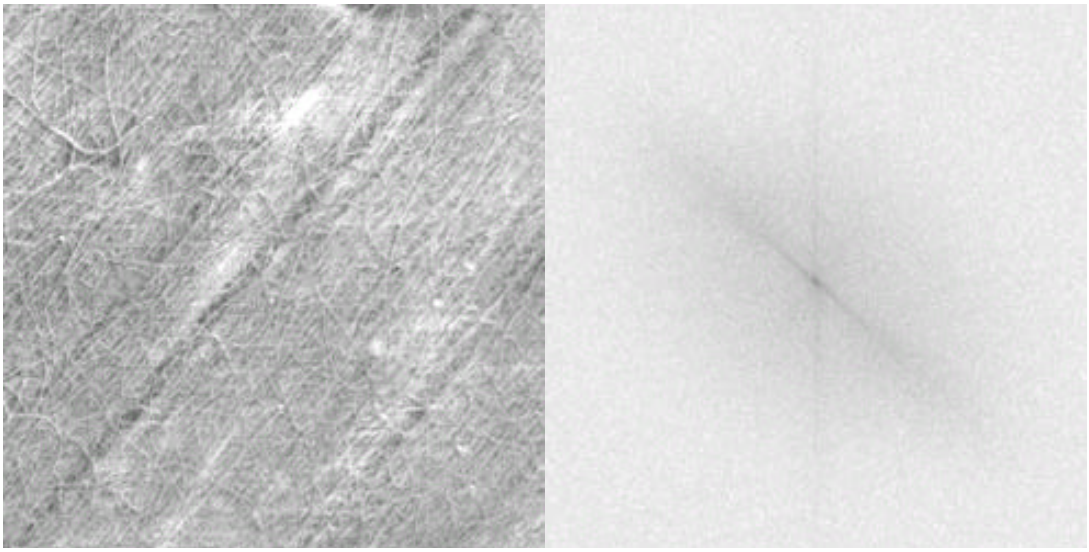

(c)

Figure 4.11 continued

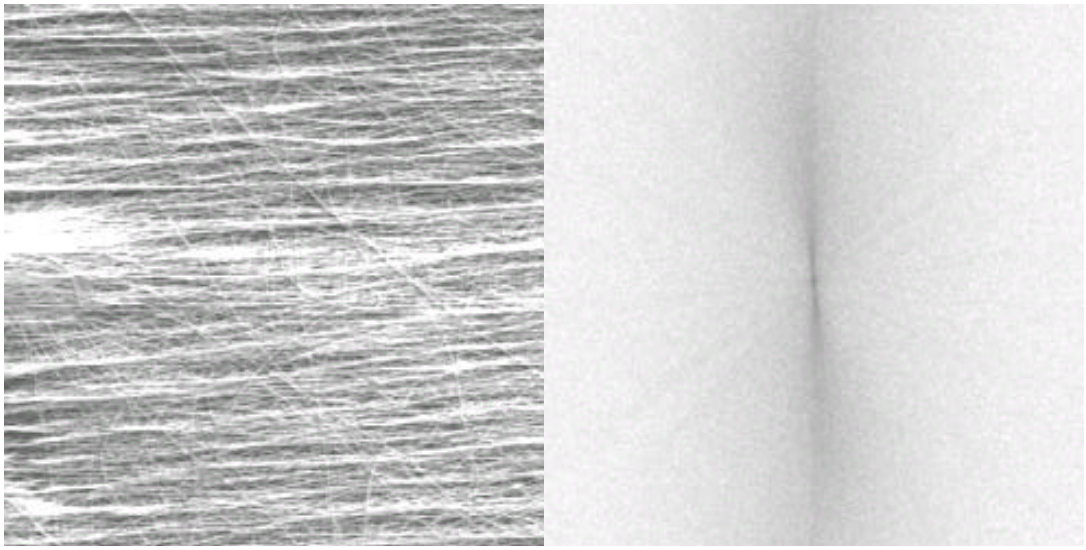

(d)

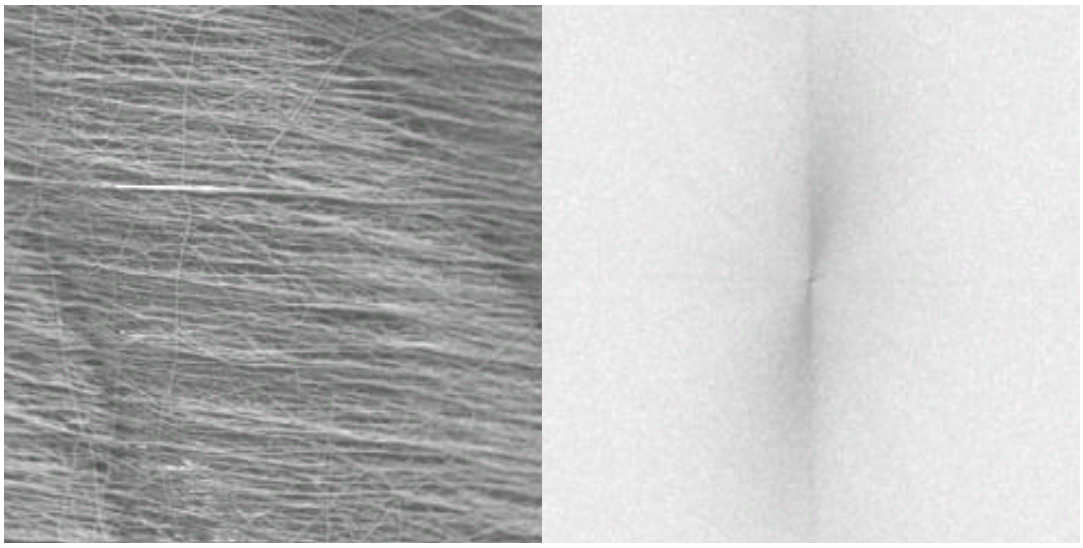

(e)

Figure 4.11 continued

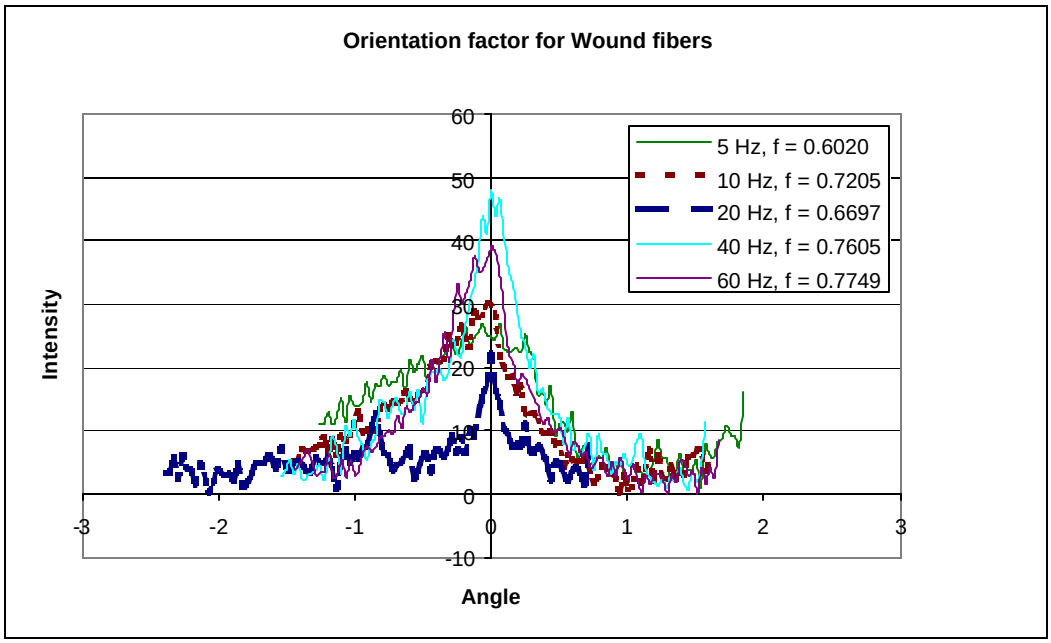

Figure 4.12 Intensity of pixels of Fourier transformed image measured at different angles

4.3.1.3.Measurement of molecular orientation using FTIR

The orientation factor and dichroic ratio are measured for the nylon 66 fibers spun at different speeds at voltage of 20 kV. The absorbance corresponding to NH stretch (3305), C=O stretch (1643), CN stretch / NH deformation (1537) and C – CO stretching (936) are used to calculate the dichroic ratio and orientation factors using the formula

$$\mathbf{D = A_{||} / A_{\perp}} \quad \text{and}$$

$$Orientation\ factor\ f = \frac{C\,(D-1)}{(D+2)}$$

The FTIR scans of the nylon 66 fibers wound at different speeds measured with the direction of IR rays parallel and perpendicular to direction of winding is given in Figure 4.13 – 4.15. The difference in the intensity of absorbance peaks is used to calculate the orientation factor. The orientation factor for all the four peaks observed increases with the increase in the speed of collection of fibers, for measurement at both the voltages. Figure

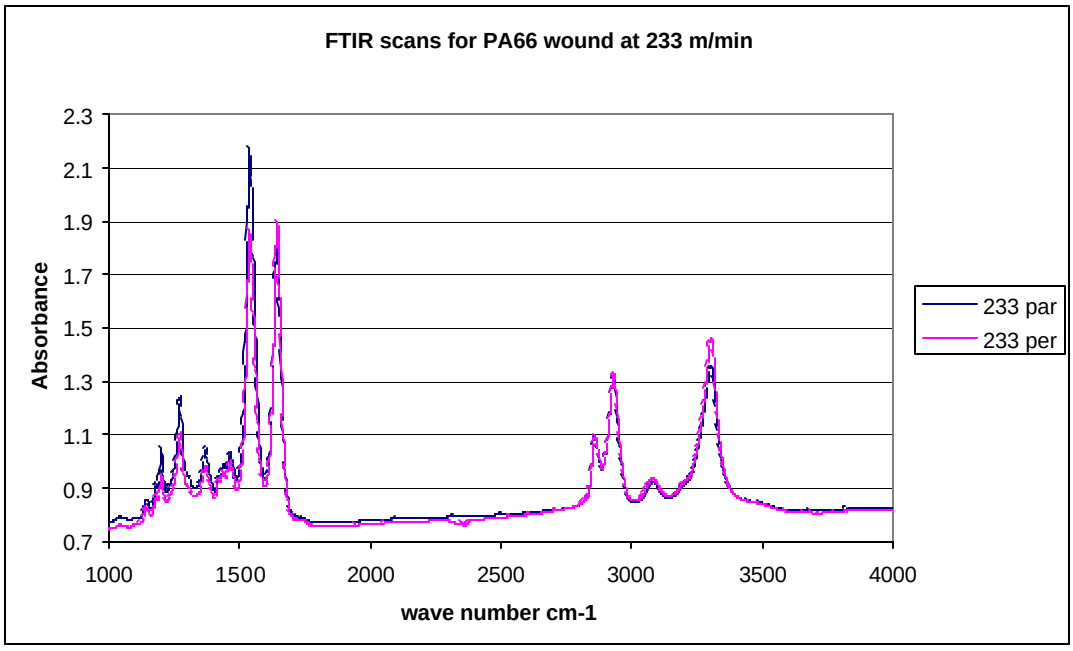

(a)

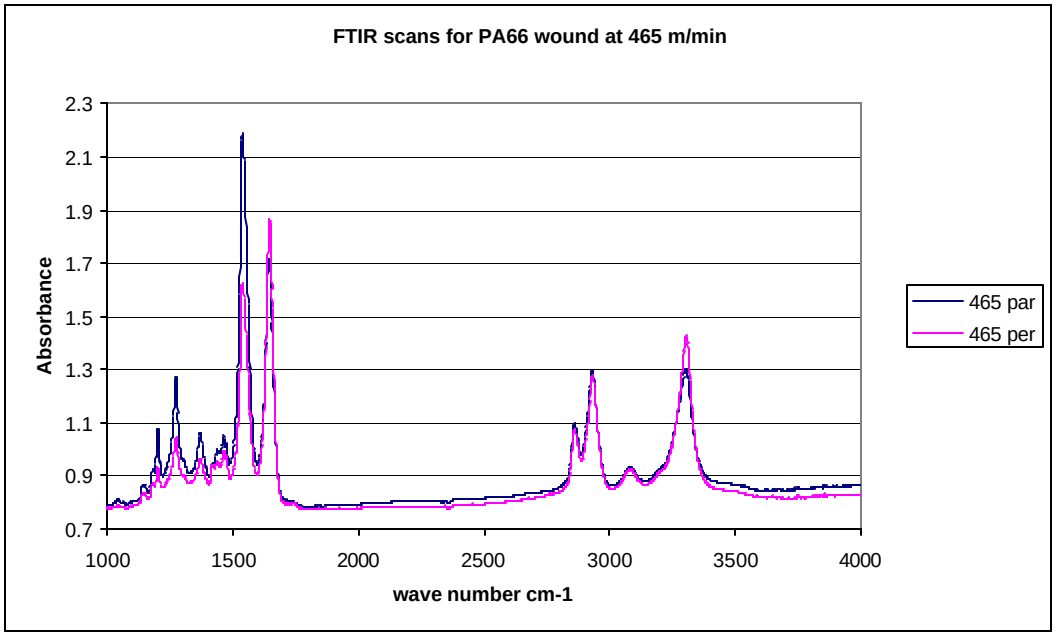

(b)

Figure 4.13 FTIR scans of nylon 66 fibers wound at 20kV with direction of IR rays parallel and perpendicular to direction of winding at speeds (a) 233 m/min (b) 465 m/min, (c) 926 m/min, (d) 1868 m/min and (e) 2833m/min

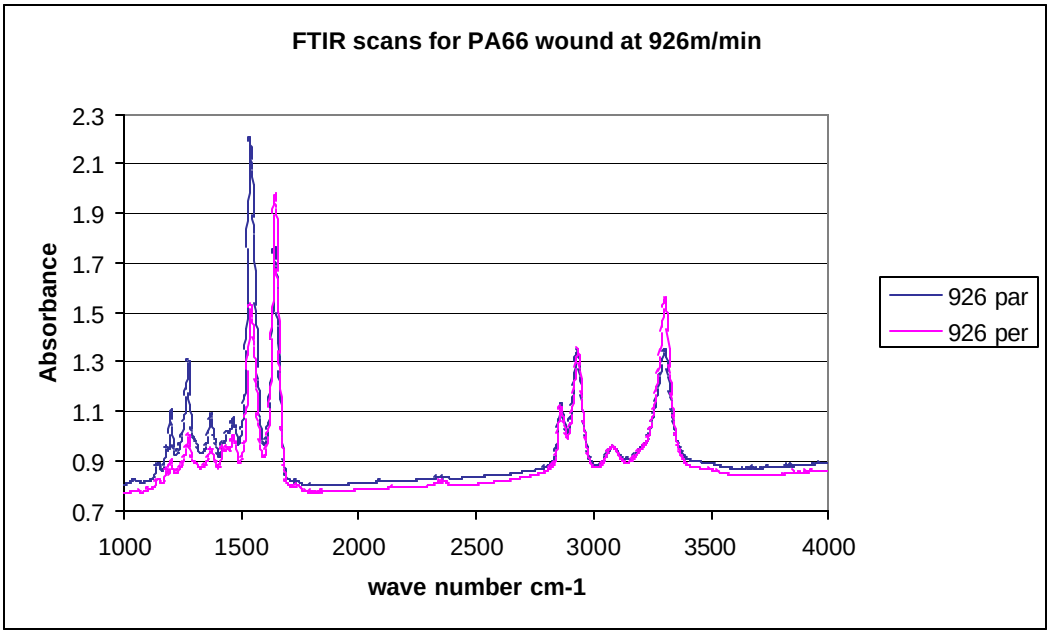

(c)

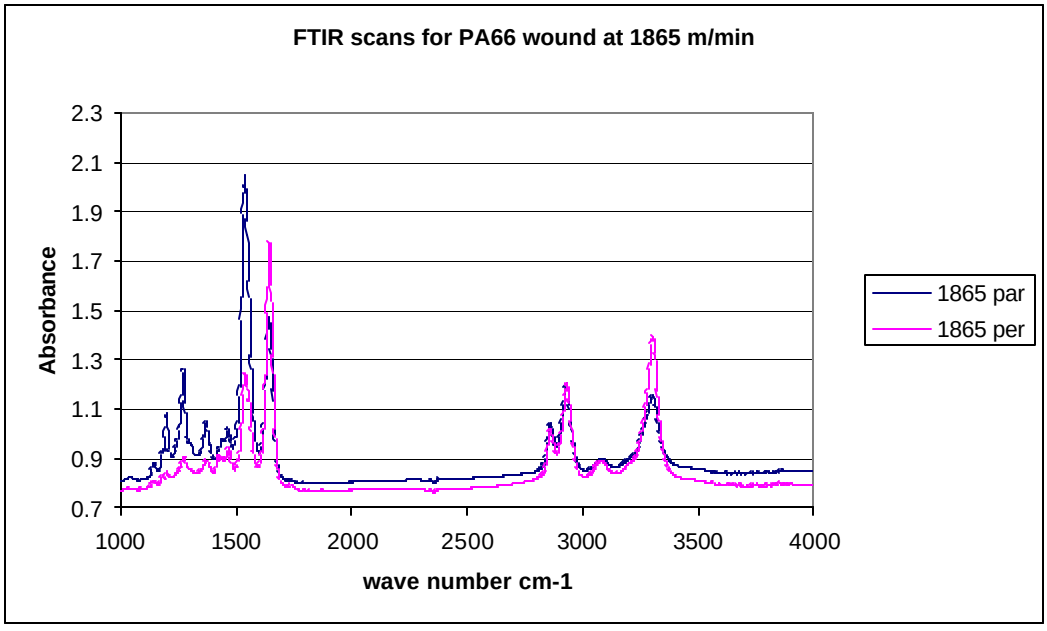

(d)

Figure 4.13 continued

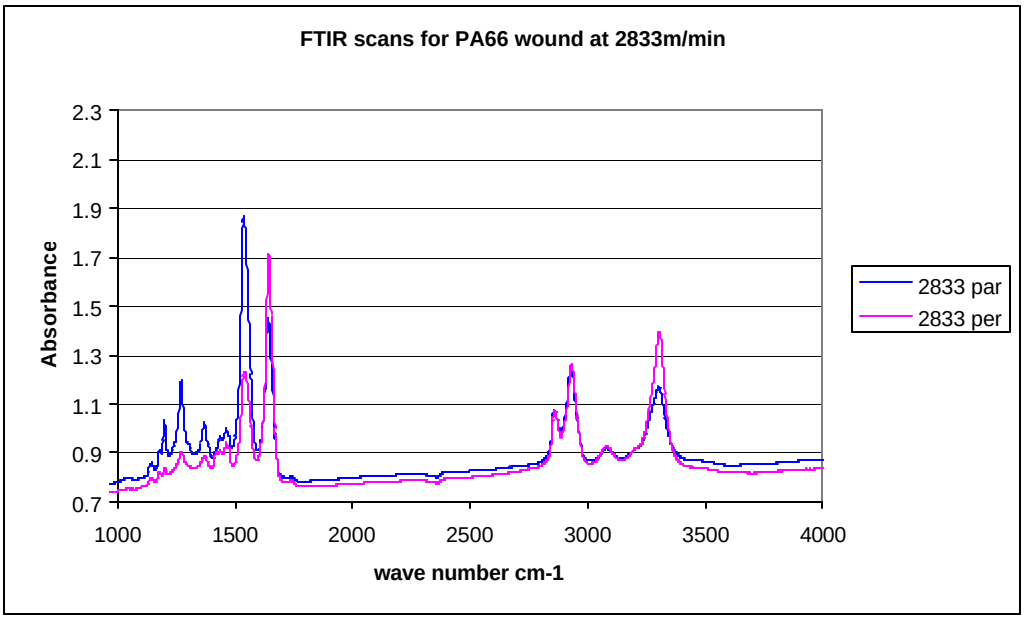

(e)

Figure 4.13 continued

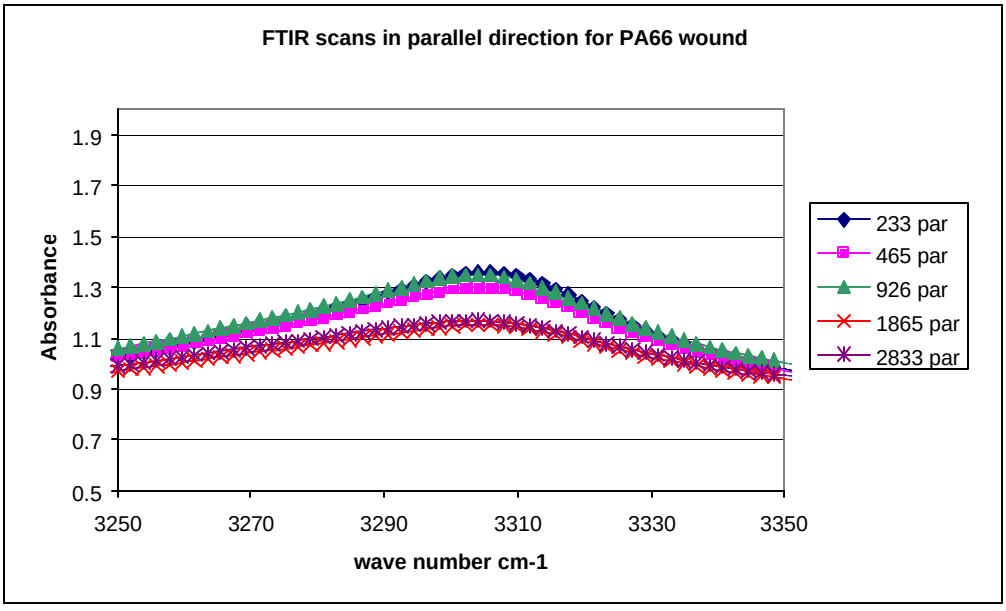

Figure 4.14 FTIR scans of nylon 66 fibers wound at different speeds measured with direction of IR rays parallel to direction of winding.

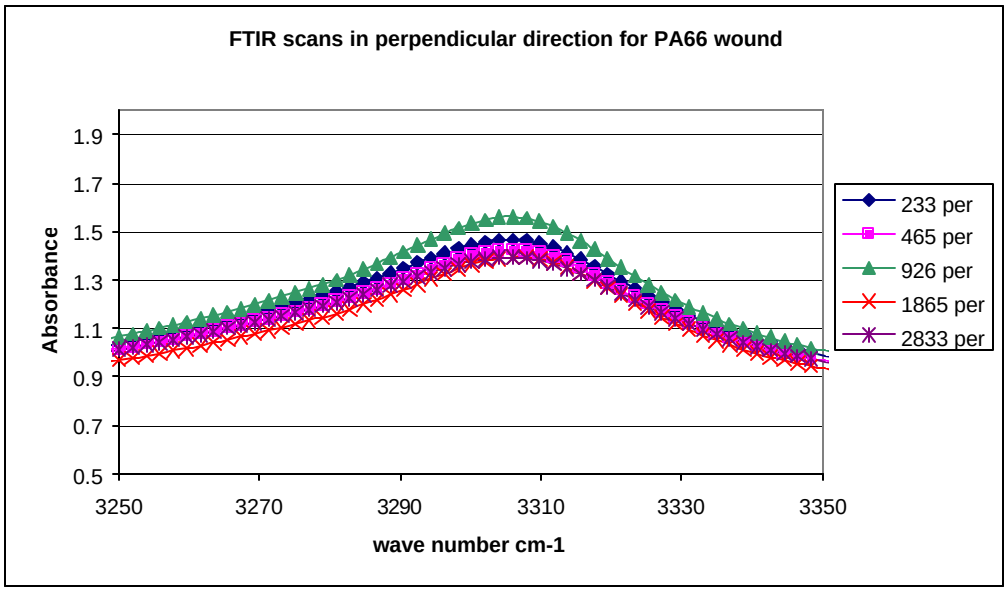

Figure 4.15 FTIR scans of nylon 66 fibers wound at different speeds measured with direction of IR rays perpendicular to direction of winding.

4.16- 4.17 shows the dichroic ratio and orientation factors for nylon 66 fibers collected at 20 kV. The absorption peak at 3305 cm^{-1} corresponds to NH stretching is used to determine molecular orientation in these samples. The N-H bond lies at an angle, ß, of 90° to the backbone of nylon 6,6, the dichroic ratio for the 3305 cm^{-1} peak will decrease as the backbone becomes oriented parallel to the winding direction. This effect can be seen in Figure 4.13. For the sample wound at a slow speed (233 m/min), the 3305 cm^{-1} peak is roughly the same size in both configurations while in the high speed sample (2833 m/min) the 3305 cm^{-1} peak in the perpendicular configuration is roughly twice as large as the same peak in the parallel configuration. Using data of this type, dichroic ratios for several peaks are plotted in Figure 4.16. These results denote that the peaks at 1537 and 936 cm^{-1} correspond to parallel dichroism and the peaks at 3305 and 1643 cm^{-1} correspond to perpendicular dichrosim similar to results of Vasanthan[18]. It is also clear that backbone orientation increased gradually with winding speed.

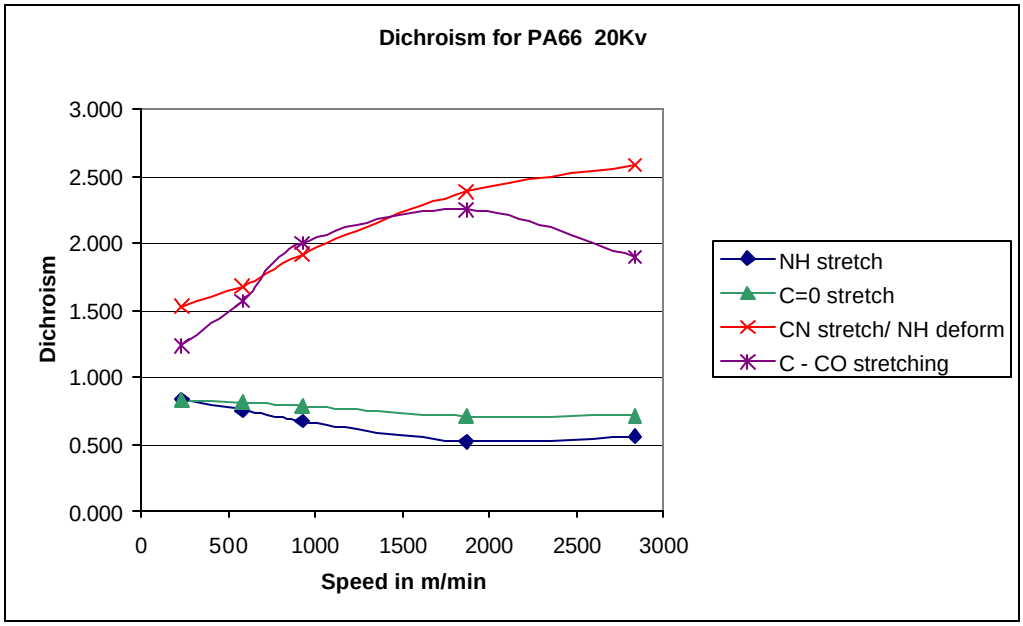

Figure 4.16 Dichroic ratio of nylon 66 fibers collected at 20 kV different speeds using FTIR

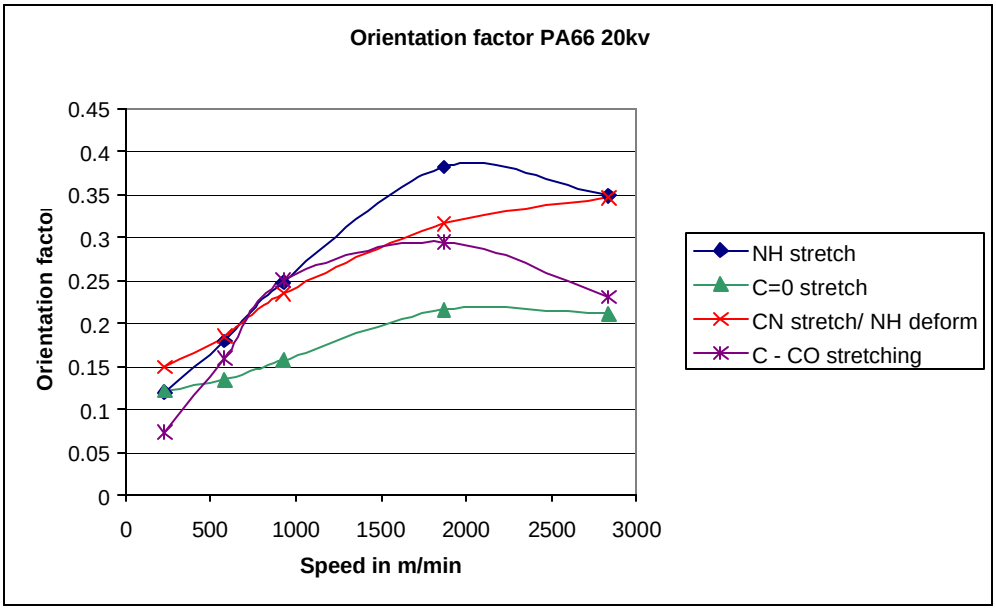

Figure 4.17 Orientation factor of nylon 66 fibers collected at 20 kV at different speeds

4.3.1.4. Measurement of crystalline orientation by psi scan in X-ray diffractometer

The nylon 66 fibers spun at maximum speed of 2833m/min are scanned in 2 – axes in x-ray diffractometer to find out all the reflections. A strong peak was noticed at 2-theta of 20.6, which corresponds to a reflection from (200) plane. Hence a psi scan was performed for the nylon 66 fibers collected at different speeds at 2-theta value of 20.6. The 2-axes scan pattern for nylon 66 fibers is shown in Figure 4.18. The results show a small degree of crystalline orientation in the wound nylon 66 samples, which is independent of the winding speed. The orientation factor shown in Figure 4.19 is then calculated using the formula

$$f_{a,z} = \frac{3 < \cos^2 f_{a,z} > -1}{2}$$

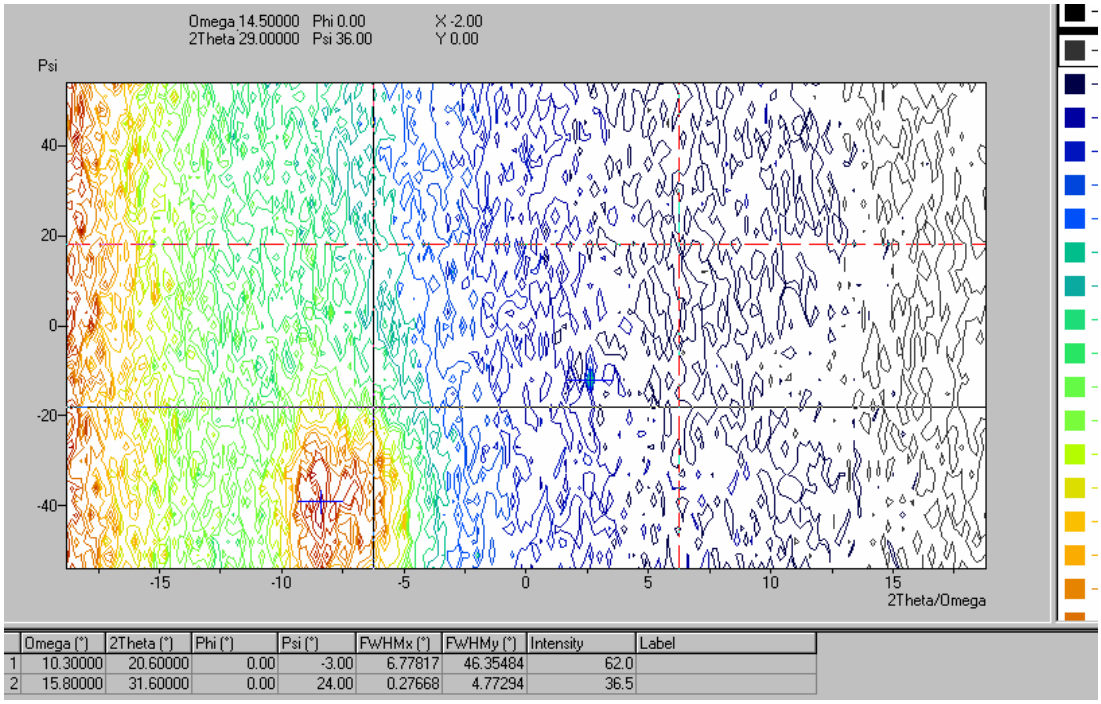

	Omega (°)	2Theta (°)	Phi (°)	Psi (°)	FWHMx (°)	FWHMy (°)	Intensity	Label
1	10.30000	20.60000	0.00	-3.00	6.77817	46.35484	62.0	
2	15.80000	31.60000	0.00	24.00	0.27668	4.77294	36.5	

Fig. 4.18 2-axes scan pattern of PA66 fibers collected at speed 2833m/min

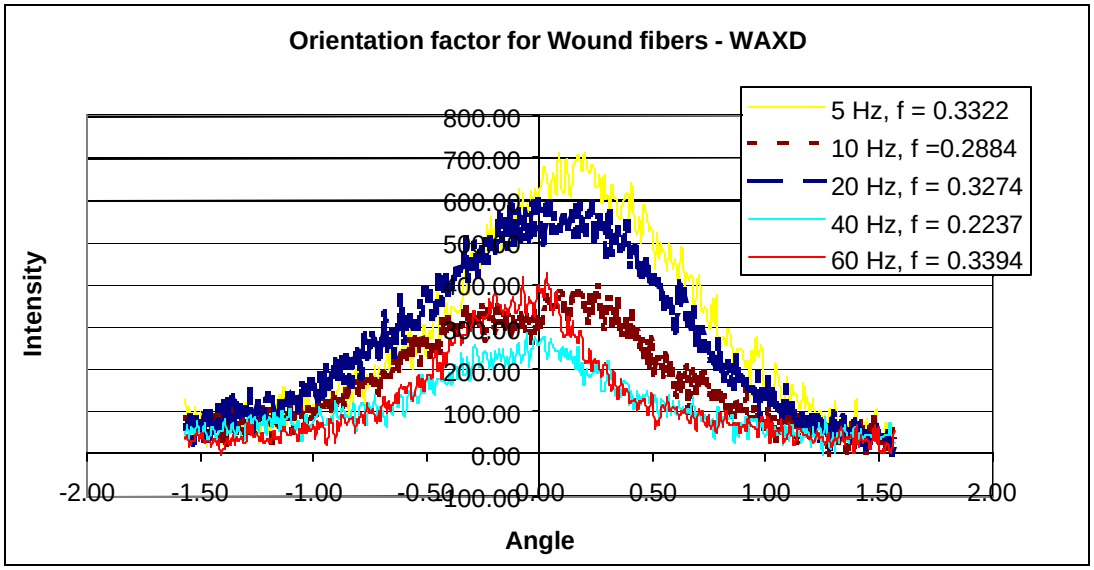

Figure 4.19 Orientation factor of PA66 measured for samples collected at different speeds using psi scan

4.3.2. Mechanical properties of wound fibers

The mechanical properties of the aligned electrospun fibers were not studied previously. Hence the nylon 66 fibers collected in rotating wheel at two different voltages are tested for tensile properties in the dynamic mechanical analyzer at a constant strain rate of 1.5% per minute. The samples collected at 15kV shows an increase in tensile modulus with the increase in speed of collection of fibers as shown in Figure 4.20. However, the sample collected at maximum speed – 2833m/min at 20kV show an abrupt increase in tensile modulus compared to samples collected at lower speeds at same voltage as shown in Figure 4.21. The tensile modulus of the samples measured at 7.5% strain rate for two different voltages is given in Figure 4.22. A significant jump in modulus of the samples collected at 15 kV and 20 kV is observed at speeds of 1865m/min and 2833m/min, respectively. This shows that the speed at which the polymers fibers travel towards the target increases with increase in voltage. At a given voltage, the speed with which the

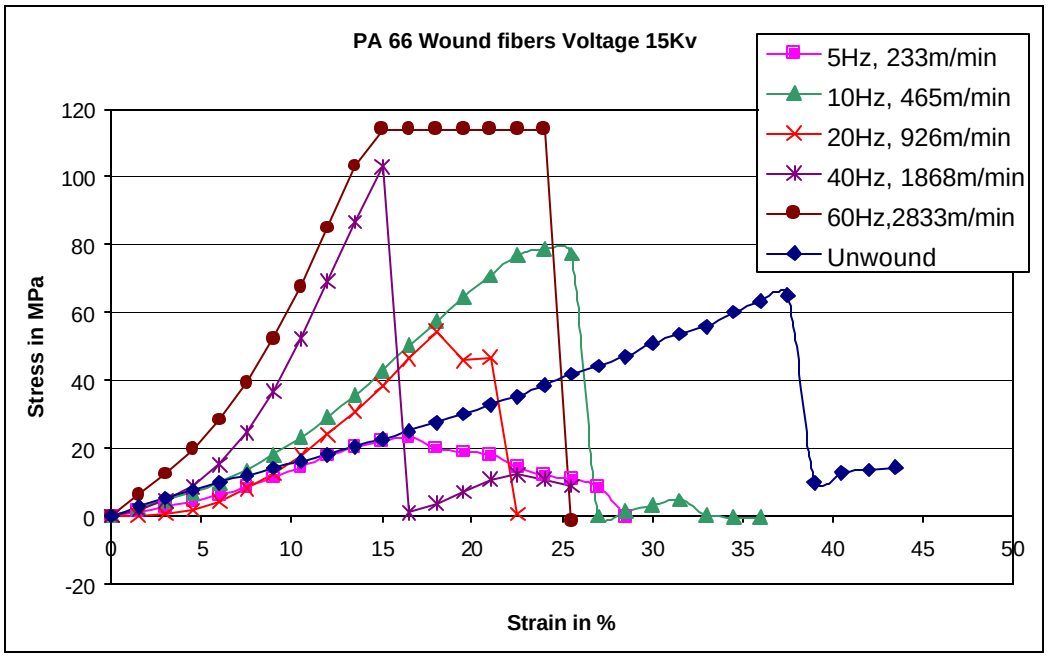

Figure 4.20 Tensile results of nylon 66 fibers collected at different speeds at 15kV

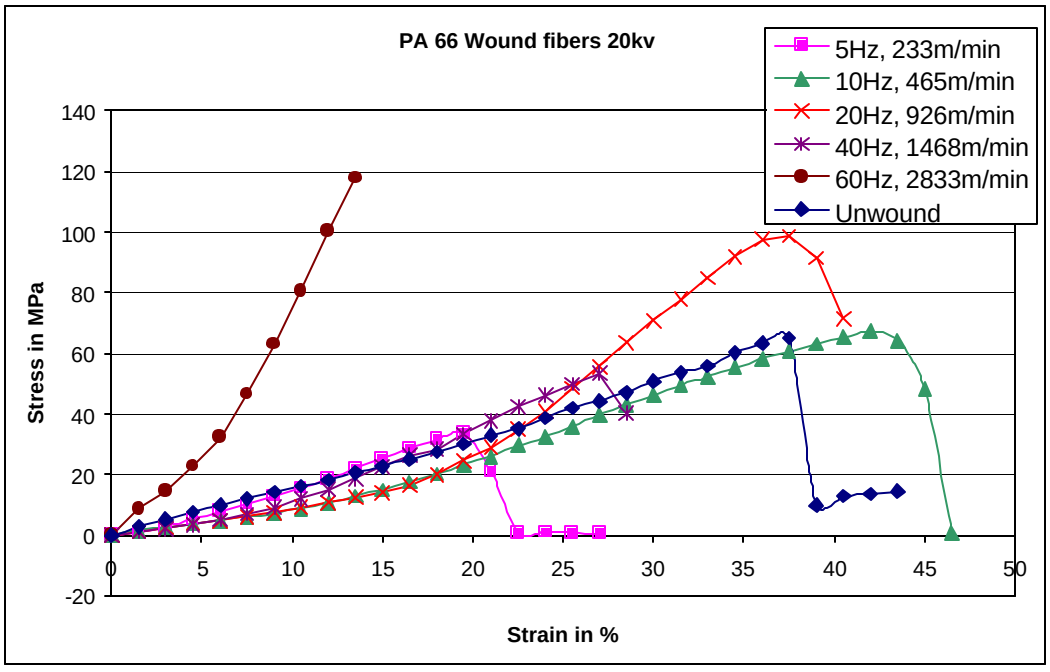

Figure 4.21 Tensile results of nylon 66 fibers collected at different speeds at 20kV

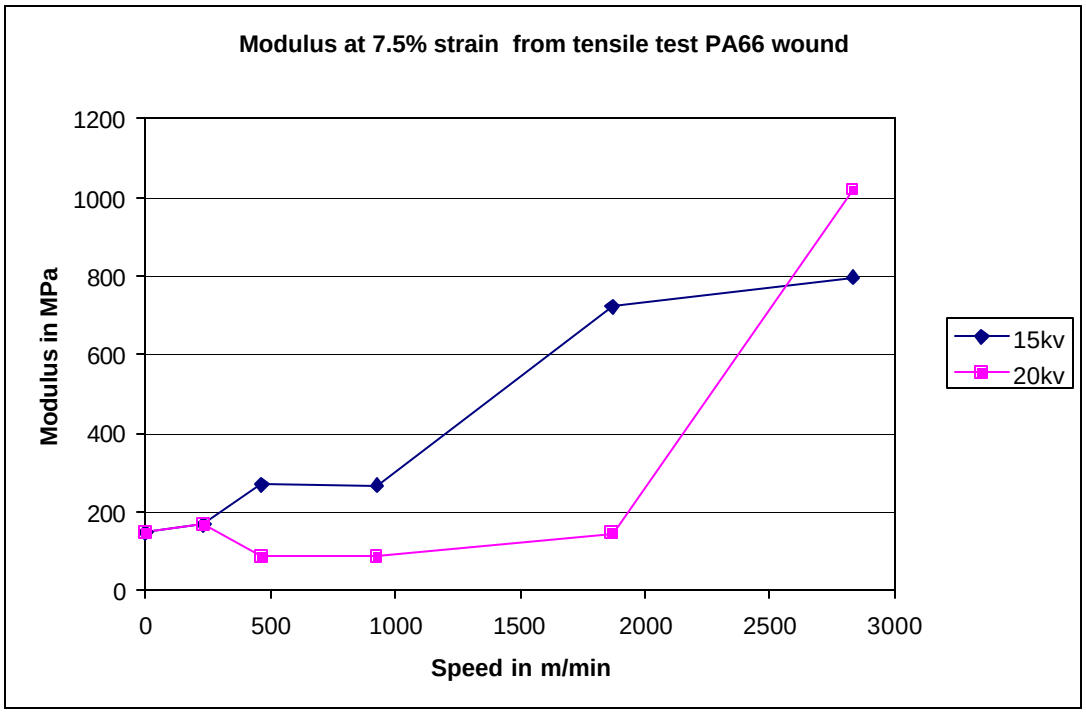

Figure 4.22 Tensile modulus of nylon 66 fibers collected at 15 & 20kV

polymer fiber travels towards the target is called the critical speed. When the speed of collection of fibers exceeds this critical speed at which the polymer fibers travels towards the target, the fibers collected are stretched and possibly oriented. Hence the speed 1865m/min and 2833m/min are likely the critical speeds at which the speed of rotation of wheel exceeds the speed of fiber travel at 15 kV and 20 kV respectively. The tensile results of wound nylon 6 fibers melt spun by Murase [23] could not be compared to our results as the spinning speed range used by them is 4000 – 14000m/min.

4.3.3. Crystallinity of wound fibers

The nylon 66 fibers collected in rotating wheel at 20kV voltage are tested for crystallinity in Philips' x'pert x-ray diffractometer and in TA instruments DSC 2590 differential scanning calorimeter. The crystallinity of nylon 66 fibers measured by the two techniques is given in Figure 4.23. The endotherm is not subtracted from the exotherm as there was

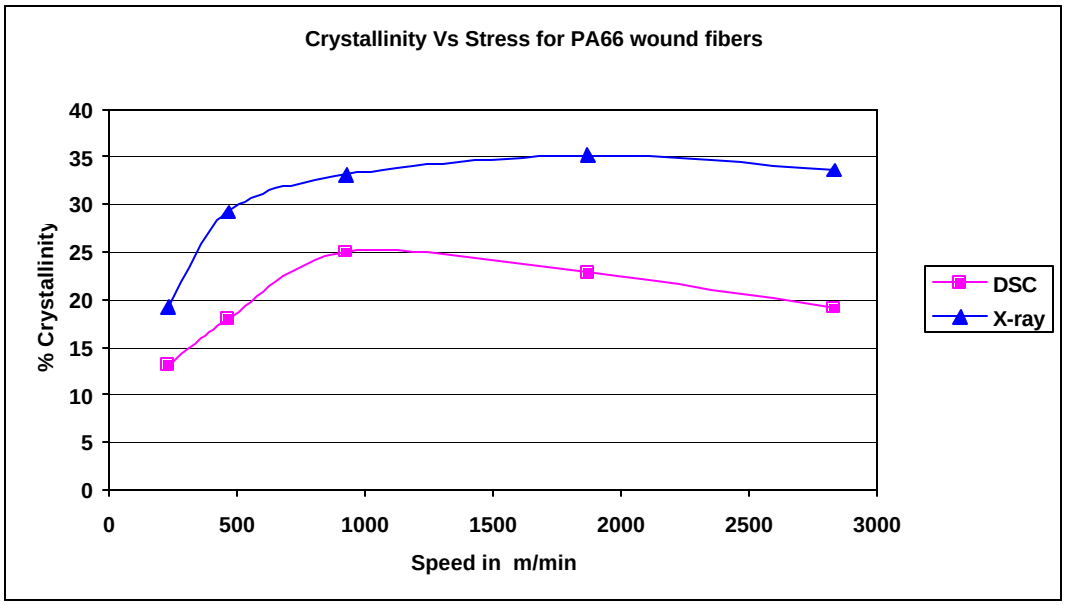

Fig. 4.23 Crystallinity of nylon 66 fibers wound at different speeds and 20 kV measured by X-ray diffraction and DSC

no well defined exotherm in the heat flow curve. Even though there is difference in values of crystallinty measured by two methods, there is a similar trend observed in the values.The crystallinity increases with speed for sample spun up to a speed of 926m/min. This increase in crystallinity can be due to stretching of the polymer fibers when collected in a rotating wheel, which can cause the stress induced crystallization. There is no significant change in the crystallinity values for samples collected at speeds more than 926m/min. The measurement from x-ray diffraction can be more accurate because it does not involve thermal gradient like DSC and hence introduces less artificial factors. This difference can also be attributed to the presence of a crystalline-amorphous interphase layer which contributes to crystalline scattering but not the heat of fusion [29]. Both sets of data, however, show that crystallinity initially increases with winding speed but then reaches a maximum and decreases at higher speeds. The initial increase in crystallinity is likely a result of stress induced crystallization, while the decrease at higher speeds cannot currently be explained. A typical 2-theta scan and DSC heat flow scan are shown in Figure 4.24-25.

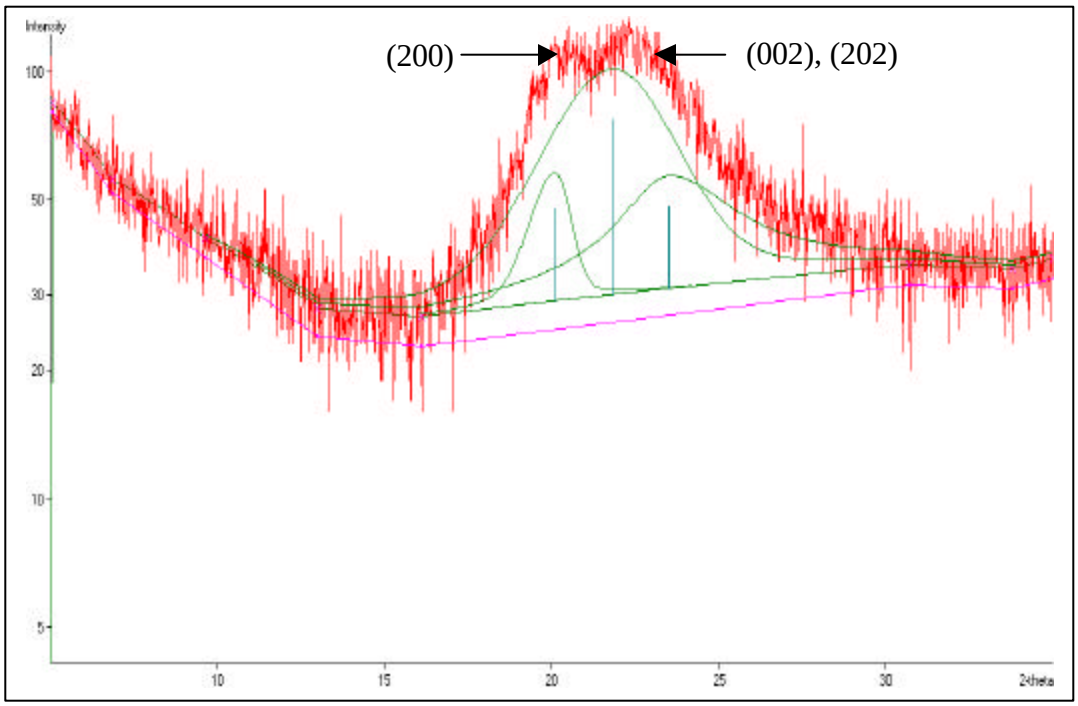

Fig. 4.24 Crystallinity of nylon 66 fibers wound 1868m/min measured by X-ray diffraction

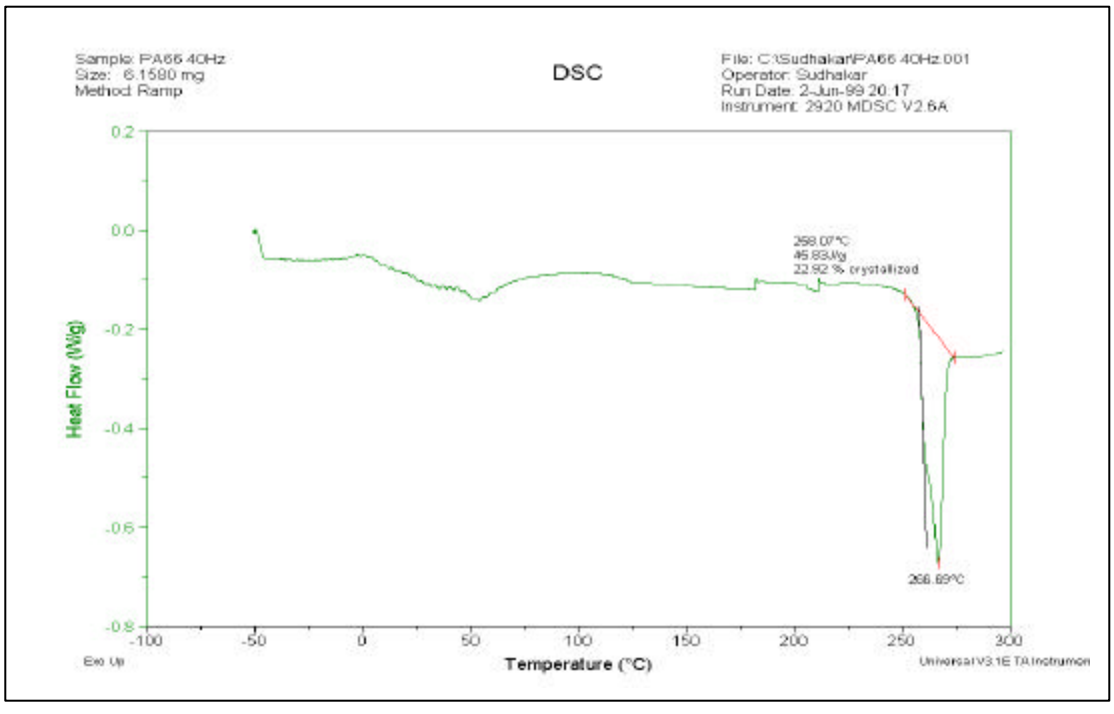

Fig. 4.25 Crystallinity of nylon 66 fibers wound at 1868m/min measured by DSC

The orientation, crystallinity and modulus of nylon 66 wound fibers are given in the figures 4.26 and 4.27. The crystallinity and orientation of the samples increases with speed for sample spun up to a speed of 926m/min and no significant change in the crystallinity values for samples collected at speeds higher 926m/min. Where as the modulus does not change significantly for nylon 66 samples collected at speeds up to 1865m/min. The orientation and crystallinity are both affected by the draw ratio as shown in Figures 4.26 – 4.27, whereas the increase in modulus after collection speed of 1865m/min can be due to molecular orientation occurring inside the polymer fibers at that speed.

The winding speed of the wheel should be more than the "natural velocity" of the fibers to elongate and align the fibers along the diameter of wheel. The fiber collected at speeds lower than this natural velocity results in random nonwoven mats. The SEM pictures show an increase in orientation of fibers between 233 and 465 m/min but only slightly for speeds greater than 465 m/min. Hence the speed around 465 m/min is more likely the natural velocity of fibers.

At winding speeds greater than 465 m/min, the winding wheel should be moving faster than the natural velocity, and a mechanical drawing of the fiber should result. This type of drawing typically results in increases in molecular orientation and tensile modulus. Molecular orientation as determined by FTIR and tensile modulus increase only slightly as the winding speed increases from 233 to 465 m/min indicating that little or no drawing of the fiber is taking place at these speeds. However, the tensile modulus of these fibers spun at 15 kV increases significantly between 926 and 1868 m/min. Since the crystalline orientation and crystallinity actually decrease over this range, it can be argued that the increase in tensile modulus is due to a significant increase in amorphous orientation within the fibers.

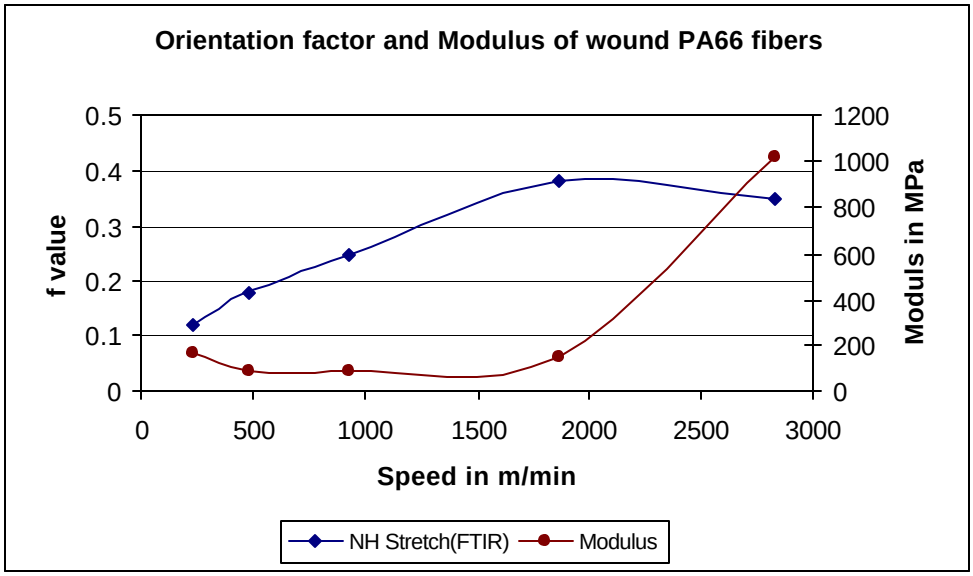

(a)

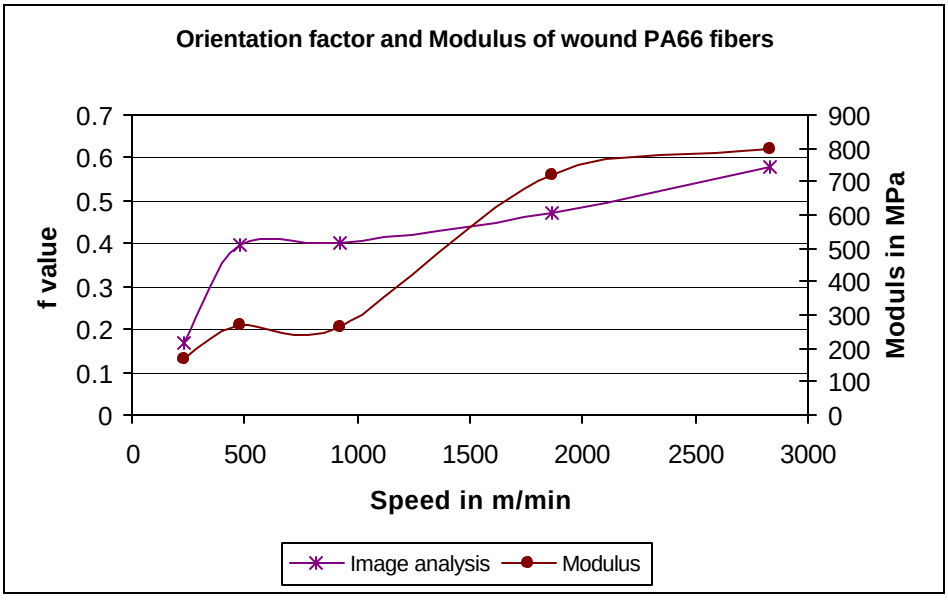

(b)

Fig. 4.26 The orientation and modulus of nylon 66 fibers collected at different speeds measured (a) at 20 kV using FTIR, and tensile test , (b) at 15 kV using image analysis and tensile test

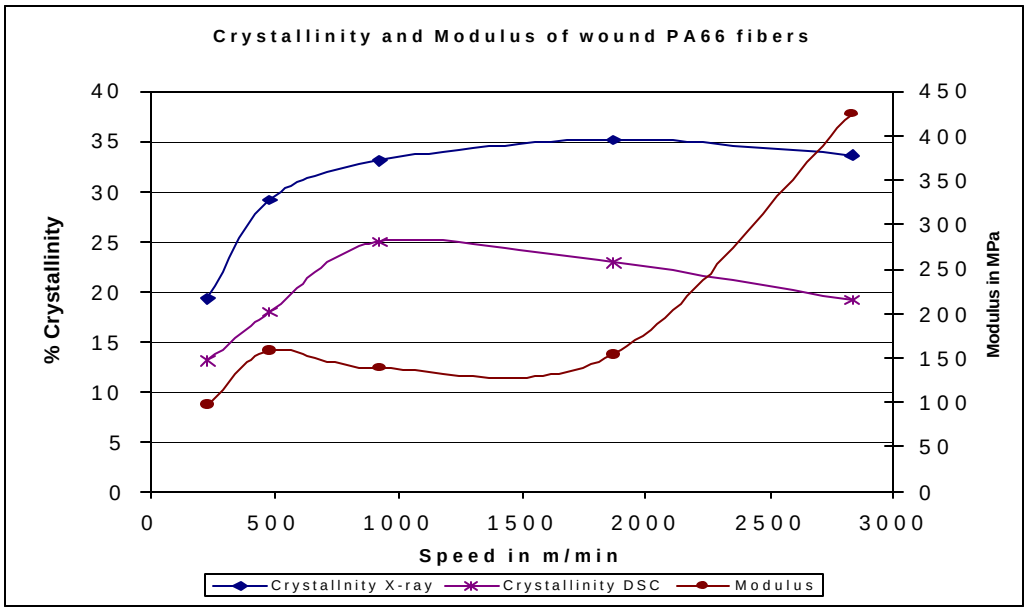

Fig. 4.27 Crystallinity modulus of nylon 66 fibers collected at different speeds at 20kV voltage measured using DSC, X-ray diffraction and tensile test.

The ratio of the speed of rotation of wheel and the natural velocity of fibers can be taken as the draw ratio represented in Figure 4.28. The degree of drawing and increases in molecular orientation and tensile modulus should be a function of both winding speed and the natural electrospinning velocity of the fiber. The latter should be a function of many variables including spinning voltage, target distance, and charge density of the jet. An increase in spinning voltage will increase the electrodynamic forces exerted on the jet, increase the natural velocity the fiber attains before it strikes the target, and therefore decrease the amount of mechanical drawing at a constant winding speed. To test this hypothesis, nylon 6,6 fibers were spun at two voltages 15 and 20 kV, and wound as described above. Figure 4.22 shows the tensile modulus and molecular orientation for fibers spun at 20 kV as a function of winding speed. This data indicates that at 20 kV a higher winding speed is necessary to achieve the equivalent modulus and orientation of the fibers spun at 15 kV. At a spinning voltage of 20 kV, the molecular orientation in consistently lower for winding speeds slower than 1000 m/min and a significant increase in modulus is only seen at the highest winding speed. A reasonable estimate of the natural electrospinning velocity at 20 kV would be between 456 and 1868 m/min.

The totality of the data presented here can be used to deduce information about the processing, structure, and properties of nylon 6,6 electrospun into a nonwoven mat onto a stationary or slowly moving target. The velocity that these fibers attain under the conditions studied is a function of spinning voltage and in the range of 465 and 1868 m/min. Due to the observation that a significant increase in modulus was only seen at high winding speeds, fibers spun into a nonwoven mat without the aid of additional mechanical drawing will have comparatively low molecular orientation and tensile modulus. Although the natural velocities were estimated to be quite significant, the electrodynamic and whipping forces exerted on the fiber were not sufficient to produce a large degree of molecular orientation with the spun fibers. This is likely due to the very fast relaxation times present in the jet before most of the solvent has evaporated, and could be an indication that the nature of the jet close to the spinneret has a large influence on the structure development of electrospun polymer fibers.

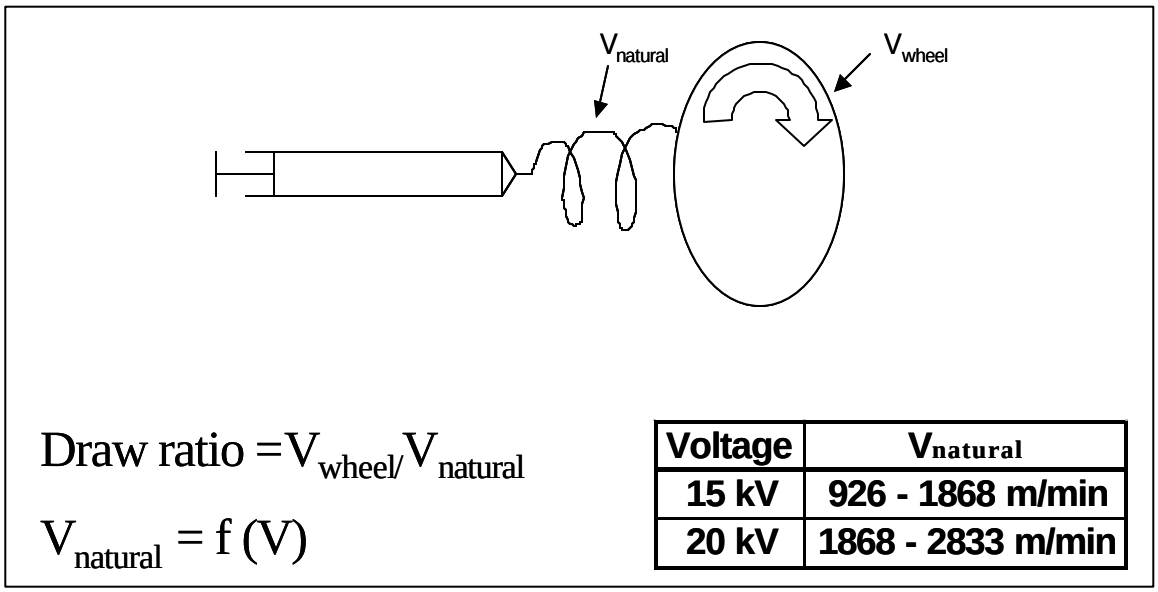

Fig. 4.28 Draw ratio and natural velocity of nylon 66 fibers.

4.4. Annealing of fibers

The mechanical properties and crystallinity of the nano size fibers can also be increased by annealing the samples at high temperature under stress. Nonwoven mats of nylon 66, PET and nylon 66/PCL fibers are annealed at 95°C under different constant loads for 1 hour and are tested for modulus, crystallinity and orientation. Figures 4.29 – 4.31 shows the morphology of the as-spun nylon 66, PET and nylon 66/PCL fibers with fiber diameters around 50 nm, 150 nm and 100 nm respectively.

4.4.1. Orientation of annealed fibers

The orientation factor and dichroic ratio are measured for the nylon 66 and poly (ethylene terepthalate) fibers annealed at different loads. The absorbance corresponding to NH stretch (3305 cm^{-1}) for nylon 66 and CH in benzene ring stretch (730 cm^{-1}) for

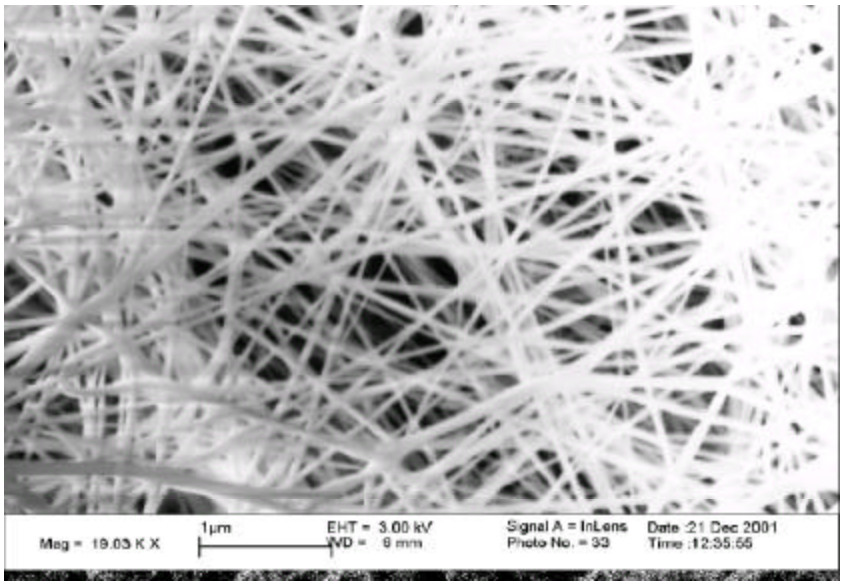

Fig. 4.29 Morphology of nylon 66 - diameter ~ 50nm

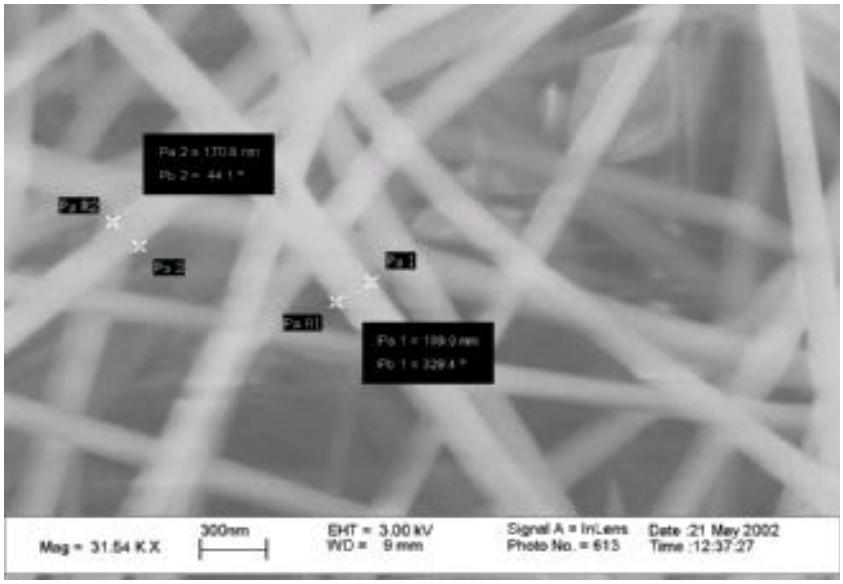

Fig. 4.30 Morphology of poly (ethylene terepthalate) – diameter ~ 150 nm

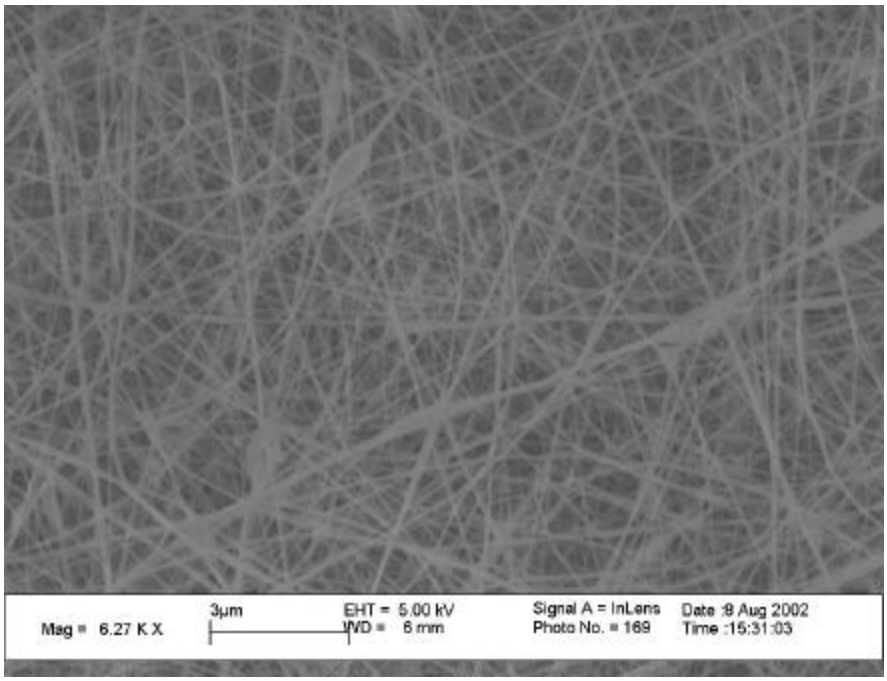

Fig. 4.31 Morphology of nylon 66 / PCL – diameter ~ 150 nm

poly (ethylene terepthalate) are used to calculate the dichoric ratio and orientation factors using the formula

$$\mathbf{D = A_{||} / A_{\perp}} \quad \text{and}$$

$$\textit{Orientation factor } f = \frac{C\,(D-1)}{(D+2)}$$

Figures 4.32 - 4.33 show the SEM pictures of the nylon 66 and poly (ethylene terepthalate) annealed at a maximum stress of 4.23 MPa and 2 Mpa, repectively. The FTIR scans of the fibers annealed at different loads with the direction of IR rays parallel and perpendicular to direction of stretching is given in Figures 4.34 for annealed nylon 66 and Figures 4.35 for poly(ethylene terepthalate) respectively. The Figures 4.40 and 4.41 show the dichroic ratio for nylon 66 and poly(ethylene terepthlate) fibers respectively.

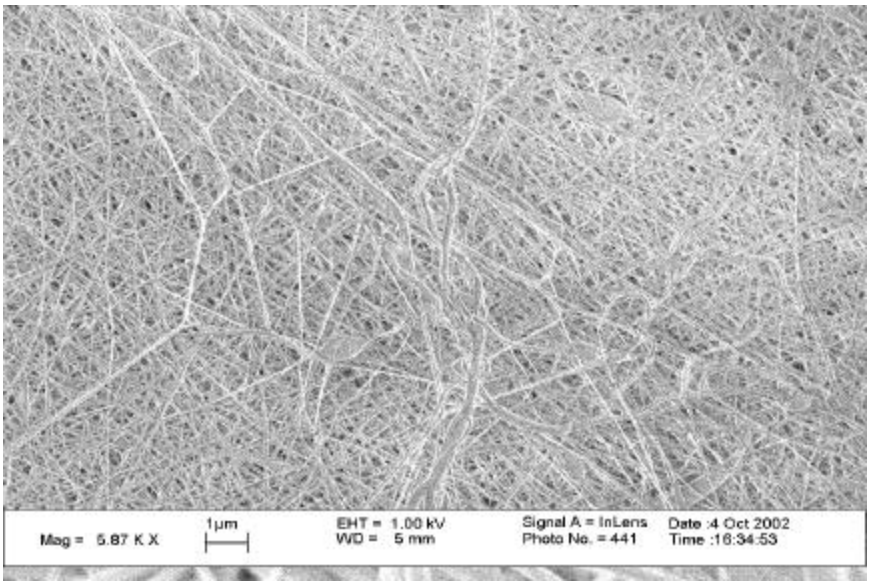

Fig. 4.32 Morphology of nylon 66 fibers annealed at 4.23 MPa stress

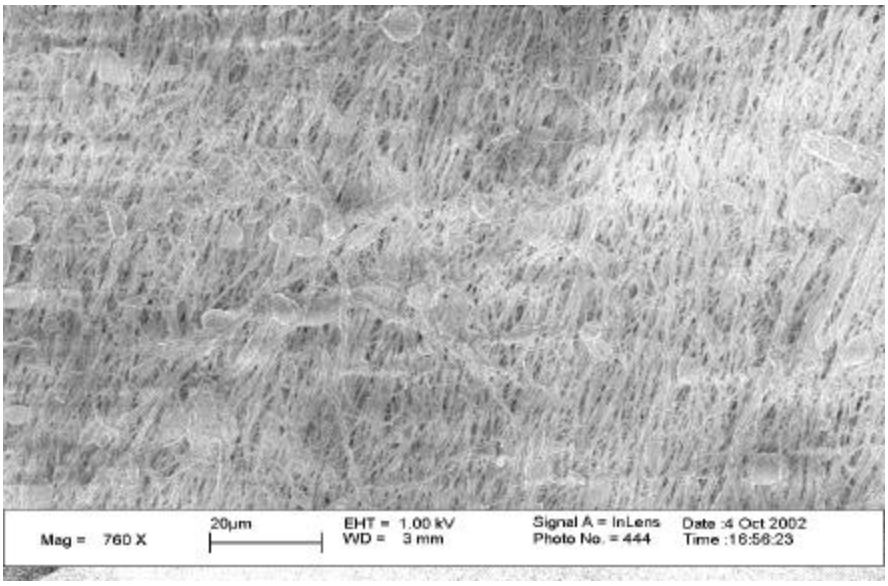

Fig. 4.33 Morphology of poly(ethylene terepthalate) fibers annealed at 2.00 MPa stress

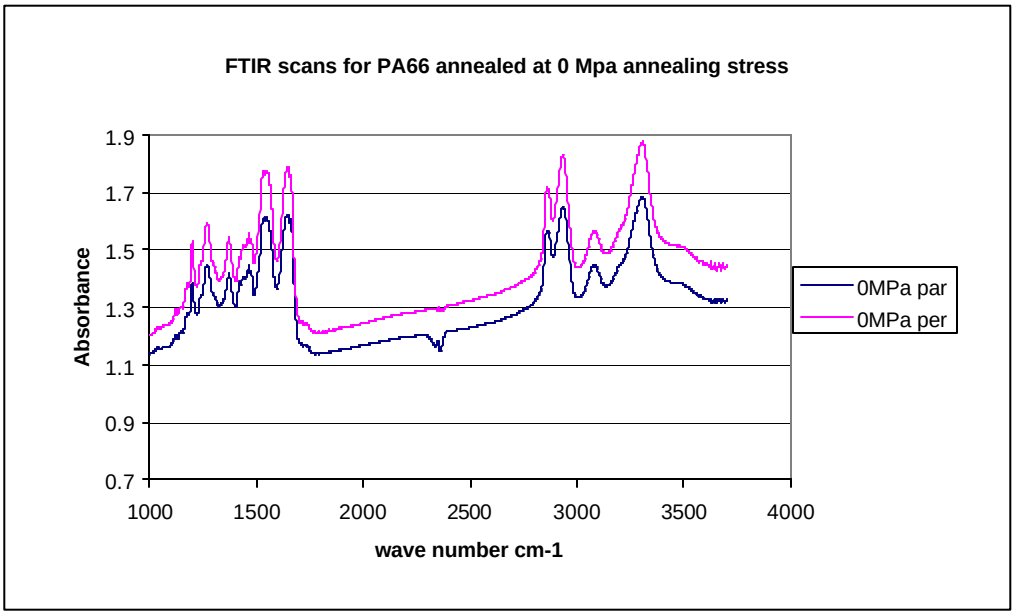

(a)

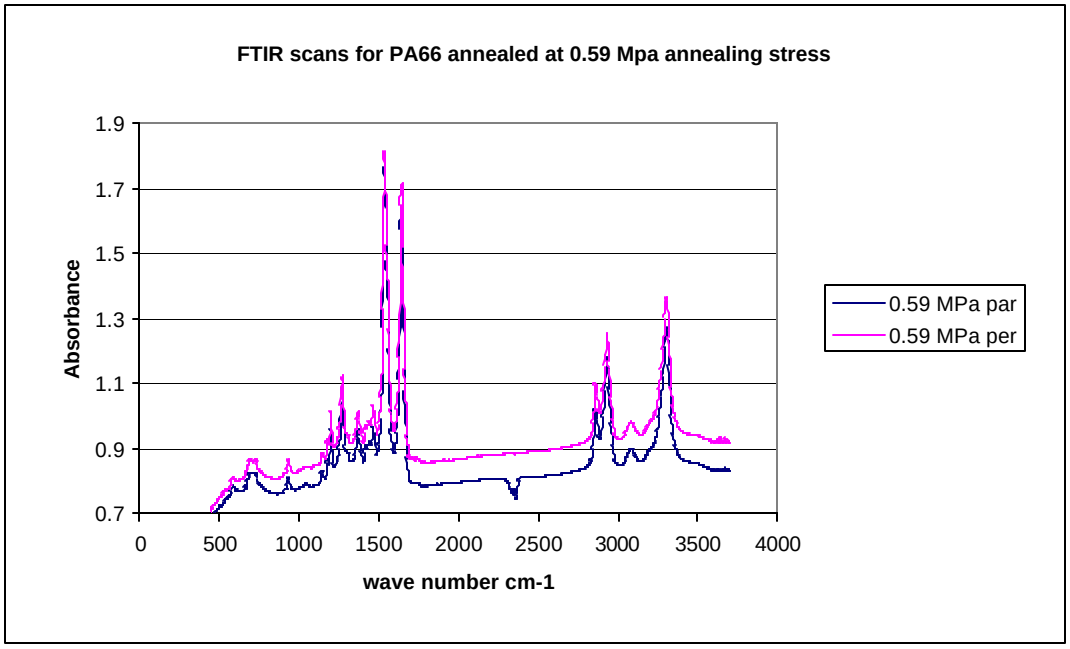

(b)

Figure 4.34 FTIR scans of nylon 66 fibers annealed measured with direction of IR rays parallel and perpendicular to direction of stretching with stress (a) 0 MPa, (b) 0.59 MPa, (c) 1.24 MPa, (d) 1.76 MPa, (e) 2.83 MPa, (f) 4.23 MPa

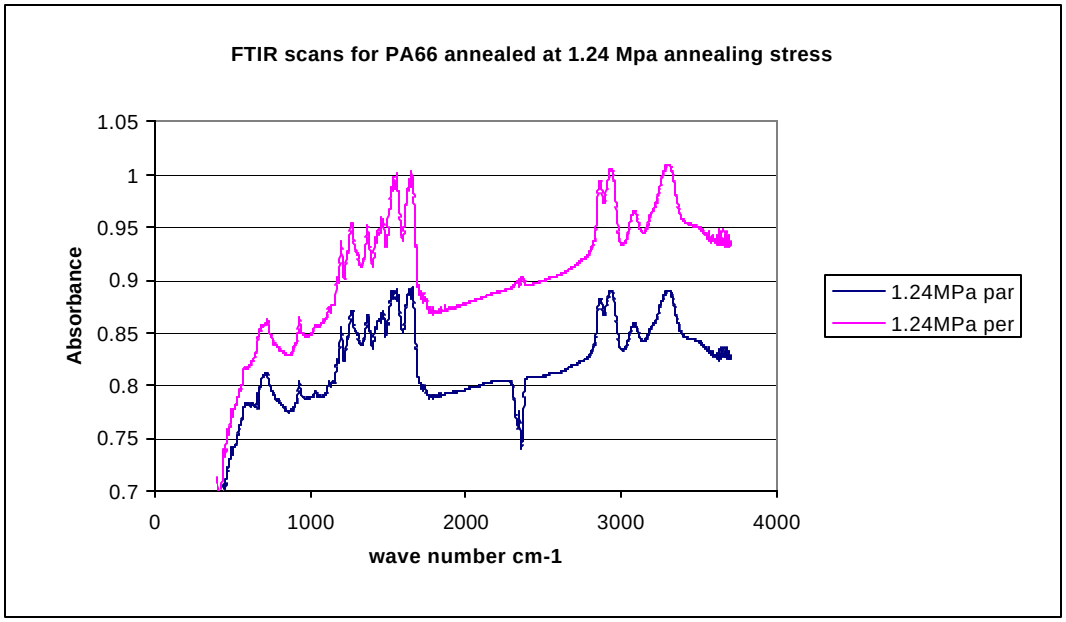

(c)

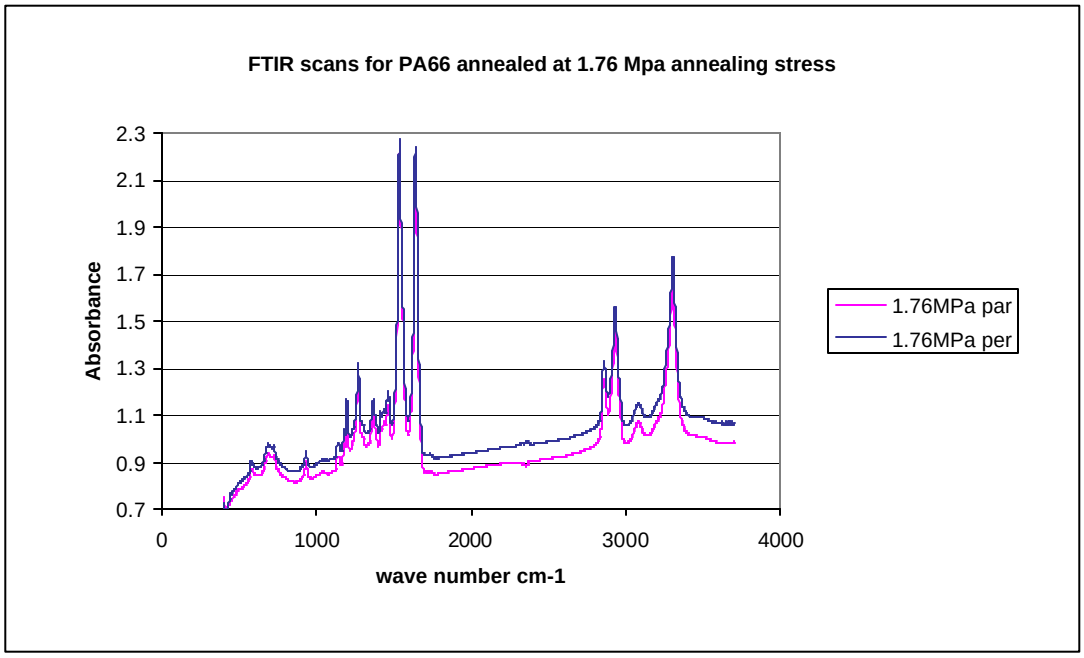

(d)

Figure 4.34 continued

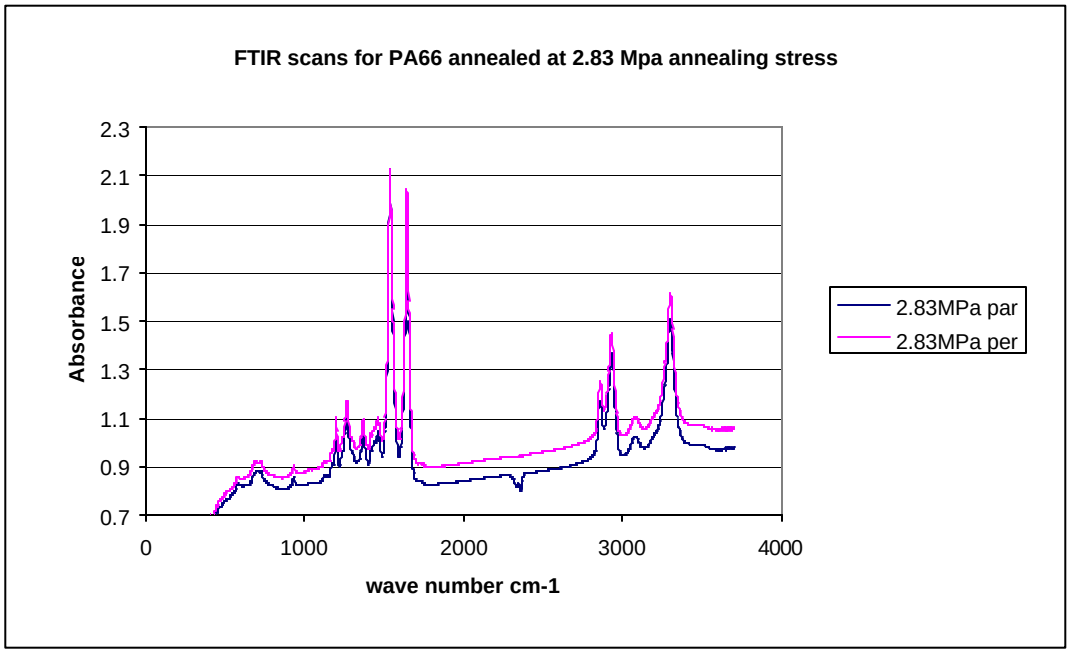

(e)

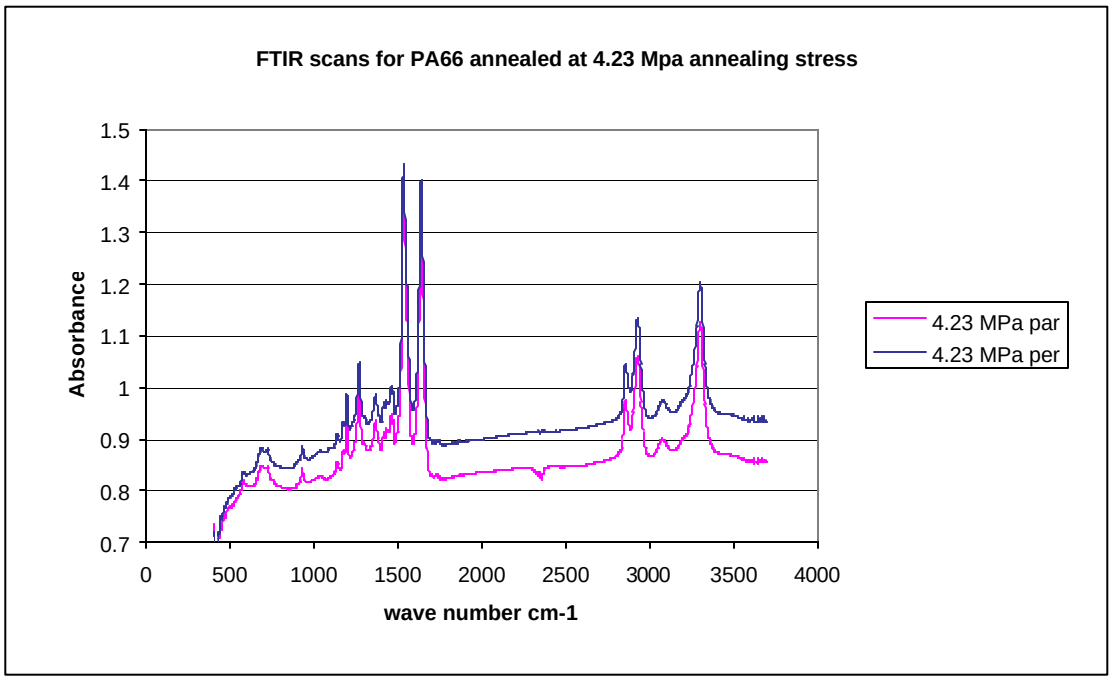

(f)

Figure 4.34 continued

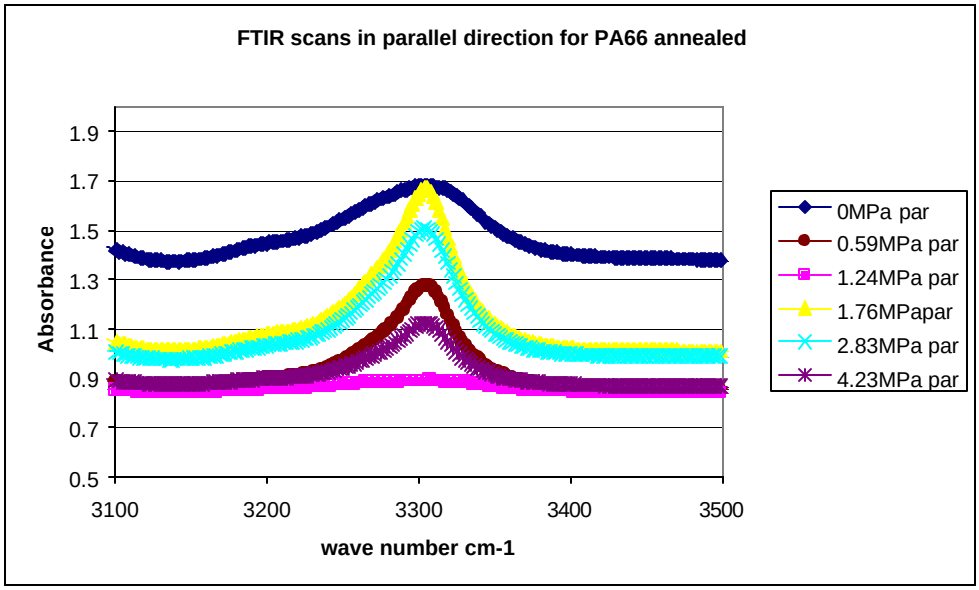

Figure 4.35 FTIR scans of anneled nylon 66 fibers measured with direction of IR rays parallel to direction of winding

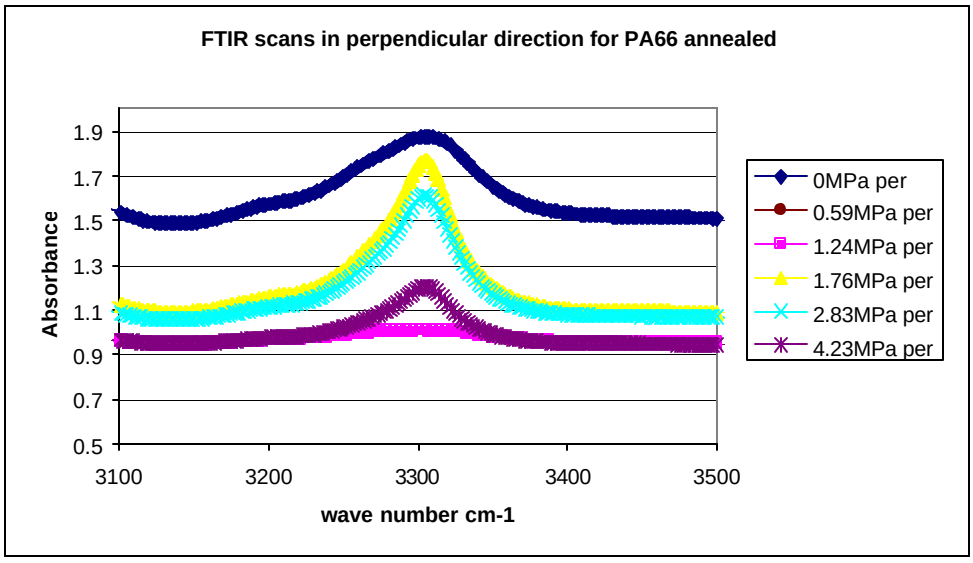

Figure 4.36 FTIR scans of annealed nylon 66 fibers measured with direction of IR rays perpendicular to direction of winding

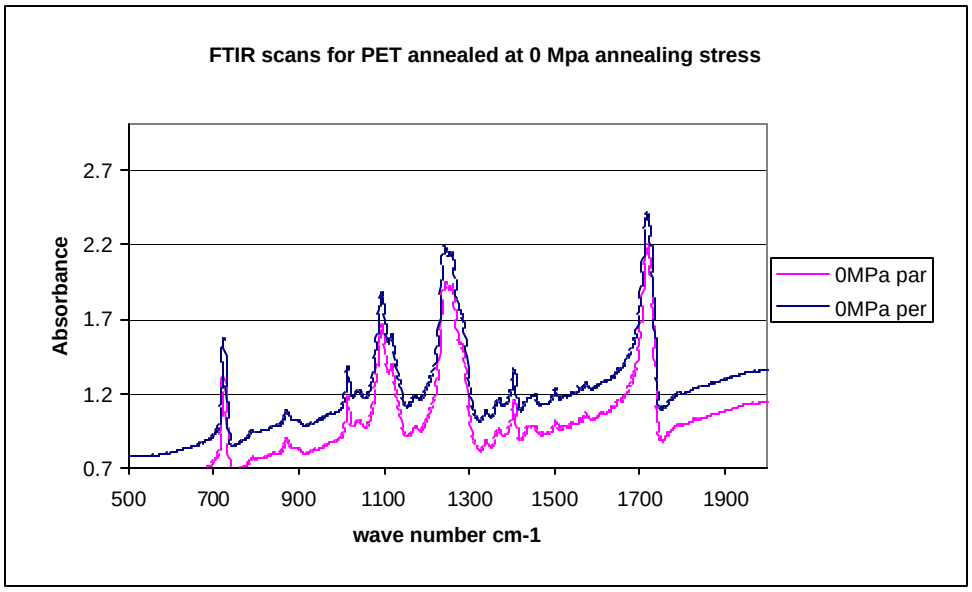

(a)

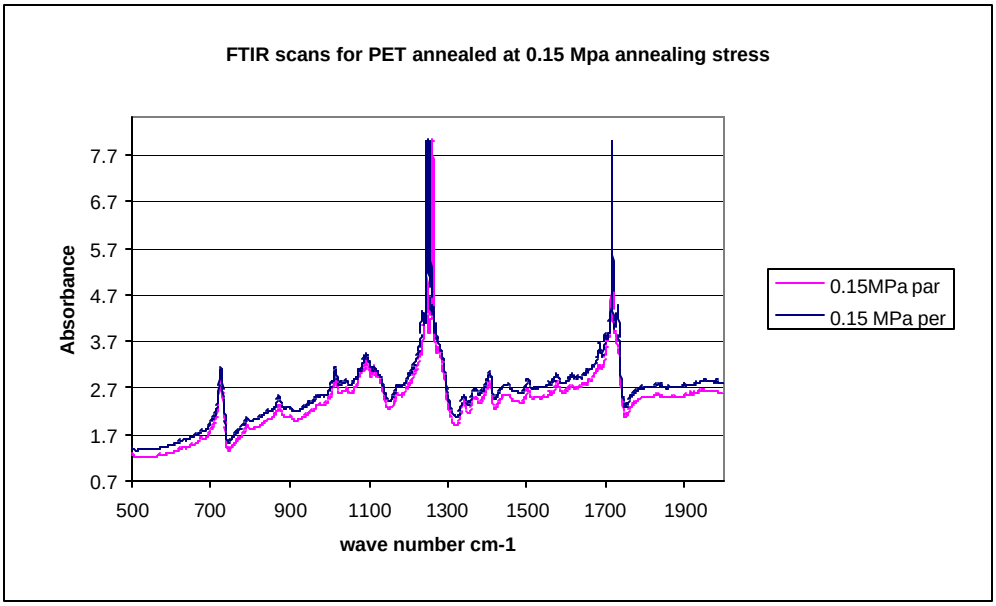

(b)

Figure 4.37 FTIR scans of PET fibers annealed measured with direction of IR rays parallel and perpendicular to direction of stretching with stress (a) 0 MPa, (b) 0.15 MPa, (c) 0.26 MPa, (d) 1.06 MPa, (e) 1.76 MPa and (f) 1.96 MPa

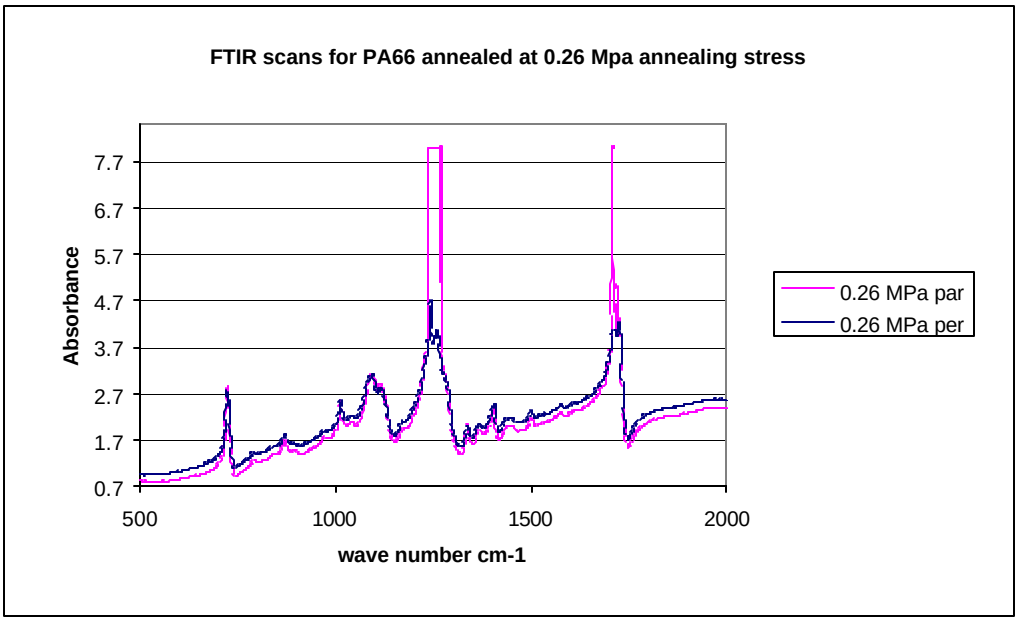

(c)

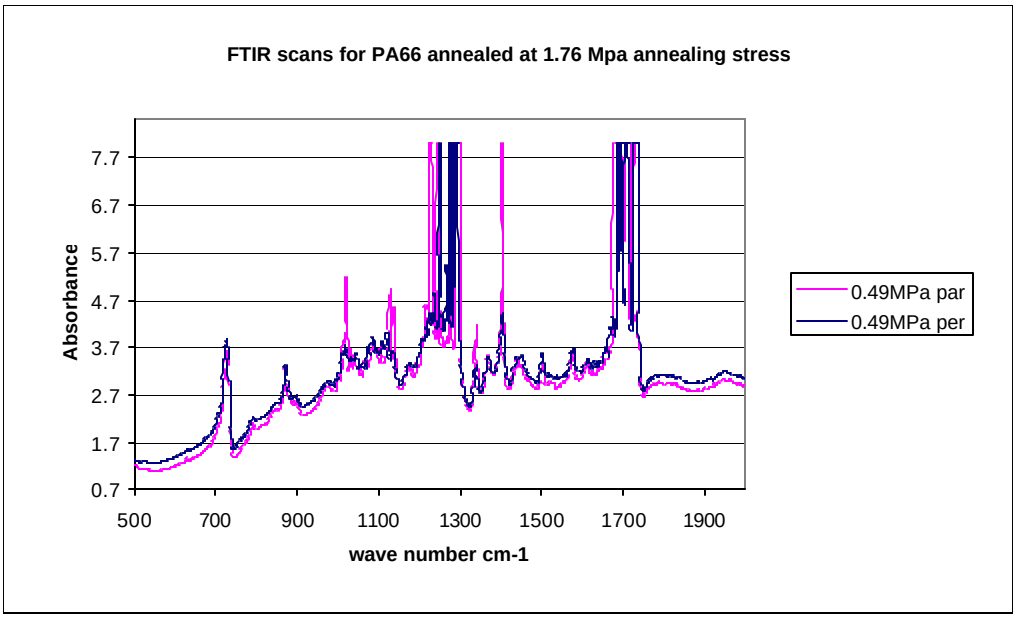

(d)

Figure 4.37 continued

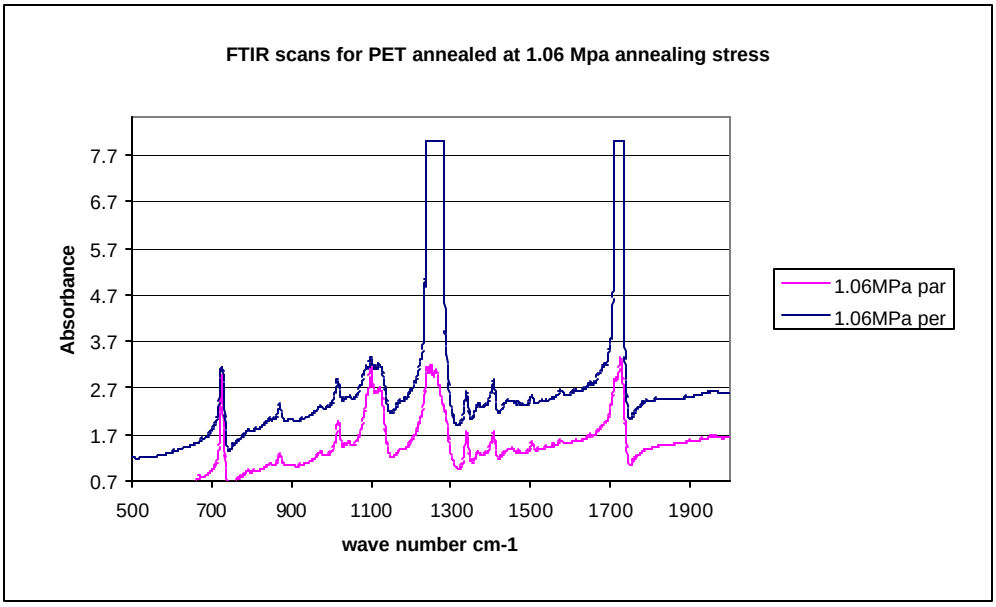

(e)

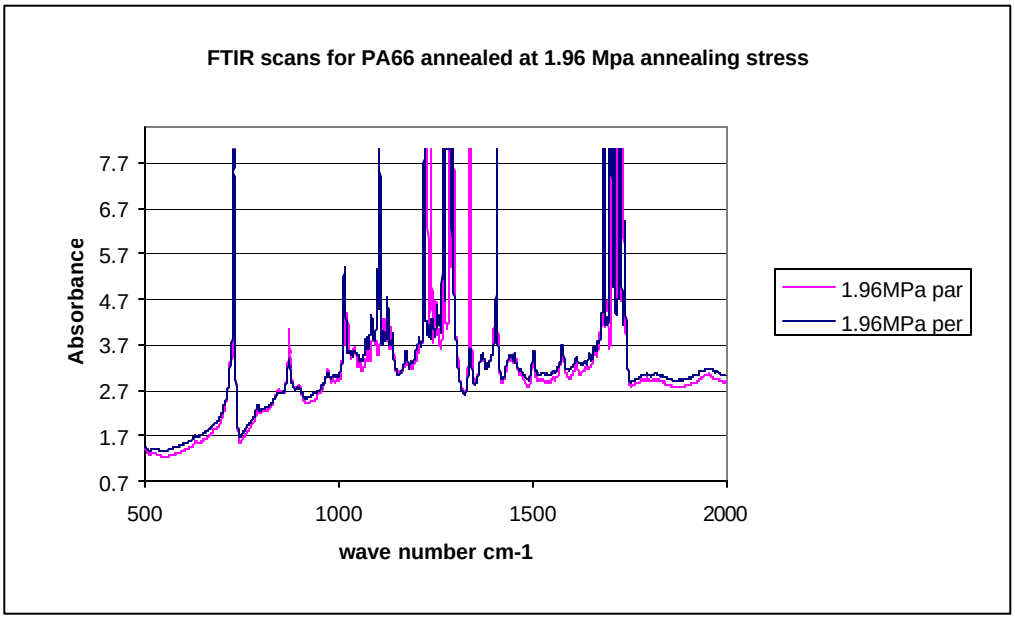

(f)

Figure 4.37 continued

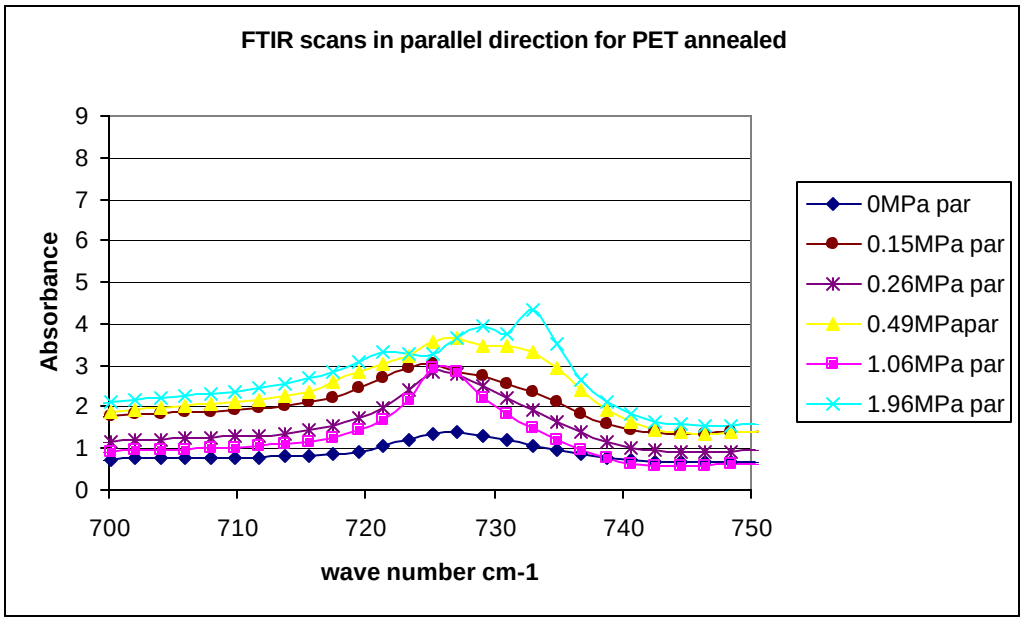

Figure 4.38 FTIR scans of annealed PET fibers measured with direction of IR rays parallel to direction of winding

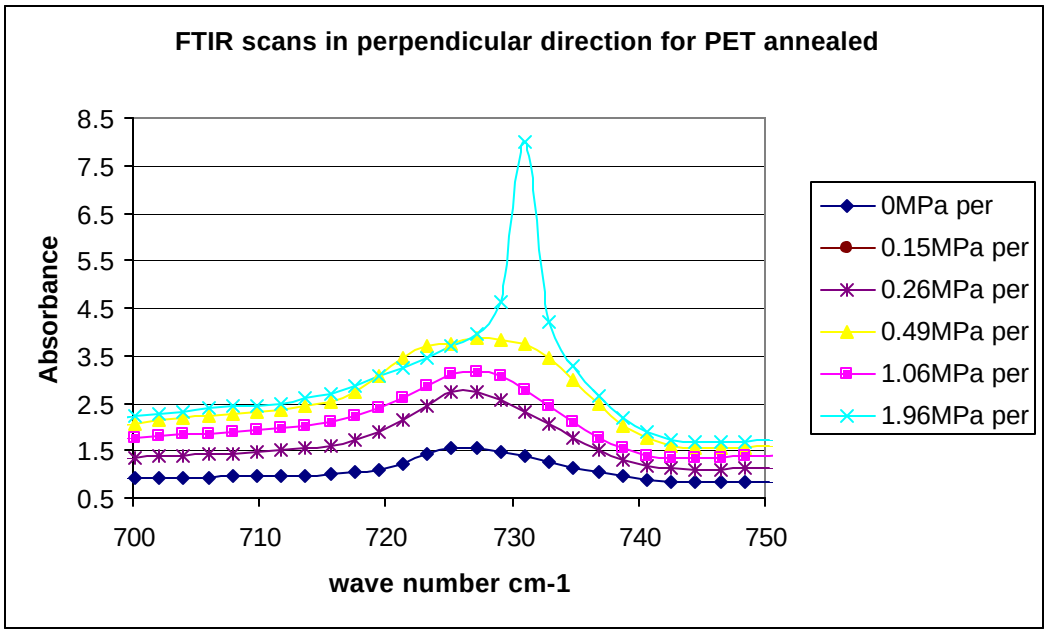

Figure 4.39 FTIR scans of annealed PET fibers measured with direction of IR rays perpendicular to direction of winding

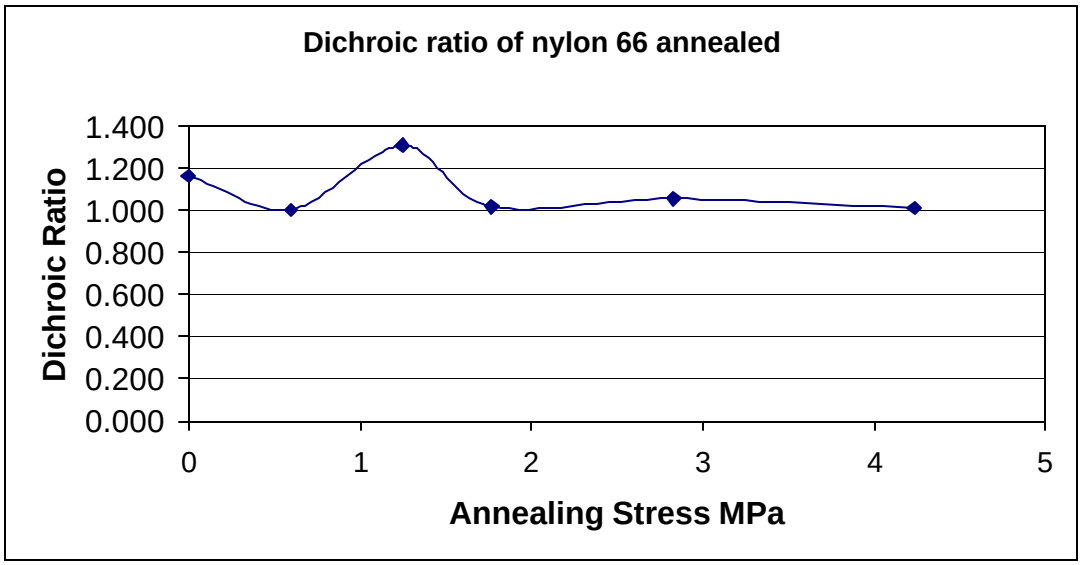

Figure 4.40 Dichroic ratio of nylon 66 fibers for peak at 3305 cm $^{-1}$ annealed at different loads.

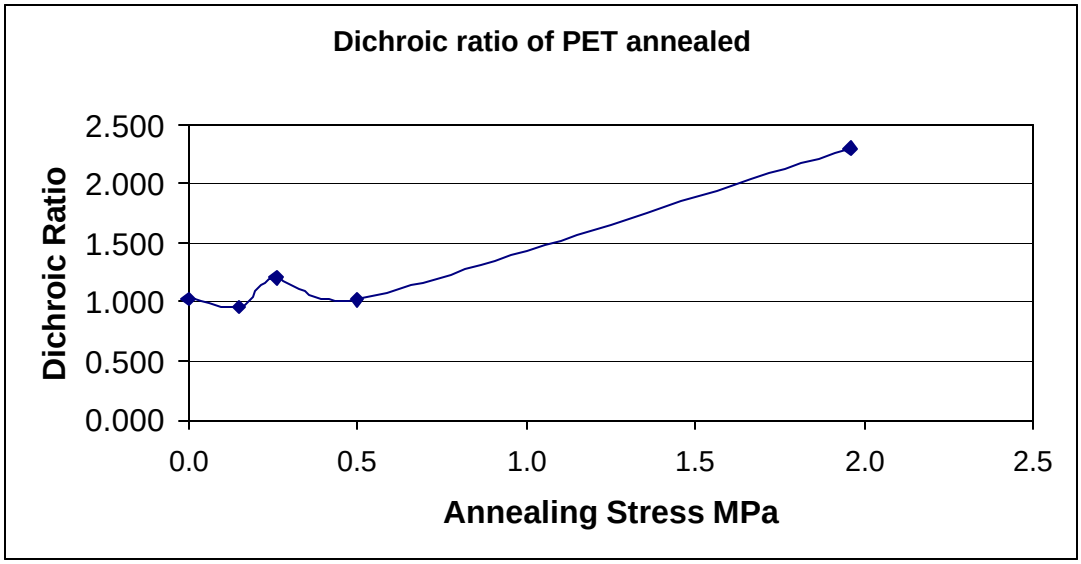

Figure 4.41 Dichroic ratio of PET fibers annealed at different loads.

The SEM pictures and the plot of dichroic ratio show that the orientation of fibers increases with annealing stress for poly(ethylene terepthalate) while no such orientation is observed in nylon 66 samples. The increase in dichroic ratio for poly(ethylene terepthalate) is comparable to the parallel dichroism observed for Vasanthan[18] for nylon 66 fibers.

4.4.2. Mechanical properties of annealed fibers

Nylon 66, PET and nylon66/PCL non woven mats annealed at 95°C under different constant loads for 1 hour are also tested for tensile modulus in the dynamic mechanical analyzer at a constant strain rate of 1.5% per minute. The Figure 4.42 shows the tensile results of fibers annealed under different loads. The nylon66 samples show an increase in tensile modulus with the increase annealing loads with a significant increase between 2 and 3 MPa as shown in Figure 4.43. The bundles of fibers of PET and nylon66/PCL were also tested for tensile modulus. The individual fibers from these samples failed at unpredictable strain percentages causing a multiple fracture of the sample. Hence an exact modulus for samples annealed at different loads could not be determined.

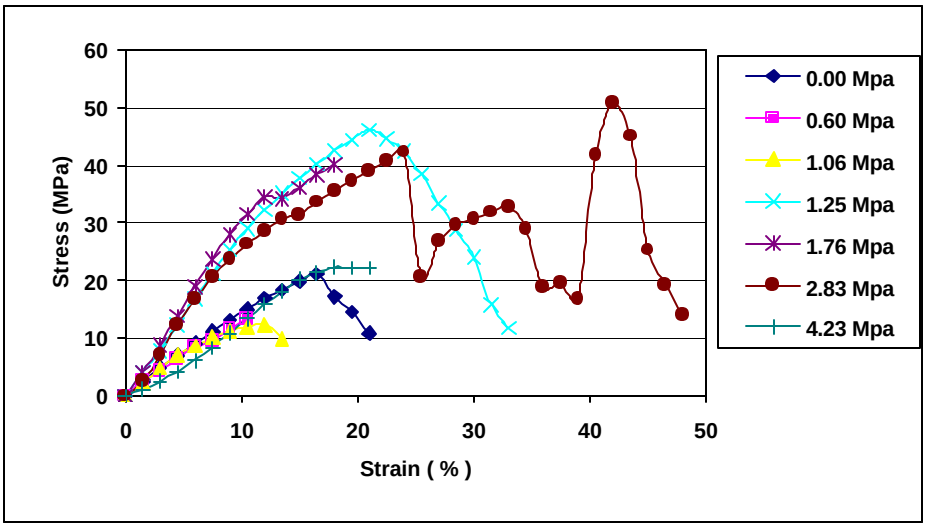

Fig. 4.42 Tensile results of nylon 66 fibers collected at different loads

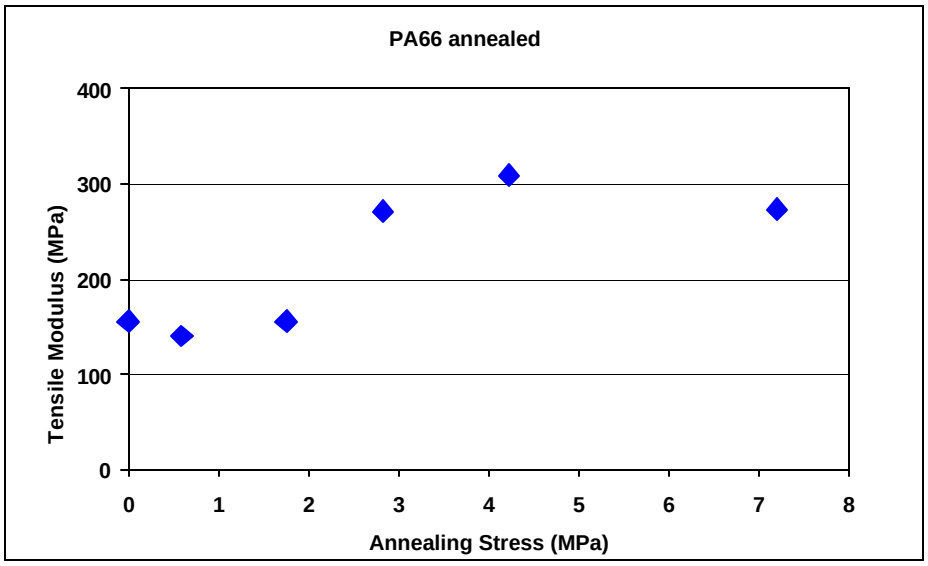

Fig. 4.43 Tensile modulus of nylon 66 fibers annealed at 95°c

4.4.3. Crystallinity of annealed fibers

The nylon 66, PET and nylon 66/PCL fibers annealed at 95°C under different constant loads for 1 hour are tested for crystallinity using the x-ray diffractometer. The DSC scans are also carried out for the annealed nylon 66 samples. Typical x-ray diffraction plot for the three samples are given in Figure 4.44- 46 and the measured crystallinity values is plotted in Figure 4.47. The PET and nylon 66/PCL samples show significant crystallinity as spun. However the crystallinity does not increase significantly with increase in annealing stress. The nylon 66 fibers show low crystallinity as spun but the crystallinity increases with the increase in annealing stress. The crystallinity of nylon 66 fibers measured by the two techniques is given in Figure 4.48. This difference, similar to the one observed for wound nylon 66 fibers, can be attributed to the presence of a crystalline-amorphous interphase layer that contributes to crystalline scattering but not the heat of fusion [29].

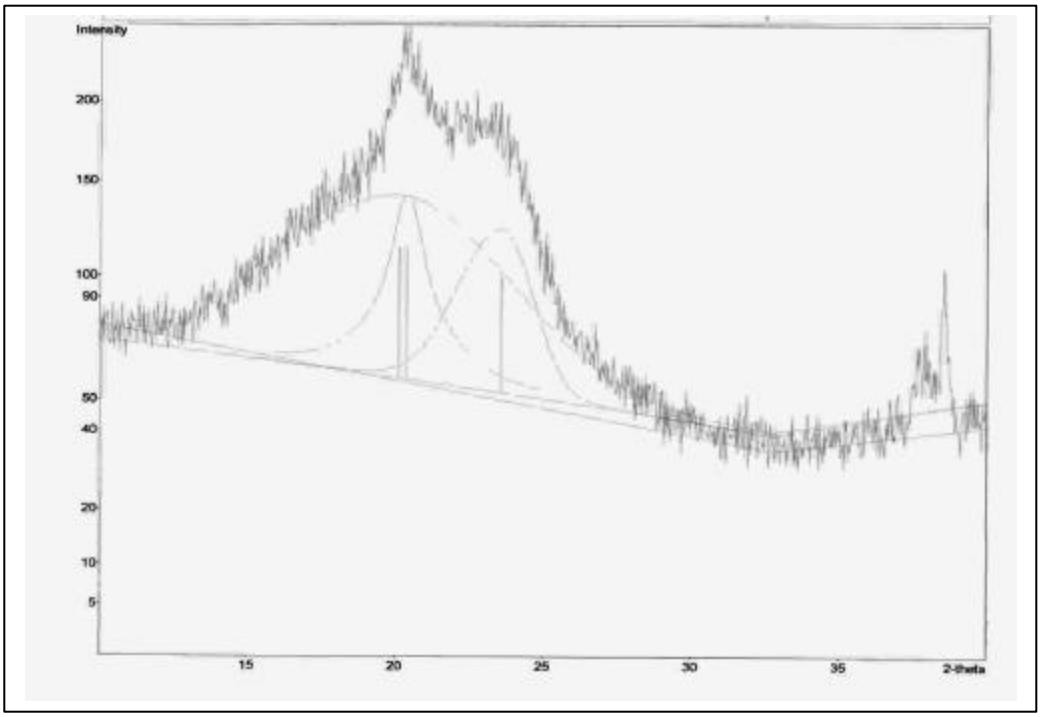

Figure 4.44 WAXD pattern for annealed nylon 66 fibers

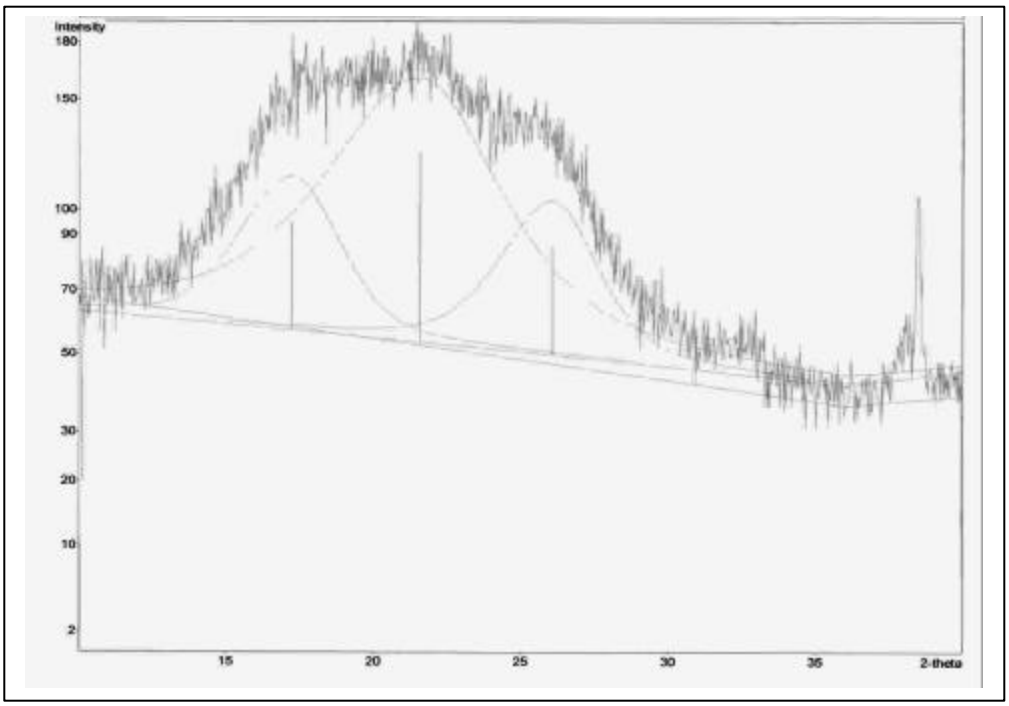

Figure 4.45 WAXD pattern for annealed PET fibers

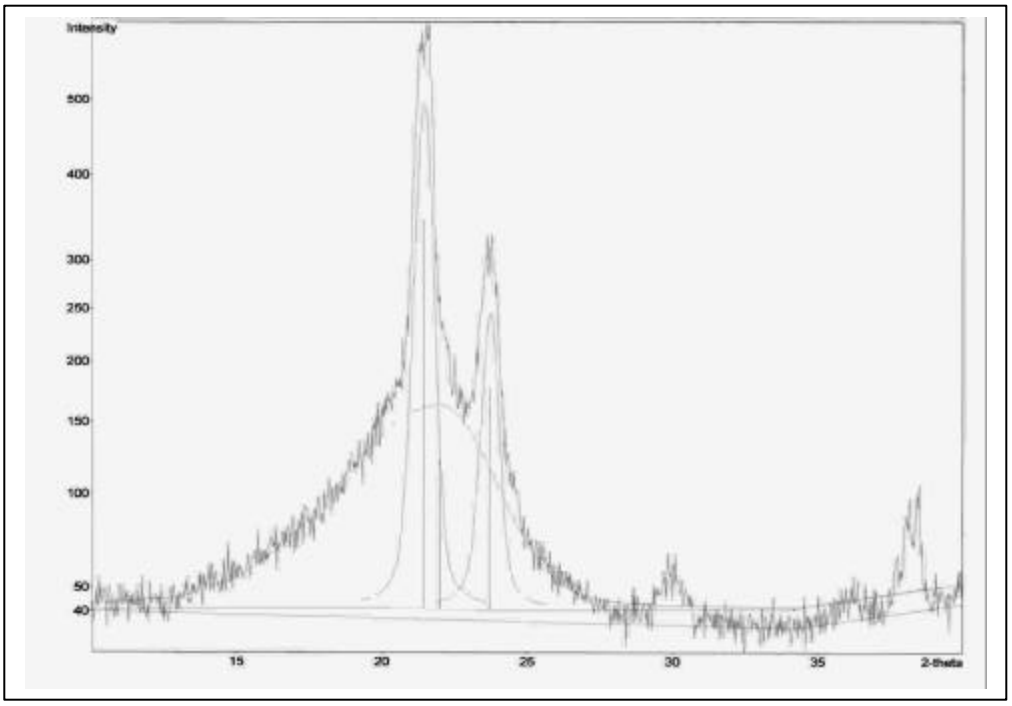

Figure 4.46 WAXD pattern for annealed nylon 66/PCL fibers

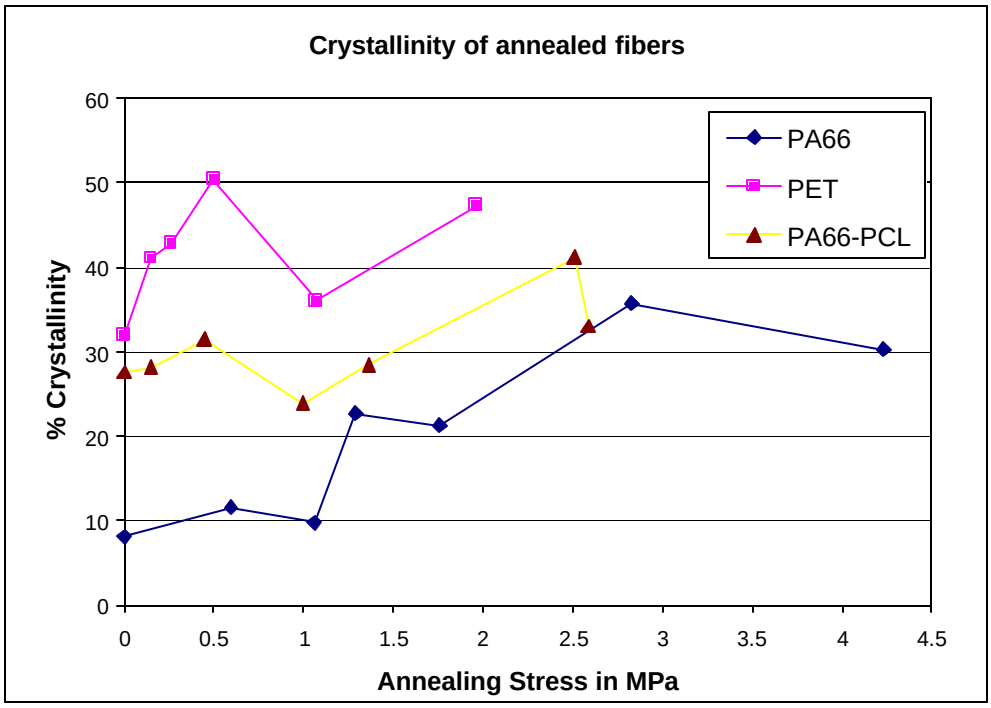

Fig. 4.47 Crystallinity of annealed fibers

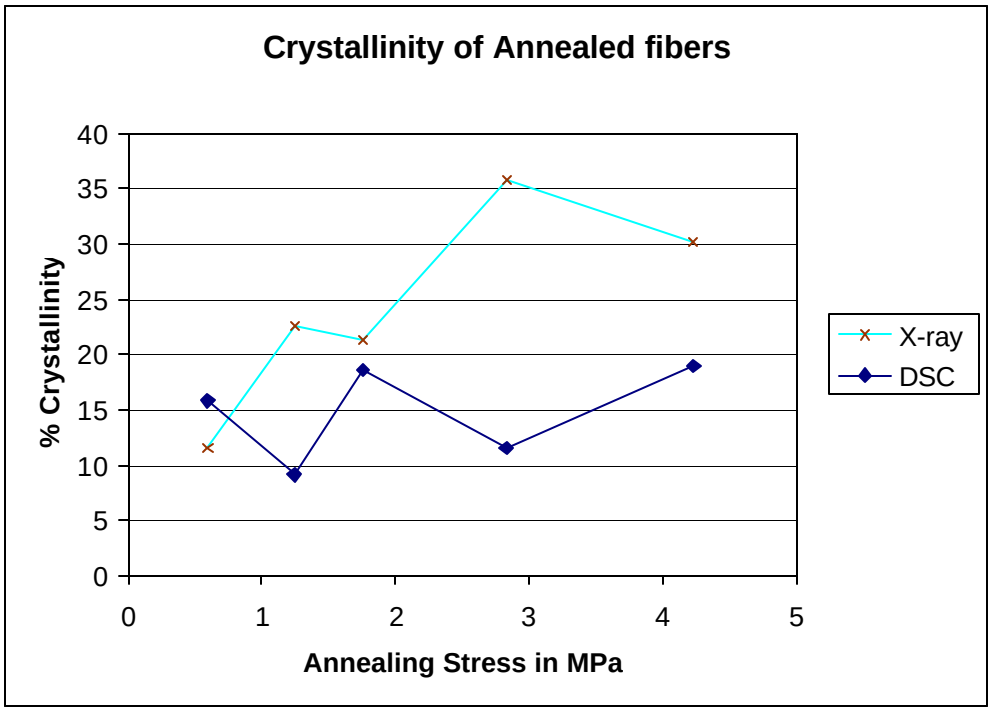

Fig. 4.48 Crystallinity of annealed nylon 66 measured by WAXD and DSC

The nylon 66, PET and nylon 66/PCL fibers were annealed at 95°C under different constant loads for 1 hour to improve the orientation of fibers, crystallinity and hence, the mechanical properties compared to the as spun fibers. The SEM picture shows a significant increase in orientation of poly(ethylene terepthalate) fibers annealed at 2 MPa stress while no such increase was noticed for the nylon 66 samples. The dichroism results of the nylon 66 and poly(ethylene terepthalate) also confirms the alignment of fibers noticed in SEM pictures. The increase in dichroism of fibers shown in Figure 4.40 indicates increase in molecular orientation along with the orientation of fiber noticed in Figure 4.32.

The PET and nylon 66/PCL samples show significant crystallinity as spun. However the crystallinity increases slightly with increase in annealing stress. The nylon 66 fibers show low crystallinity as spun but the crystallinity increases with the increase in annealing stress as given in Figure 4.46. These results are similar to the crystallinity values measured for nylon 66 by Vasanthan[18] and Salem[22]. This shows that stress induced crystallization may be occuring for nylon 66 samples while PET and nylon 66/ PCL samples does not show such change. The increase in modulus of the nylon 66 samples given in Figure 4.42 could be due to the increase in stress induced crystallization than molecular orientation of fibers.

Hence the modulus of the nylon 66 samples increases with annealing load due to the increase in percent crystallinity and crystalline orientation while the molecular orientation of fibers does not improve. The crystallinity of as spun poly(ethylene terepthalate) and nylon 66/PCL fibers is high but does not increase with increase in annealing load. However the molecular orientation of the poly(ethylene terepthalate) fibers increases with annealing load and can likely improve the mechanical property of fibers.

4.5. Effect of moisture on polymer fibers

The electrospun fibers spun do not always have regular morphology and is often characterized by bead defects in regular array. The morphology of nylon 6 fibers spun during the earlier stages of the project showed a membrane like structure given in Figure 4.51. This membrane like structure is likely due to incomplete evaporation of solvent. An attempt was made to produce a blend of nylon 6 and nylon 66 so that the membrane like morphology observed in nylon 6 could be used to increase the bonding between more homogenous nylon 66 fibers as shown in Figure 4.49. This could result in superior mechanical properties compared to the fibers of individual polymers.

Figures 4.50 - 52 shows the effect of variation in composition on fiber structure of nylon 6, nylon 66 and their blend. The nylon 66 polymer at 10 wt% concentration, as shown in figure 4.50, resulted in more of fiber morphology when spun at voltage of 10 kV with target at 10 cm from the capillary. The nylon 6 polymer, given in figure 4.51, produced a structure more like a condensed mat. The blends of the two polymers, given in figure 4.52, showed regions characteristic of the individual polymers with increase in fiber like structure with increase in the concentration of the nylon 66 fibers. However, we were not able to reproduce the membrane like morphology more than once. The nylon 6 fibers produced more uniform fibers like nylon 66 on the second attempt to produce them. The distance between tip of the syringe and the target is also varied from 10 cm to 30 cm to see if there is difference in morphology. The SEM images given in Figure 4.53 show no significant changes in the morphology. Hence, nylon 6 and nylon 66 fibers are spun from solution with different concentrations of water in terms of weight percentage to test the effect of moisture on the structure of these fibers. The morphology of nylon 66 fibers with different weight percentage of water is shown in Figure 4.54. Similar effects were also found in nylon 6 fibers. The increase in water content results in inconsistency in the morphology of fibers with increase in amount of beads in the fibers. The tensile results of these fibers with varying moisture

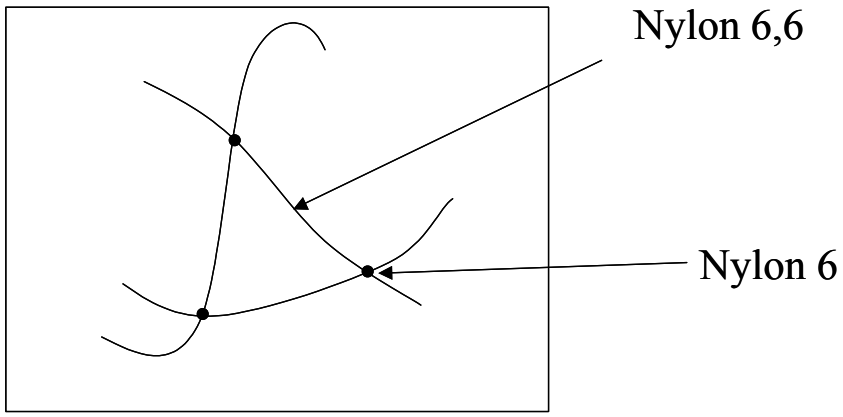

Figure 4.49 Assumed morphology of nylon 66 with small amount of nylon 6 added to improve the mechanical property.

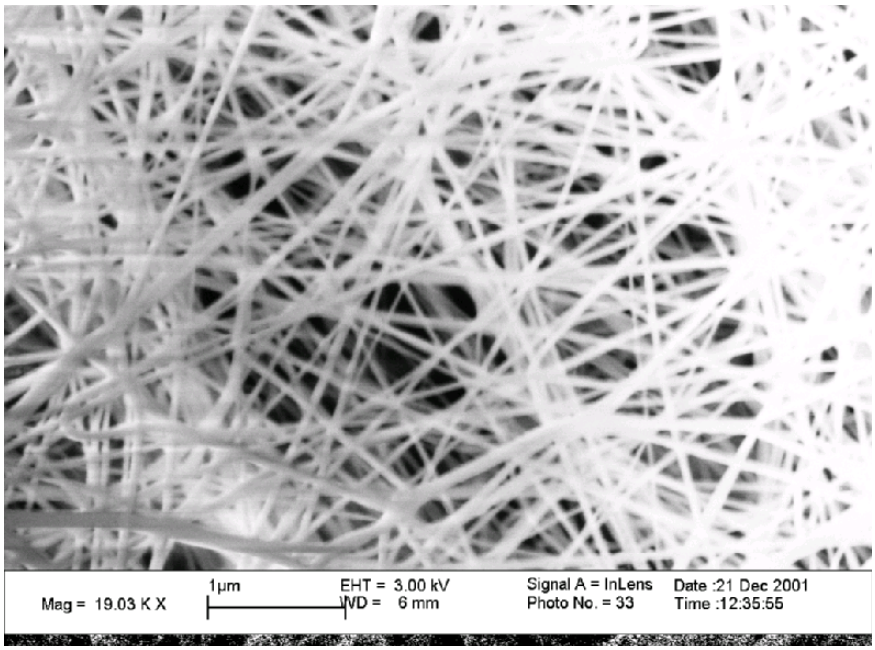

Figure 4.50 Neat nylon 66 fibers at 10 % solution concentration

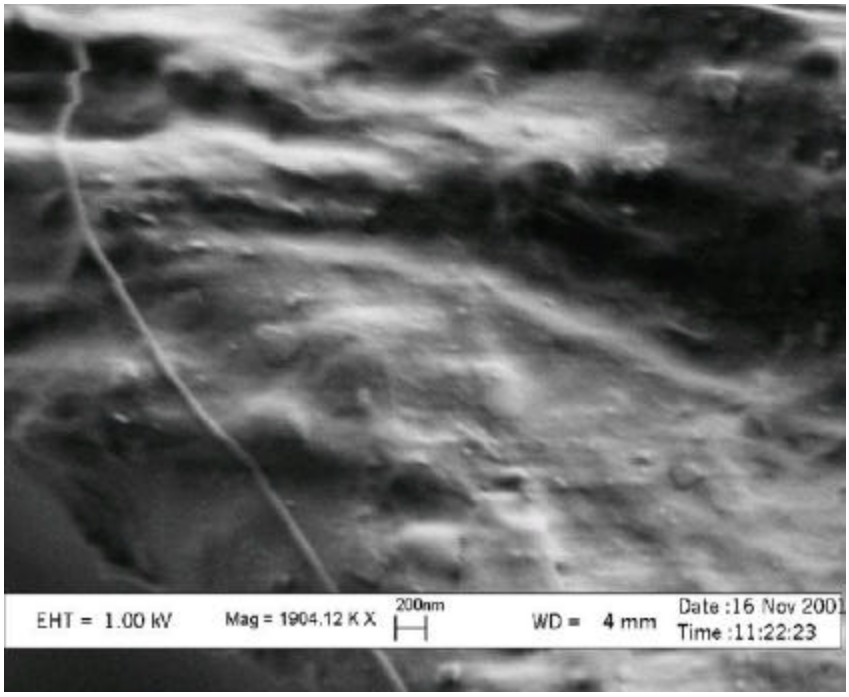

Figure 4.51 Neat nylon 6 fibers at
10 % solution concentration

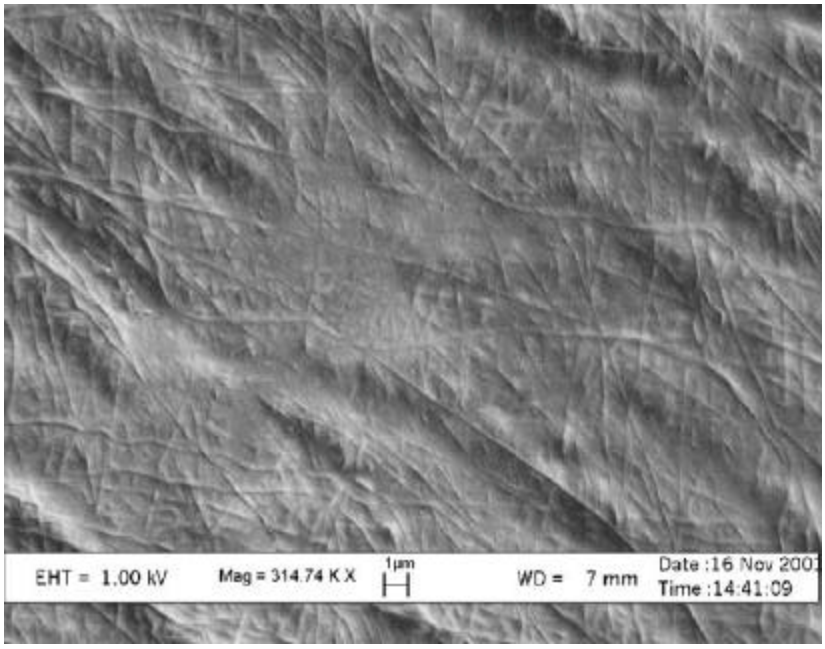

Figure 4.52 Nylon 6-66 50 – 50 blend
at 10% solution concentration

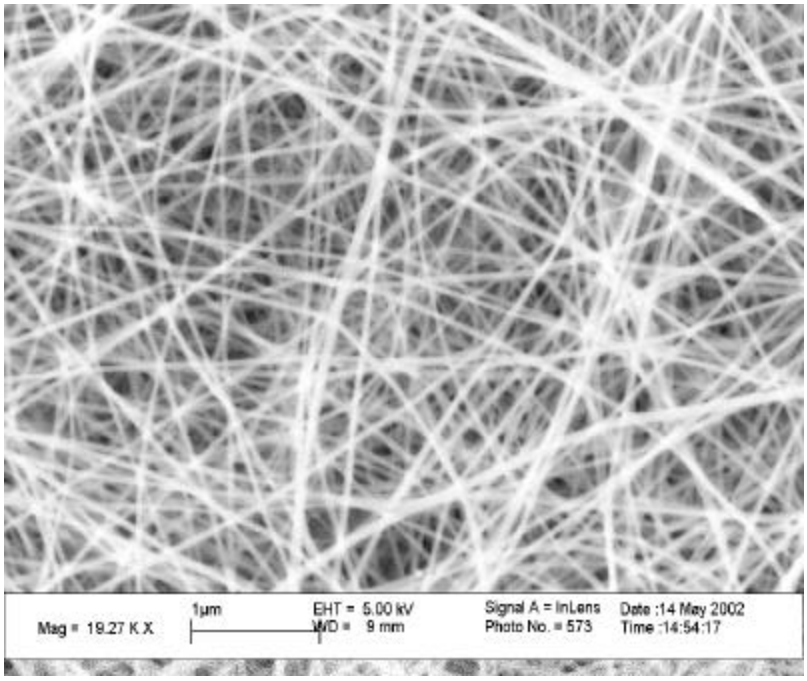

(a)

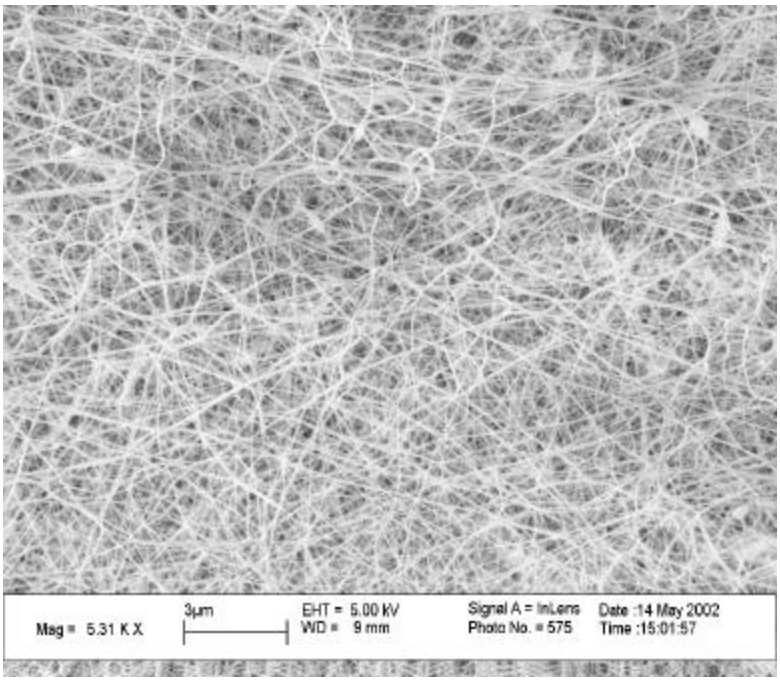

(b)

Figure 4.53 Morphology of nylon 6 spun from a target distance from the syringe (a) 10cm, (b) 20cm and (c) 30cm

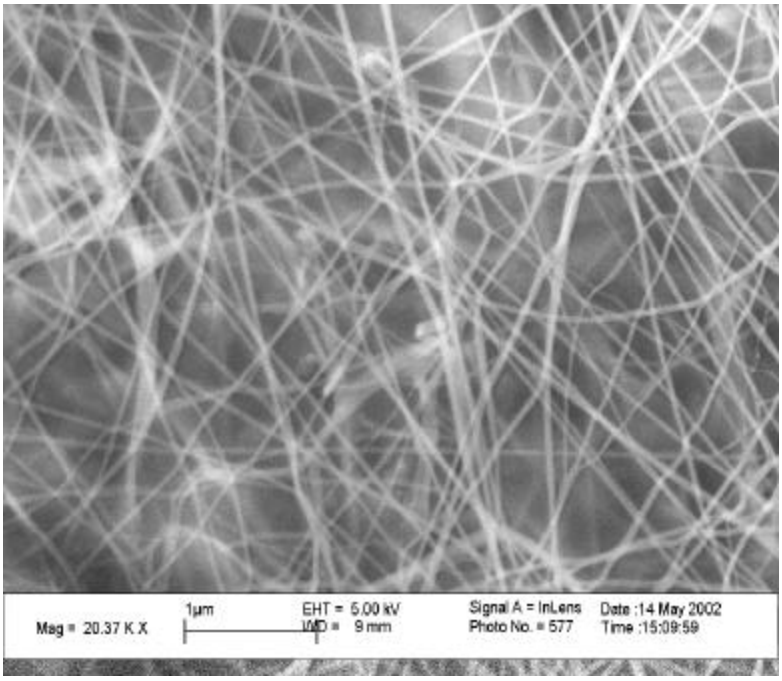

(c)

Figure 4.53 continued

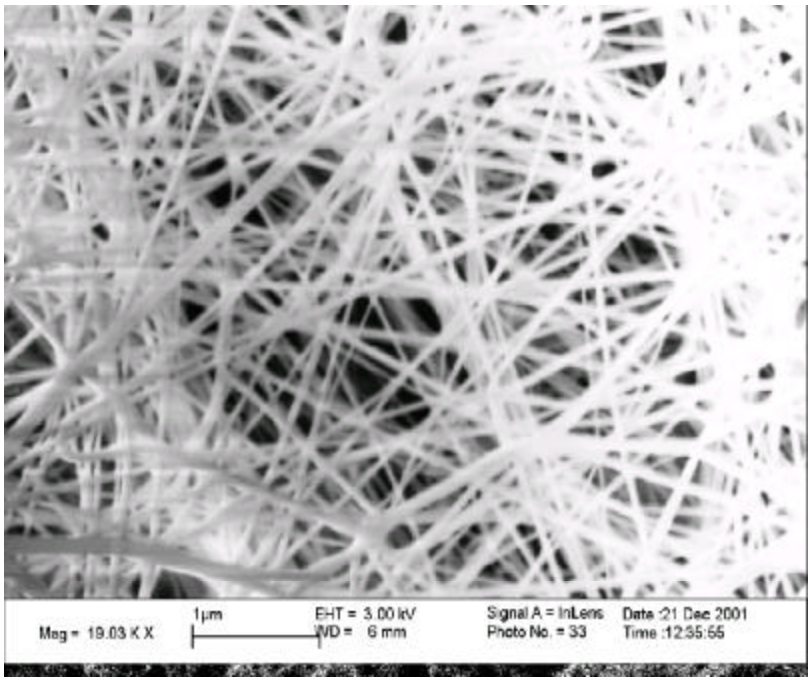

(a)

Figure 4.54 Morphology of nylon 66 spun with water (a) 0%, (b) 5%, (c) 10% and (d) 20%

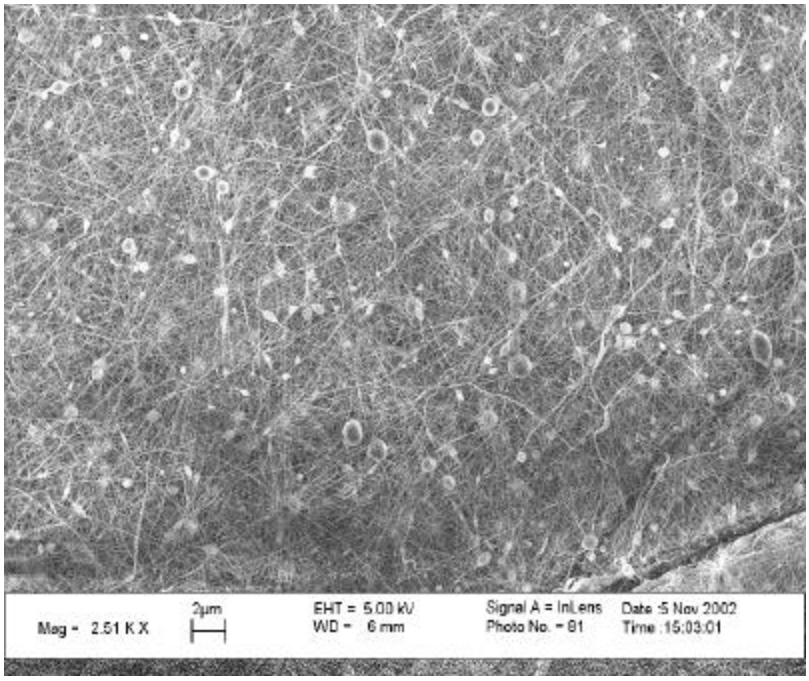

(b)

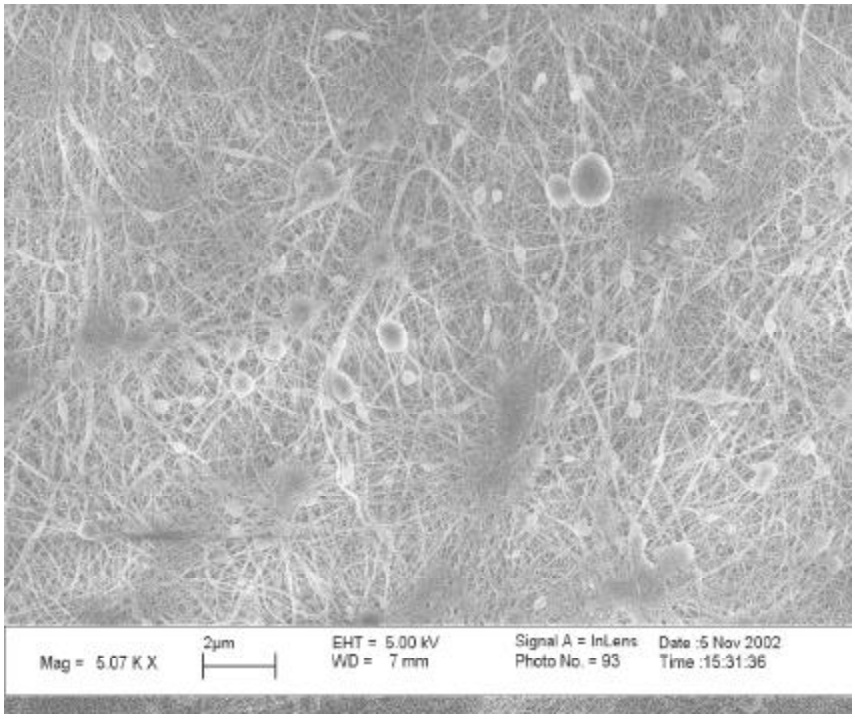

(c)

Figure 4.54 continued

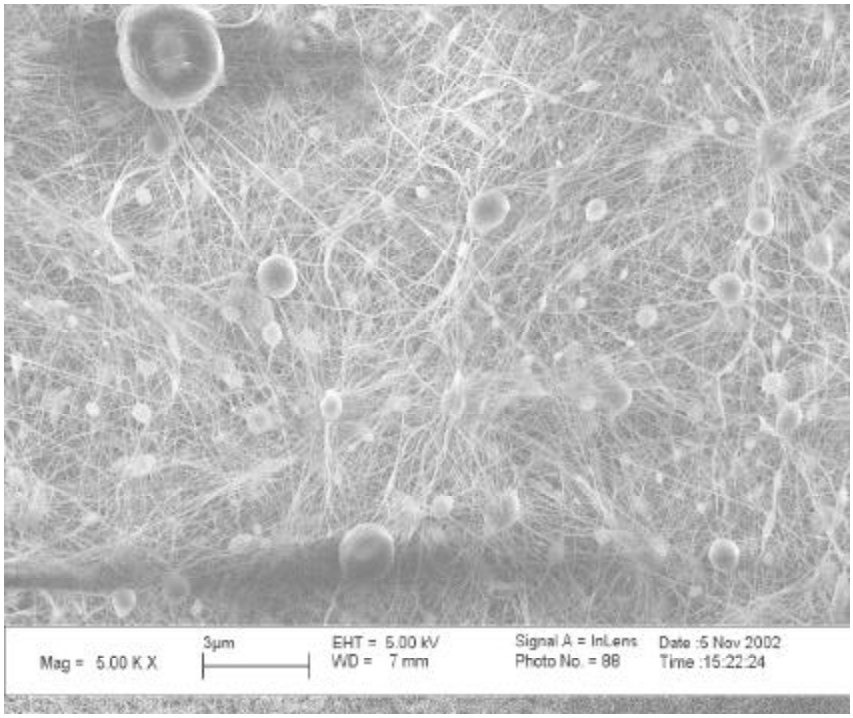

(d)

Figure 4.54 continued

content are shown in Figure 4.55 – 56. The presence of water also causes a plasticizing effect on the electrospun fibers as the tensile strength of the fibers decreases with increase in water content. The improvement in the mechanical properties expected is overwhelmed by the plasticizing effect of the water present. The Figure 4.57 shows the tensile results of nylon 6 fibers dried at room temperature for 24 hours and at 40°C for 24 hours. A significant improvement in modulus of the fibers is also observed for the dried samples compared to the as-spun as shown in Figure 4.57.

4.6. Electrospinning from organic solvents

Previous studies show that polymers spin well from acidic solutions having higher charge density. However experiments done to spin polymers like polystyrene and

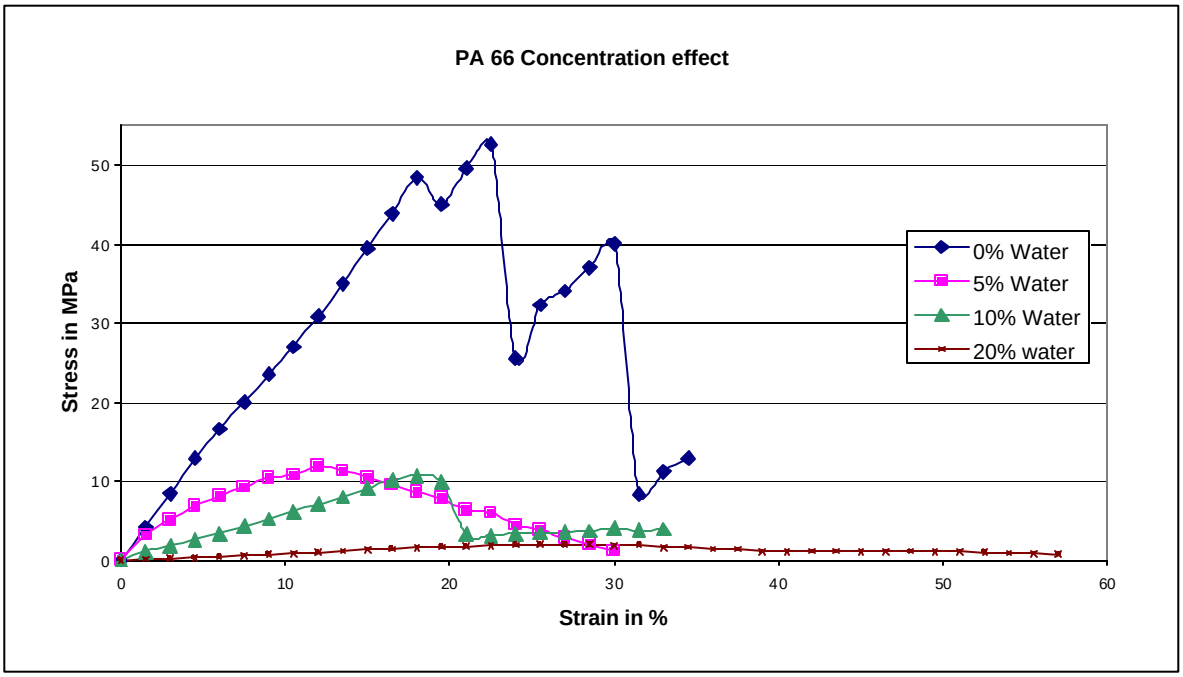

Figure 4.55 Tensile results of nylon 66 with 5, 10, 20 wt% concentrations of water

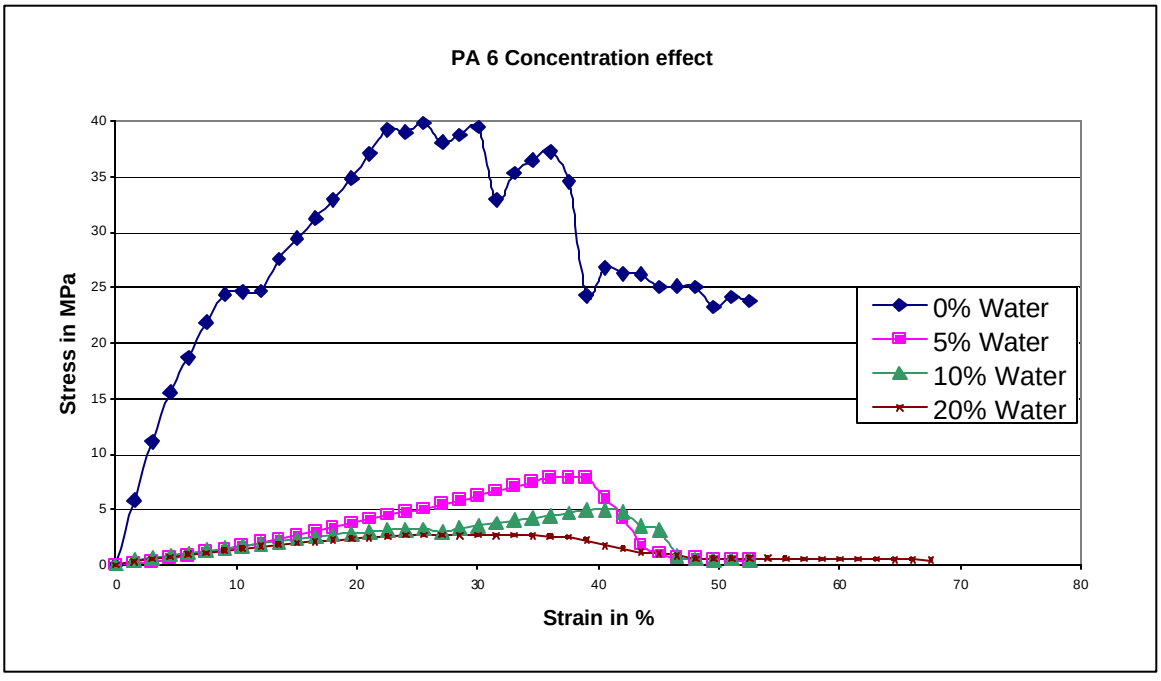

Figure 4.56 Tensile results of nylon 6 with 5, 10, 20 wt% concentrations of water

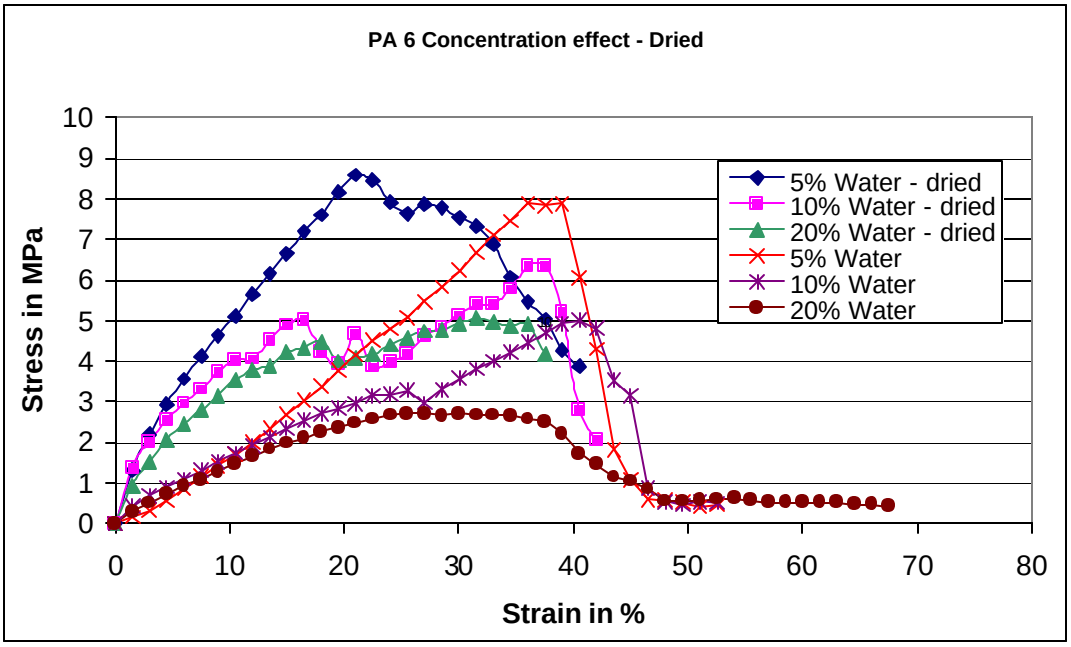

Figure 4.57 Tensile results of nylon 6 with 5, 10, 20 wt% concentrations of water and samples dried at room temperature / 40°C.

poly(methylmethacrylate) from organic solvents have shown poor processability due to low charge carrier density in organic solvents. The conductivity resistivity meter YSI model 34 with standard dip type cell with constant 10 S/cm was calibrated with a solution of sodium chloride in water. The conductivity of THF and a solution of THF with different concentrations of salts – lithium perchlorate, sodium chloride, potassium chloride and potassium iodide are measured to find the solution with maximum charge carrier density. The conductivity of solutions with various salts is given in Figure 4.58. The solution of $LiClO_4$ and KI in THF shows the maximum conductivity and hence were used spin the polystyrene and poly(methylmethacrylate).

The morphology of polystyrene/poly(methylmethacrylate) spun from THF with approximate diameter of fiber as 2 microns and that of beads as big as 10 microns without addition of any salt is shown in Figure 4.59. A non-uniform morphology was observed with many bead defects in the fibers. However, the PS/PMMA system produced more uniform and smaller fibers when electrospun with the charge enhancing agent

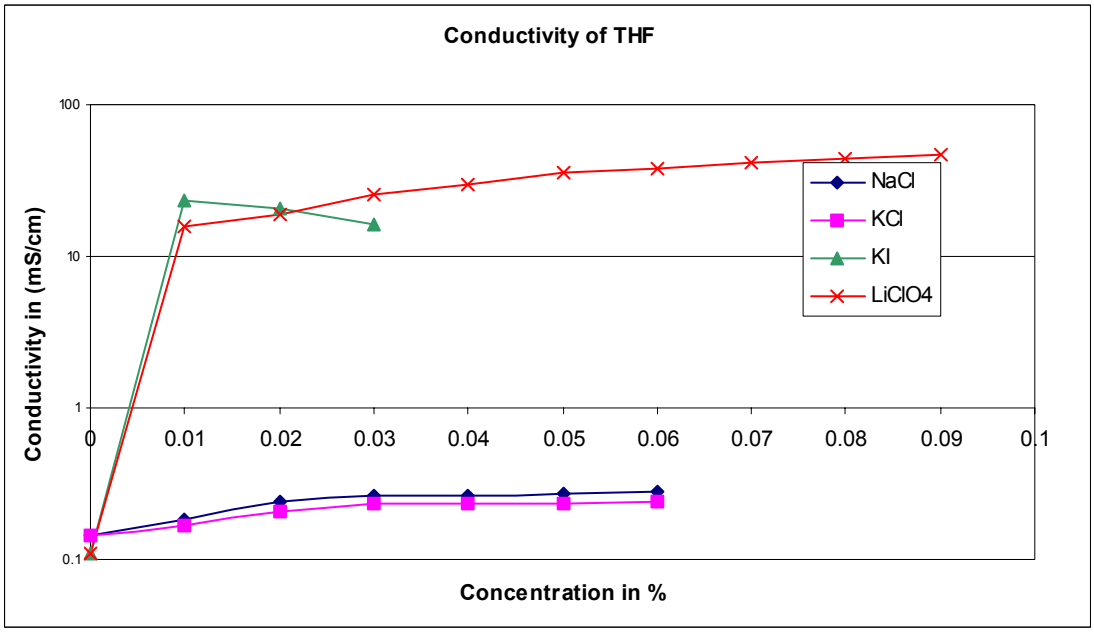

Figure 4.58 Increase in conductivity of tetrahydrofuran with addition of salts

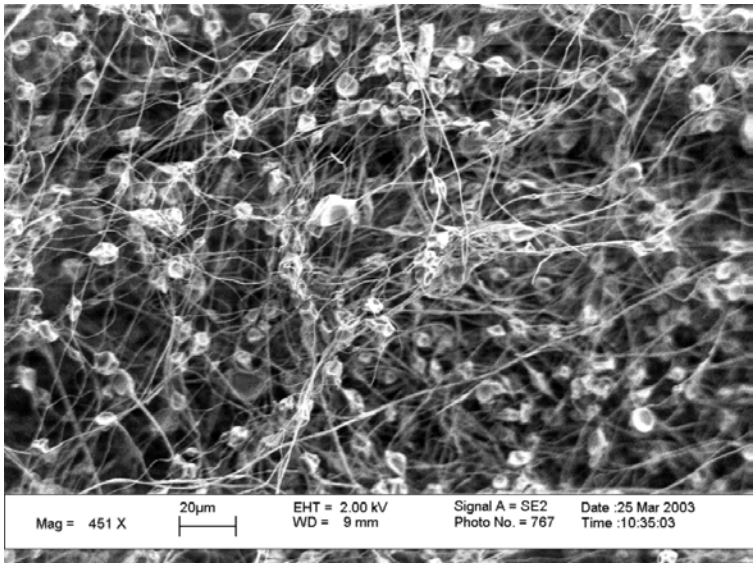

Figure 4.59 Morphology of PS/PMMA spun from THF

$LiClO_4$ shown in Figure 4.60. The bead defects were completely eliminated and fibers with more uniform morphology is produced. Similar effects were observed when the polystyrene and PMMA were spun alone with THF. The PS fibers spun with the additive $LiClO_4$ show more uniform morphology than those spun with KI as shown in Figure 4.61-62. Elimination of bead defect is extremely important if homogenous non-equilibrium blend is desired as a fine morphology in which solvent can evaporate very quickly is required.

4.7. Electrospinning of polymer blends

When polymer blends are spun from a common solvent using the electrospinning process, there is possibility of phase separation like any other method used to produce polymer fibers. But the rapid evaporation of the solvent may prevent phase separation;

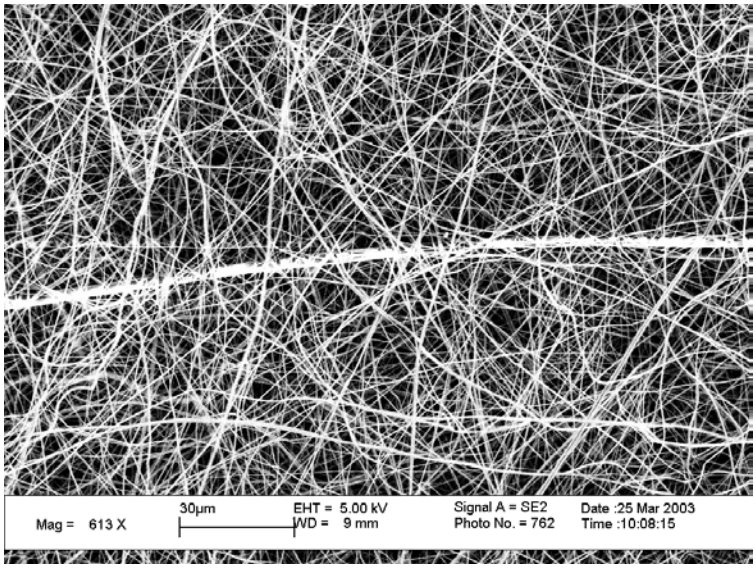

Figure 4.60 Morphology of PS/PMMA spun from

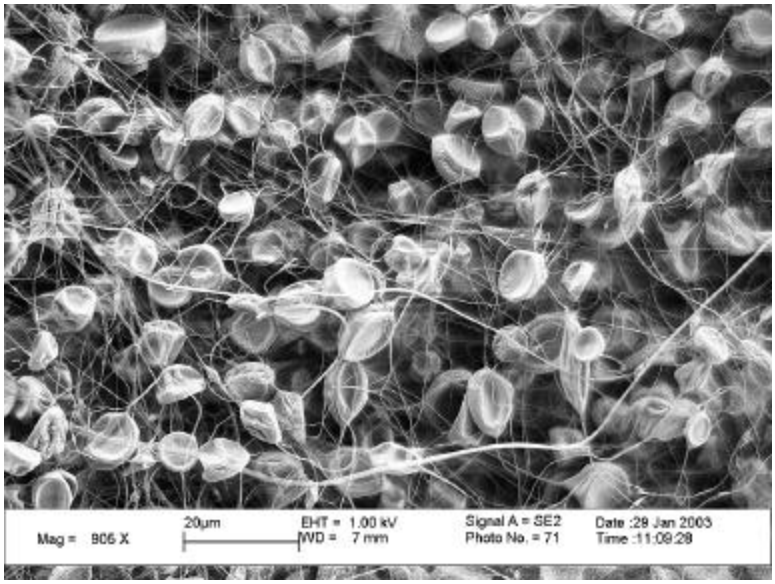

Figure 4.61 Morphology of PS spun from THF/1% KI

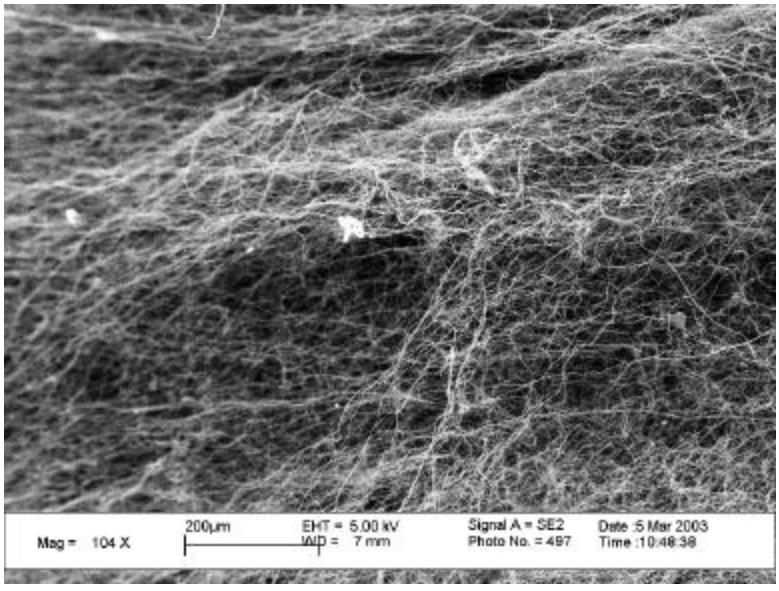

Figure 4.62 Morphology of PS spun from THF/1%LiClO4

making this method suitable to produce a homogenous phase for almost any polymer pair that is melt immiscible but soluble in a common solvent. The homogenous blend can be annealed to allow phase separation to occur which can result in very fine nano-scale morphology, depending on annealing conditions. The final morphology of these immiscible blends, often difficult to control, is determined by the processing conditions and the properties of its components. The polymer systems listed in the Table 4.2. are used to study the possibility of formation of polymer blends fibers produced by the electrospinning process. The clarity of the solution is checked inside the syringe and at the tip of the capillary to assure the miscibility of the system. The solutions that were cloudy either in the bulk solution or at the tip of capillary are phase separated, and hence were not spun.

Table 4.2 Polymer blend systems used to study the formation of fibers of polymer blends by electrospinning process

Polymer (10 wt%) + Solvent	**Bulk Solution**	**Solution at Capillary Tip**	**Comments**
nylon 6/nylon 66 in formic acid	clear	clear	Phase separated?
PC/PS in toluene/chloroform	clear	clear	Phase separated?
PMMA/PS in THF	clear	clear	Phase separated?
PMMA/PVC in THF	clear	clear	Powder only
PMMA/PC in THF	clear	clear	Powder only
nylon 66/nylon 6(3)T in formic acid	clear	cloudy (even at 2.5%)	Did not spin

As given in Table 4.2, nylon 66/ nylon 6(3) T polymers in formic acid were phase separated even in liquid phase and hence were not spun. The poly(vinyl chloride) / poly(methyl methacrylate) system and polycarbonate / poly(methyl methacrylate) systems did not produce any fibers when spun from a solution of tetrahydrofuran. The nylon 6/66, polycarbonate/polystyrene, polystyrene/poly(methyl methacrylate) and the nylon 66 / polycaprolactone systems produced fine fibers when spun from a common solvent. The Tg of polystyrene, polycarbonate and poly(methyl methacrylate) are 90, 155 and 100°C respectively. The polycarbonate/polystyrene and polystyrene/poly(methyl methacrylate) systems seem to be phase separated due to the presence of 2 Tgs as shown in DMA results given in Figures 4.63 – 66. The shift in Tg's observed in PS/PMMA system may be due to the presence of $LiClO_4$ salt in it. The increase in modulus noticed can be due to evaporation of solvents noticed at those temperatures. The reason for the lower value of modulus observed is that the dynamic mechanical test was conducted in the web structure instead of individual fibers. Further studies have to be made to spin polymer blends as a single phase by trying different solvents and use of different salts to improve conductivity of solvents.

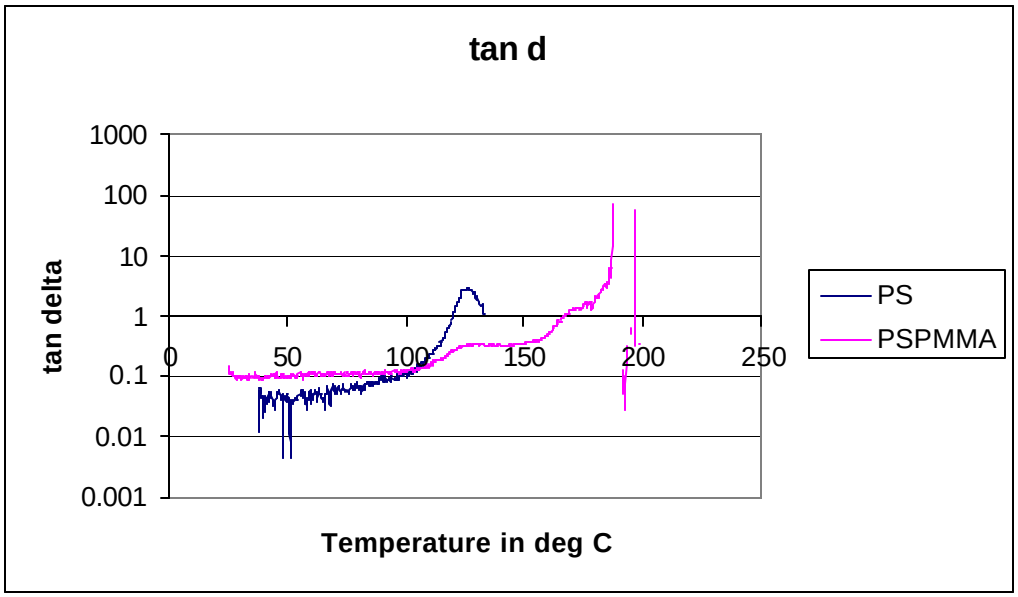

Figure 4.63 Tan delta of polystyrene/
poly (methyl methacrylate).

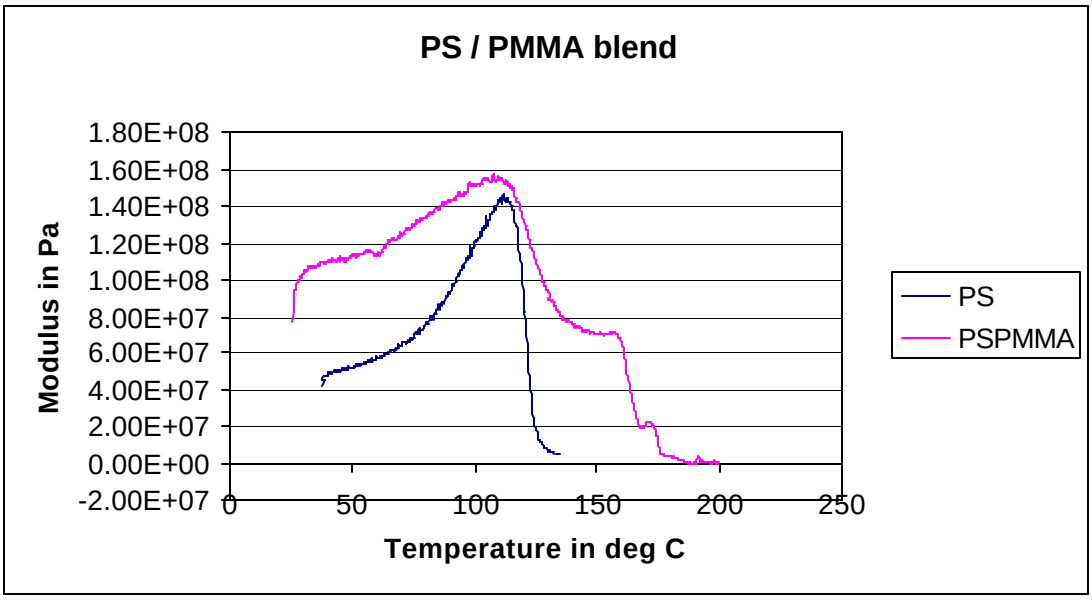

Figure 4.64 Storage modulus of polystyrene/
poly (methyl methacrylate).

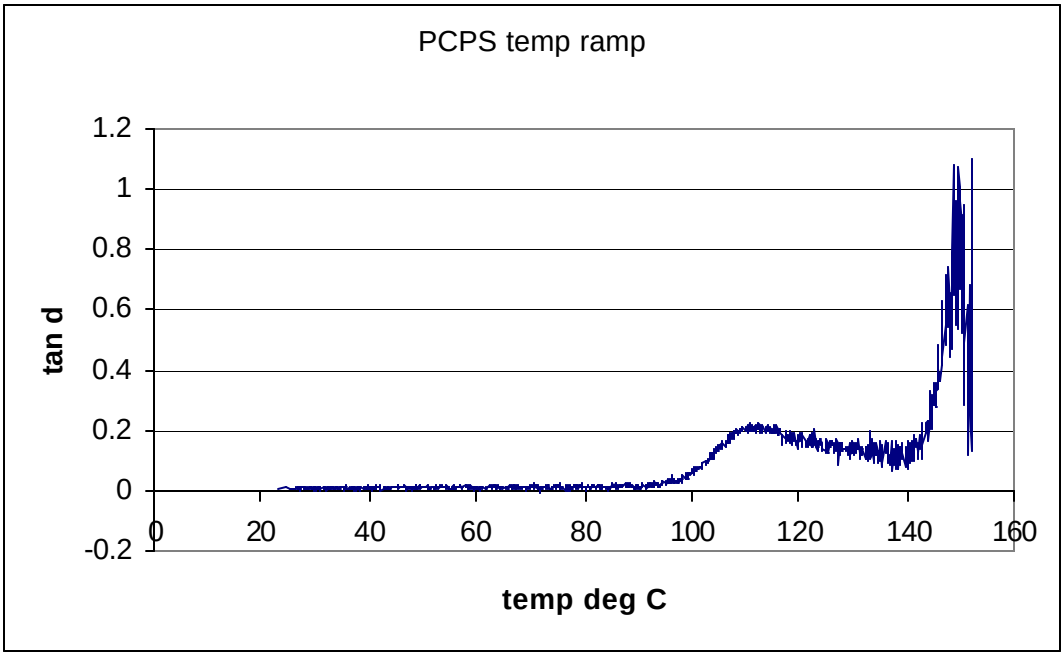

Figure 4.65 Tan delta values for polystyrene/polycarbonate.

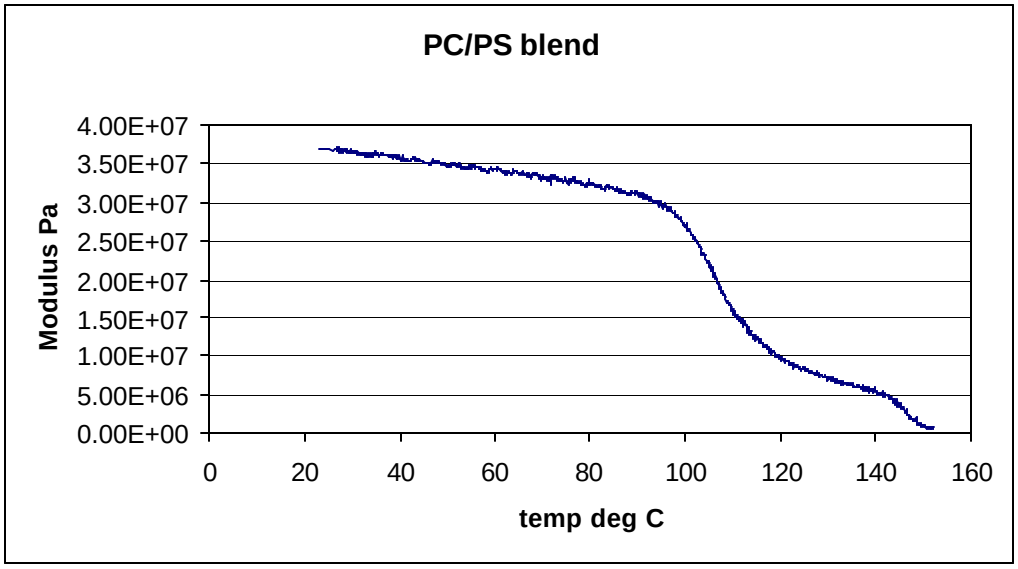

Figure 4.66 Storage modulus of polystyrene/polycarbonate.

Chapter 5

Summary and Conclusions

Electrospinning is an effective process to increase the surface area of the polymer fabric by reducing the diameter of fibers. The polymers used for electrospinning are nylon 6, nylon 66, poly(ethylene terepthalate), polystyrene, polycarbonate, poly(methyl methacrylate), poly(vinyl chloride), poly(caprolactone) and poly(trimethyl hexamethylene terepthalamide) in different solvents. The type of polymer used in the preparation of the solution affects the viscosity of solution and in turn the fiber structure formed. Nylon 6, nylon 66, poly(ethylene terepthalate), poly(caprolactone) and poly(trimethyl hexamethylene terepthalamide) produced fine fibers with different diameters, while polystyrene, polycarbonate and poly(methyl methacrylate) produced fibers with some bead defects. The poly(methyl methacrylate) and poly(vinyl chloride) in solutions studied did not have enough viscosity to produce fibers. These polymers produced only powders that are collected at the target.

This electrospinning process was used to produce PA66 fibers as small as 15 nm. The fibers were produced by electrospinning process only if the applied voltage is above a given limiting value. The diameter of the fiber obtained varied with the solution concentration, which in turn depends on solution charge density, type of polymer, and the solvent used. The diameter of nylon 66 fibers under conditions studied here does not depend on the target distance from the tip of syringe and the voltage applied. The amount of fibers spun by electrospinning process increases with the applied voltage.

The orientation of fibers can be increased by collecting the fiber in a rotating wheel or annealing the fibers at high temperature and load. The winding speed of the wheel should be more than the “natural velocity of the fibers to elongate and align the fibers along the diameter of wheel. The fiber collected at speeds lower than this natural velocity results in random nonwoven mats. The winding wheel moving faster than the natural velocity can cause mechanical drawing of the fiber and results in increases in molecular orientation and tensile modulus for nylon 66 fibers.

The ratio of the speed of rotation of wheel and the natural velocity of fibers can be taken as the draw ratio. The degree of drawing, the increase in molecular orientation and tensile modulus should be a function of both winding speed and the natural electrospinning velocity of the fiber. The latter should be a function of many variables including spinning voltage, target distance, and charge density of the jet. An increase in spinning voltage will increase the electrodynamic forces exerted on the jet, increase the natural velocity the fiber attains before it strikes the target, and therefore decrease the amount of mechanical drawing at a constant winding speed.

The fiber and molecular orientations and tensile modulus of electrospun nylon 6,6 fibers increase with winding speed. Significant orientation of the fibers occurs at lower winding speeds than those needed to cause significant increases in molecular orientation and tensile modulus. Nylon 6,6 fibers electrospun under the conditions studied only develop a large amount of molecular orientation due to mechanical drawing and the forces imposed on the jet due to electrodynamic forces and the whipping instability are not sufficient to impart significant molecular orientation. Fibers spun at a higher voltage exhibited less molecular orientation and lower tensile modulus at the same winding speed, indicating that these fibers attained a higher natural velocity due to higher electrodynamic forces. It can be inferred that nylon 6,6 fibers electrospun into a nonwoven mat under conditions similar to those reported here will exhibit little or no molecular orientation and a low tensile modulus.

The annealing of the electrospun polymer fibers increases their mechanical properties. The modulus of the nylon 66 samples, measured from a tensile test, increases from a lower value with annealing load due to the increase in percent crystallinity and crystalline orientation while the molecular orientation of fibers does not improve. The crystallinity of as spun poly(ethylene terepthalate) and nylon 66/PCL fibers is high but does not increase with increase in annealing load. However the molecular orientation of the poly(ethylene terepthalate) fibers increases with annealing load and can likely improve the mechanical property of fibers.

Nylon 6 and nylon 66 fibers are spun from solution with different concentration of water in terms of weight percentage to predict the effect of plasticizer on the structure of fibers. The increase in water content results in inconsistency in the morphology of fibers with increase in amount of beads in the fibers. The presence of water causes a plasticizing effect on the electrospun fibers as the tensile strength of the fibers decreases with increase in water content. A significant improvement in modulus of the fibers was also observed for the dried samples compared to the as-spun.

The polymers like polystyrene and poly(methylmethacrylate) electrospun from organic solvents shows poor processbility due to low charge carrier density in organic solvents like tetrahydrofuran. The conductivity of THF increases with the addition of LiClO4 and KI salts. The bead defects, observed before, were completely eliminated and fibers with more uniform morphology is produced with the addition of these salts

Attempts made to electrospin two polymers from a common solvent did not produce a single phase. The PA6/PA66 system spun from formic acid, produced fine fibers, has the transition temperature too close to predict presence of a single phase. The PS/PC system spun from toluene as well as from chloroform produced fine fibers but was found to be phase separated. The PMMA/PS, PMMA/PVC and PMMA/PC systems produced only powders and did not spin as fibers. The PA66/PA6(3)T in formic acid produced a cloudy solution showing phase separation even in solution, hence was not spun.

5.1 Recommendations for future work

Future work, which will contribute to better understanding of the electrospinning process and the structure – property relationship of the fibers produced will include

1. In addition to solution concentration, voltage and target distance, the effect of molecular weight, viscosity and polarity of the polymer and its solvent have to be studied.
2. Further study have to be made on producing polymer blend by electrospinning process by trying various solvents, mixture of solvents or addition of conductive agents.
3. The mass throughput, the main disadvantage of electrospinning process, has to be increased by using multiple syringes.
4. The changes in mechanical properties, orientation and crystallinity of other polymers can be studied by winding them in a rotating wheel.
5. The limiting voltage and the natural velocity for a given voltage should also be determined for other polymers.
6. Adequate means have to be found to test single fiber spun from electrospinning process for better understanding of the properties of electrospun fibers.
7. The effect of moisture on other polymers should also be determined.

References

1. Vaidya, A A. *Production of synthetic fibers*, 1988.
2. Deitzel, J M, J. Kleinmeyer, D. Harris, N.C. Beck Tan. *The effect of processing variables on the morphology of electrospun nano fibers and textiles*, Polymer, 42 (2001), 261 – 272.
3. Ziabicki, A. *Fundamentals of fiber formation: the science of fiber spinning and drawing*, 1978.
4. Gibson, Phillip, Heidi Schreuder Gibson, Donald Rivin. *Transport properties of porous membranes based on electrospun nanofibers*, Colloids and surfaces A: Physicochemical and Engineering Aspects, 187-188 (2001), 469-481.
5. Audrey Frenot, Ioannis S. Chronakis. *Polymer nanofibers assembled by electrospinning*, Current opinion in Colloid and Interface science, 2003(article in press).
6. Shin Y M, Hohman M M, Brenner M P, Rutledge G C, *Experimental characterization of electrospinning: the electrically forced jet and instabilities*, Polymer, 42(2001) 9955 – 9967.
7. Larrondo L, John Manley R.St., *Electrostatic fiber spinning from Polymer melts. I. Experimental observations on fiber formation and properties*, Journal of polymer science: Part B: Polymer physics, 19 (1981), 909 – 920.
8. Reneker, Darell H and Iksoo Chun. *Nanometre diameter fibers of polymer, produced by electrospinning*, Nanotechnology, 7 (1996), 216 – 223.
9. Jaeger, Raimund, Micheal M. Bergshoel, Cristina Martin I Batlle, Holger Shonherr, G. Juilius Vancso. *Electrospinning of ultra thin polymer fibers*, Macromolecular symposia, 127, (Feb 1998), 141 – 150.
10. Reneker DH, Sureeporn Koombhongse, wenxia liu, *Flat polymer ribbons and other shapes by electrospinning*, Journal of polymer science: Part B: Polymer physics, 39 (2001), 2598-2606.
11. Reneker, Darell H and Gokul Srinivasan. *Structure and morphology of small diameter electrospun aramid fibers*, Polymer international, 30, No 2 (1995), 195 – 201.

12. Kim JS, Reneker DH, *Polybenzimidazole nanofiber produced by electrospinning,* Polymer engineering and science, 39(1999), 849-854.
13. Zussman, E, Theron A, Yarin AL. *Electrostatic field assisted alignment of electrospun nanofibers*, Nanotechnology, 12 (2001) 384 – 390.
14. Buchko, CJ, Chen LC, Yu Shen, David C. Martin. *Processing and microstuctural characterization of porous biocompatible protein polymer thin films,* Polymer, 40 (1999), 7397 – 7407.
15. Xinhua Zong, Kwangsok Kim, Dufei Fang, Shaofen Ran, Benjamin S.Hsiao, Benjamin Chu, *Structure and process relationship of electrospun bioabsorbable nanofiber membranes,* Polymer 43(2002) 4403-4412.
16. Fong, H, Chun I, Reneker DH. *Beaded nanofibers formed during electrospinning,* Polymer, 40 (1999) 4585 – 4592.
17. Wang Ping, Hongfei Jia, Guangyu Zhu, Bradley Vugrinovich, Woraphon Kataphinan and D H Reneker. *Enzyme-carrying polymeric nanofibers prepared via electrospinning for use as unique biocatalysts,* Biotechnol, 18 (2002), 1027-1032.
18. Vasanthan, Nadarajah, Sigrid B. Ruetsh, David R. Salem. *Structure development of Polyamide 66 fibers during drawing and their microstructure characterization,* Journal of Polymer science: Part B: Polymer Physics, 40 (2002), 1940 – 1948.
19. Lee S H, Yoon J W and Suh M H, *Continous nanofibers manufactured by electrospinning technique,* Macromolecular Research, 10(2002), 282 – 285.
20. Gianchandani J, J. E. Spruiell, E. S. Clark, *Polymorphism and orientation development in melt spinning, drawing, and annealing of nylon-6 filaments,* Journal of Applied Polymer Science, 27, (1982), 3527-3551.
21. Jerold M. Schultz, Joshua M. Samon, Jing Wu, Benjamin Hsiao, Fengji Yeh, Rainer Kolb, *Study on structure development during the melt spinning of Nylon 6 fiber by online wide angle synchrotron x ray techniques,* Journal of polymer science: Part B: Polymer physics, Vol. 37, 1277 –1287 (1999).
22. D. R. Salem, R. A. F. Moore, H.-D. Weigmann, *Macromolecular order in spin-oriented nylon 6 (polycaproamide) fibers,* Journal of Polymer Science Part B: Polymer Physics, 25,(1987), 567-589.

23. Shigemitsu Murase, Masaru Kashima, Kazushige Kudo, Matsuo Hirami, *Structure and properties of high-speed spun fibers of nylon 6*, Macromolecular Chemistry and Physics, 198, (1997), 561-572.
24. Joseph I. Goldstein, A.D. Romig, Jr., Dale E. Newbury, Charles E. Lyman, Patrick Echlin, Charles Fiori, David C. Joy, Eric Lifshin, *Scanning Electron Microscopy and X-ray microanalysis, 2nd Ed., 1992.*
25. Murayama, Takayuki *Dynamic mechanical analysis of polymeric material*, 1978.
26. Mcrum N G et al, *Anelasitic and dielectric effects in polymeric solids*, 1967.
27. shah, Visu *Handbook of plastics testing technology*, 2 , 1998, 195-197&203-205.
28. Zhishen Mo & Hongfang Zhang, *The degree of crystallinity in polymers by wide angle x-ray diffraction.* Journal of Macromolecular symposia – macromolecular chemistry and physics, C35(4), (1995), 555-580.
29. Kendall, David N. *Applied Infrared spectroscopy*, 1, 1966,11.
30. Manual for the Mettler Toledo differential scanning calorimeter DSC 821.
31. Wilkes, G L. *The measurement of molecular orientation in polymeric solids*, Advances in polymer science, 8, 1971, 91 – 137.
32. Osswald, Tim A., Hernandez, Juan P. , Tschohl, Keith, Wagner, Heike. *A novel fiber orientation evaluation using a directional imagine processing technique*, ANTEC 2003, 2178 – 2182.
33. L. Torre L, J. M. Kenny, A. Recca, V. Siracusa, A. Tarzia, and A. Maffezzoli, *Journal Of Thermal Analysis And Calorimetry*, 61, 565-578 (2000).
34. Demir, M. M., Yilgor I, Yilgor E, Erman B. *Electrospinning of polyurethane fibers*, Polymer, 43 (2002), 3303-3309.
35. Martuscelli, Ezio. *Polymer blends - processing, morphology and properties*, 1979, 1-3.
36. Schultz J M, Samon. J M, J. Wu, B. S. Hsiao, F. Yeh and R. Kolb. *Study on structure development during the melt spinning of Nylon 6 fiber by online wide angle synchrotron x ray techniques*, Journal of polymer science: Part B: Polymer physics, 37 (1999), 1277 –1287.
37. Suphaphol, Pitt, Chidchanok Mit-uppatham and Manit Nithitanakul. *Influence of nylon-6 concentration on appearance of resulting electrospun fibers,* Extended

Abstracts of the 28th Congress on Science and Technology of Thailand, http:// pioneer.netserv.chula.ac.th/~spitt/papers/ STT28Gift. pdf.

38. Micheal T. Postek, Karen S. Howard, Arthur H. Johnson & Kathyln L. McMicheal, *Scanning Electron Microscopy - a student's handbook*, 1980
39. Heywood VH, *Scanning Electron Microscopy systematic and evolutionary applications*, 1971.

Appendix

Fortan 77 program to calculate orientation of fibers

```
c   read greyscale data into g(x,y)
c   g(0,0) at upper left corner
c   g(512,512) at lower right corner


      program avecos
       REAL g(512,512), gg(512), ig(512)
      INTEGER a

c read datafile
      open(unit=1, file='5hzFFT.txt')
      open(unit=2, file='5rad.txt')
      do 10 j = 1,512
      read(1,*) (g(i,j),i=1,512)
      gg(j) = 0.0
      ig(j) = 0.01
      ic = 0
   10 continue
      close(1)

c define variables
      pi = acos(-1.0)
      a = 256
      ir = 64
      r = real(ir)
      r2 = r*r
      sumi = 0.0
      sumcos2 = 0.0
      sumig = 0.0
      gmax = -1000

c calculate gg(i) = radial average
      do 20 i = a-r,a+r
      jm = int(sqrt(r2 - (real(a-i))**2))
c       write(2,200) i, a-jm, a+jm
c 200 format(1x, 3I8)
      do 20 j = a-jm,a
      ic = ic+1
      x = real(i-a)
      y = real(a-j)
      theta = acos(x/sqrt(x*x + y*y))
      itheta = int(theta*100/pi)
```

```
    gg(itheta) = gg(itheta) + g(i,j)
    ig(itheta) = ig(itheta) + 1
 20 continue
    write(*,*) "ic = ", ic
    do 30 i = 1,100
    sumig = sumig + ig(i)
    write(2,100) real(i*pi/100), ig(i), gg(i)/ig(i)
 30 continue
100 format(1x,3f16.5)
    close(2)


    write(*,*) "sumig = ", sumig


    end
```

VITA

Sudhakar Jagannathan was born in Madras, India on 24th August 1978 to J. Kasthuri and J. Jagannathan. He received his Bachelor of Technology degree in Polymer Technology with overall rank II from University of Madras, India in the year 2000. He worked for one year (2000-01) in MK Electric (India) Ltd. as Plastics Engineer. He joined the Polymer Engineering program in Department of Material Science and Engineering at University of Tennessee, Knoxville in August 2001 and completed the degree of Masters of Science in August 2003.